Whey protein fibrils – a new approach to modify the functionality of milk protein concentrate and nonfat dry milk

by

Gunvantsinh Indrasinh Rathod

B. Tech., Anand Agricultural University, 2011
M. Tech., ICAR-National Dairy Research Institute, 2013

AN ABSTRACT OF A DISSERTATION

submitted in partial fulfillment of the requirements for the degree

DOCTOR OF PHILOSOPHY

Food Science

KANSAS STATE UNIVERSITY
Manhattan, Kansas

2022

Abstract

Milk-derived ingredients such as milk protein concentrate (MPC) and isolate are the preferred choice to provide nutritional and functional benefits in a wide range of dairy and food products. Milk proteins provide nutritional benefits by providing several essential amino acids. Besides nutrition, milk proteins also provide several functional properties such as thickening, gelling, emulsification, and foaming. These functional properties can be further enhanced by altering protein configuration and protein-protein interactions between milk proteins that can open doors for new product applications. Among several techniques, fibrillation is a technique that converts globular proteins such as whey proteins into a fibrillar form. Compared to globular proteins, fibrillar proteins have a higher aspect ratio (due to a few nanometers diameter and few microns length), which consequently provide improved functionality in terms of thickening, gelation, emulsification, foaming, and interfacial properties. As a first step, milk-derived whey proteins were selectively converted into fibrils and mixed with micellar casein, keeping the casein to whey protein ratio (80:20) to develop fibrillated model MPC (F-MPC) in liquid form. This F-MPC showed the presence of fibrils and consequently resulted in significantly ($P<0.05$) higher viscosity at a 5% (w/w) protein level. Acid gels prepared using F-MPC also resulted in firmer gels compared to control MPC. To further increase the convenience, liquid F-MPC was spray dried to produce in powder form. The F-MPC powder was reconstituted to 5% protein and confirmed the presence of fibrils using transmission electron microscopy. Further, reconstituted F-MPC showed enhanced viscosity, emulsification capacity, foaming capacity and stability, and lower surface and interfacial tension compared to control MPC. In a different study, nonfat dry milk (NDM) containing whey protein fibrils was also developed using microfiltration and ultrafiltration to yield fibrillated skim milk which was spray dried to get fibrillated NDM.

Reconstituted fibrillated NDM (10% w/w) total solids also showed improved viscosity, emulsification, and foaming capacity. Therefore, it could be said that selective fibrillation of whey proteins can enhance the functionality of milk protein powders that can impart functionality to a range of dairy products. These fibrillated ingredients can aid in reducing the use of non-dairy ingredients and can be termed as clean-label ingredients.

Whey protein fibrils – a new approach to modify the functionality of milk protein concentrate and nonfat dry milk

by

Gunvantsinh Indrasinh Rathod

B. Tech., Anand Agricultural University, 2011
M. Tech., ICAR-National Dairy Research Institute, 2013

A DISSERTATION

submitted in partial fulfillment of the requirements for the degree

DOCTOR OF PHILOSOPHY

Food Science

KANSAS STATE UNIVERSITY
Manhattan, Kansas

2022

Approved by:

Major Professor
Dr. Jayendra Amamcharla

Abstract

Milk-derived ingredients such as milk protein concentrate (MPC) and isolate are the preferred choice to provide nutritional and functional benefits in a wide range of dairy and food products. Milk proteins provide nutritional benefits by providing several essential amino acids. Besides nutrition, milk proteins also provide several functional properties such as thickening, gelling, emulsification, and foaming. These functional properties can be further enhanced by altering protein configuration and protein-protein interactions between milk proteins that can open doors for new product applications. Among several techniques, fibrillation is a technique that converts globular proteins such as whey proteins into a fibrillar form. Compared to globular proteins, fibrillar proteins have a higher aspect ratio (due to a few nanometers diameter and few microns length), which consequently provide improved functionality in terms of thickening, gelation, emulsification, foaming, and interfacial properties. As a first step, milk-derived whey proteins were selectively converted into fibrils and mixed with micellar casein, keeping the casein to whey protein ratio (80:20) to develop fibrillated model MPC (F-MPC) in liquid form. This F-MPC showed the presence of fibrils and consequently resulted in significantly ($P<0.05$) higher viscosity at a 5% (w/w) protein level. Acid gels prepared using F-MPC also resulted in firmer gels compared to control MPC. To further increase the convenience, liquid F-MPC was spray dried to produce in powder form. The F-MPC powder was reconstituted to 5% protein and confirmed the presence of fibrils using transmission electron microscopy. Further, reconstituted F-MPC showed enhanced viscosity, emulsification capacity, foaming capacity and stability, and lower surface and interfacial tension compared to control MPC. In a different study, nonfat dry milk (NDM) containing whey protein fibrils was also developed using microfiltration and ultrafiltration to yield fibrillated skim milk which was spray dried to get fibrillated NDM.

Reconstituted fibrillated NDM (10% w/w) total solids also showed improved viscosity, emulsification, and foaming capacity. Therefore, it could be said that selective fibrillation of whey proteins can enhance the functionality of milk protein powders that can impart functionality to a range of dairy products. These fibrillated ingredients can aid in reducing the use of non-dairy ingredients and can be termed as clean-label ingredients.

Table of Contents

List of Figures

List of Tables

Acknowledgements

I would like to thank my advisor Dr. Jayendra K. Amamcharla for his support and guidance before and during my doctoral program at K-State. I also would like to express my gratitude to my committee members, Dr. Scott Smith, Dr. Karen Schmidt, and Dr. Hari Meletharayil for serving on my committee and providing guidance. I would also like to thank my professor and former Director at ICAR-NDRI, Dr. RRB Singh, for his motivation, direction, and endless support to pursue a doctorate.

I am thankful to National Dairy Council and Midwest Dairy Foods Research Center (St. Paul, MN) for their financial support. I would like to acknowledge Dr. Dan Boyle for his help and guidence in transmission electron microscopy, scanning electron micrography, and confocal laser scanning microscopy. I would also like to thank Dr. Kaliramesh Siliveru, Jared, and Anu for their help with powder rheology and Morphology G3. I would also like to thank Jared Parsons and the whole dairy plant team for helping in my dairy plant related activities. I would also like to thank Steve, Rachel, and Sajeev for my plant trial at SDSU. I am also very grateful to all of my lab mates Emily, Luke, Baheeja, Karthik, Priya, Sam, Kavya, Suchismita, Silas, Kaitlynn, Jack, Antonio, Jill, and Emma.

I would like to express my sincere gratitude to my Pappa, Mummy, my lovely brother, niece, and sister-in-law. They unconditionally loved me and endlessly supported me throughout my graduate studies. I would also thank and appreciate my wife and my son for witnessing my ups and downs in life and always supporting, strengthening, and motivating me to move forward. This page would be incomplete without giving thanks to my lovely friends Prakash, Ganesh, Suyog, Amogh, Biswa, Nitin, Dipesh, Rajesh, Taruna, Sweta, Supriya, Deepika, Snehal, Sneha, Priyal, and Priyanka for making journey of Ph.D joyful and being a family far from home.

Dedication

To my beloved father, late Mr. Indrasinh Khumansinh Rathod. Words are not enough to express how special you are to me in my life. A friend and father with whom I can share anything. I really miss you. I hope you could have seen me graduating from K-State.

.

Chapter 1 - Introduction

United States is the second largest milk producer in the world with total annual milk production of 101.25 Million Tons (MT) in 2020 (FAOSTAT, 2022), and is the largest cow milk producer in the world. The total value of the US dairy industry is estimated to be $753 Billion contributing to 3.5% of the US Gross Domestic Product (IDFA, 2021). Apart from milk production, the United States is the largest producer of non-fat dried milk with a total production of 1.1 MT (25% of total world production) (FAOSTAT, 2022). In 2022, it is forecasted to export 0.874 MT of nonfat dried milk (USDA, 2022). With an increase in global demand for dietary proteins and advancements in membrane technology, fractionation of milk proteins and the development of protein dense ingredients such as milk protein concentrates/isolates, whey protein concentrates/isolates, and micellar casein concentrates has increased (Meena et al., 2017; Khalesi and FitzGerald, 2021). The global market for milk protein concentrates was valued at $3009.9 million in 2019 and is projected to reach $3923.6 million by 2027 with a compound annual growth rate (CAGR) of 5.3% (Allied Market Research, 2021). Similarly, the global whey protein market was $10.26 billion in 2021 which is expected to grow to $18.12 billion by 2029 with a projected CAGR of 7.4% (Fortune Business Insight, 2022). Likewise, the global market for micellar casein is also expected to reach $1050 million by the end of 2027 with a CAGR of 6.1% (Coherent Market Insight, 2020). Considering sensory and nutritional attributes, milk proteins are the first choice of ingredients in high protein products and sports drinks. Further, milk proteins possess many functionalities such as thickening, emulsification, and foaming due to their structure and amino acid makeup (Wong et al., 2009). Therefore, fortification of dairy and food product formulations with protein-dense ingredients is preferred to improve the overall quality and functionality of dairy products. However, milk proteins are one of the most

expensive ingredients in the formulation which elevates the overall cost of the product. Therefore, common industry practice is to add non-dairy ingredients such as thickener, emulsifier, surfactant, and foaming agents (Khubber et al., 2021). However, consumer wants product free from non-dairy ingredients or with clean label ingredients (Maruyama et al., 2021) which create a need for an alternative solution to make commercial products keeping similar quality and shelf-life. As discussed earlier, apart from nutrition, protein can fulfill functional need of a given product and their functionality can be further enhanced by altering native protein structure. Therefore, number of attempts were made to enhance functionality of milk proteins using various physical (such as ultrasonication, high pressure processing), chemical (such as succinylation) and enzymatic (such as transglutaminase) methods, which are well documented in the coming section (Review of literature). In the current study, we have focused on the fibrillation technique which converts globular proteins such as whey proteins into fibrils and enhances the functionality of proteins in terms of enhanced viscosity, gelation, emulsification, foaming, and antioxidant properties (Meng et al., 2022). Details about the fibrils' structure, manufacture, and functionality enhancement of protein, are well discussed in the coming section (Review of literature).

References

FAOSTAT. 2022. FAOSTAT. Accessed September 6, 2022. https://www.fao.org/faostat/en/#data/QCL/visualize.

IDFA. 2021. U.S. Dairy Industry’s Economic Impact Totals $753 Billion - IDFA. Accessed September 6, 2022. https://www.idfa.org/news/u-s-dairy-industrys-economic-impact-totals-

753-billion.

Insight, C.M. 2020. Micellar Casein Market Size, Trends And Forecast To 2027. Accessed September 6, 2022. https://www.coherentmarketinsights.com/market-insight/micellar-casein-market-3717.

Insight, F. business. 2022. Whey Protein Market Size, Share & Growth Report [2022-2029]. Accessed September 6, 2022. https://www.fortunebusinessinsights.com/whey-protein-market-106555.

Khalesi, M., and R.J. FitzGerald. 2021. Insolubility in milk protein concentrates: potential causes and strategies to minimize its occurrence. https://doi.org/10.1080/10408398.2021.1908955. doi:10.1080/10408398.2021.1908955.

Khubber, S., K. Chaturvedi, N. Thakur, N. Sharma, and S.K. Yadav. 2021. Low-methoxyl pectin stabilizes low-fat set yoghurt and improves their physicochemical properties, rheology, microstructure and sensory liking. Food Hydrocoll. 111:106240. doi:10.1016/J.FOODHYD.2020.106240.

Maruyama, S., N.A. Streletskaya, and J. Lim. 2021. Clean label: Why this ingredient but not that one?. Food Qual. Prefer. 87:104062. doi:10.1016/J.FOODQUAL.2020.104062.

Meena, G.S., A.K. Singh, N.R. Panjagari, and S. Arora. 2017. Milk protein concentrates: opportunities and challenges. J. Food Sci. Technol. 54:3010–3024. doi:10.1007/S13197-017-2796-0/FIGURES/2.

Meng, Y., Z. Wei, and C. Xue. 2022. Protein fibrils from different food sources: A review of fibrillation conditions, properties, applications and research trends. Trends Food Sci. Technol. 121:59–75. doi:10.1016/J.TIFS.2022.01.031.

Research, A.M. 2021. Milk Protein Concentrate Market Size, Share, Trends & Forecast, 2027.

Accessed September 6, 2022. https://www.alliedmarketresearch.com/milk-protein-concentrate-market-A10558.

USDA. 2022. United States Department of Agriculture Foreign Agricultural Service Dairy Production and Trade Developments.

Wong, D.W.S., W.M. Camirand, A.E. Pavlath, D.N. Parris, and D.M. Friedman. 2009. Structures and functionalities of milk proteins∗. https://doi.org/10.1080/10408399609527751 36:807–844. doi:10.1080/10408399609527751.

Chapter 2 - Review of literature

Introduction

Milk is considered a complete food, having almost all essential nutrients for infants to adults. Regarding milk composition, milk contains fat (3-3.5%), proteins (3-3.5%), sugar (lactose) (4.5-5%), and minerals/ash/salt (0.8%), while water (87%) is a major component (Walstra et al., 2005). Milk proteins are composed of ~80% casein and ~20% whey proteins. Casein is present in colloidal form and possesses a micellar structure while whey proteins are in true solution and have a globular structure. Caseins are subdivided into four different fractions, αS_1, αS_2, β, and κ-casein. Among them, calcium insensitive κ-casein forms a hairy outer layer around the casein micelles while calcium sensitive αS_1, αS_2, and β caseins remain within the casein micelles, which are joined together by colloidal calcium phosphate. The colloidal calcium within the casein micelles is in equilibrium with ionic calcium present in the serum phase, and depending on the serum calcium level, calcium in the casein micelles is released into the serum to keep calcium in equilibrium (Fox et al., 2015a). Unlike casein micelles, whey proteins are globular proteins having tertiary and quaternary structures and remain in true solution in milk (Walsta et al., 2005). Among whey proteins, β-lactoglobulin contributes to ~75% of total whey proteins, while α-lactalbumin contributes around ~25%. Other than these major whey proteins, bovine serum albumin and immunoglobulins are also present as minor proteins. The β-lactoglobulin comprises two disulfide bonds and one free -SH (sulfhydryl) bond which makes β-lactoglobulin the most reactive milk protein. Unlike β-lactoglobulin, α-lactalbumin has four disulfide bonds, while bovine serum albumin has seventeen disulfide bonds (Gunasekaran and Solar, 2012; Fox et al., 2015b). Upon heating to 62 to 78°C, whey proteins are denatured. Among them immunoglobulins denature first, followed by bovine serum albumin, β-

lactoglobulin, and finally α-lactalbumin (Borad et al. 2017). Contrary to whey proteins, casein is heat stable, as casein has a primary structure and is also called a naturally denatured protein (Darewicz et al., 2006). However, during heat processing, when casein and whey proteins both are in the solution, κ-casein interacts with β-lactoglobulin by forming a disulfide bond. This interaction increases the rennet coagulation time, as a complex of β-lactoglobulin with κ-casein (Gunasekaran and Solar, 2012) over shed the site for the rennet to act upon the κ-casein (Met105-Phe106) and delays rennet gelation (Kethireddipalli et al., 2010). However, during gel formation by pH reduction, whey proteins bound to the casein micelles also take part in gel network formation and provide higher gel strength and firmer gel (Lucey et al., 2022). Heat-induced denaturation of whey proteins also helps in increasing heat stability and reducing age gelation (Anema, 2017). Calcium, a divalent cation, also plays a key role in the structure of casein micelles (as colloidal calcium phosphate) and gel formation. Depending on the level of serum calcium, calcium on the casein dissociates from casein, comes to the serum phase, and enhances the gelation by forming salt bridges (Fox et al., 2015a).

Similar to gelation, milk proteins also provide thickening and increased viscosity depending upon the protein content of the solution, due to swelling upon protein hydration and protein-protein crosslinking (Power et al., 2020). An increase in viscosity and thickening also helps to retain air in aerated dairy products such as ice cream. Increase in viscosity, limit the air cell movement in the solution and delay coalescence, Ostwald ripening, and escape of air cell from the solution. Besides raising the viscosity, milk proteins can also unfold and adsorb to the air-water interface due to the presence of both hydrophilic and hydrophobic amino acids. Therefore, they can stabilize air cells in the solution and give good foaming capacity and foam stability in terms of longer retention of foam (Zhao et al., 2022). Like the air-water interface,

milk proteins can also be adsorbed at the oil-water interface and stabilize the oil droplet. Due to this feature milk proteins can also provide good emulsification capacity which is exploited in dairy foods formulation for decades (Silva et al., 2020). A common example is the homogenization of milk. During homogenization of milk, the milk fat globule membrane ruptures, and the milk fat globule is broken down into tiny fat globules. These newly formed milk fat globules are covered by milk proteins specifically casein (Lu et al., 2021).

Despite having inherent functionalities of milk proteins, the dairy industry needs further enhancement in the functional properties of milk proteins to increase product quality, stability, shelf-life, and lower defects, to meet consumer demand. Therefore, the dairy industry used gums and stabilizer/texture modifiers to achieve thickening and gelling in products. Also, they used emulsifiers, stabilizers, thickeners, and surfactants to prevent defects such as oiling off and fluffy products. However, these additives are non-dairy-based, and these days consumers want products free from non-dairy-based additives. It creates demand for dairy-based clean-label ingredients with enhanced functionality (Dairy Reporter, 2020). Therefore, the existing functionality of milk proteins such as gelling, thickening, emulsification, and foaming (Mirmoghtadaie et al., 2016) can be further improved (Figure 2.1). The basic mechanisms of these functional properties could be different, and they are (1) hydration of proteins that affect the absorption of water/oil, wettability, solubility, and thickening of protein; (2) surface activity properties of protein due to charged groups, such as hydrophobicity, hydrophilicity, net charge, or charge distribution, which can affect the movement of protein to oil-water or air-water interface and thereby the formation of protein-lipid films, foaming, and emulsifying activities; (3) modification in protein structure, such as size, shape, amino acid sequence and composition which can modify rheological properties, including the viscosity of the solution, elasticity, aggregation and gelation

characteristics (Speroni et al., 2009). These inherent functional properties can be further altered and improved by modification of proteins using different physical, enzymatic and chemical treatments.

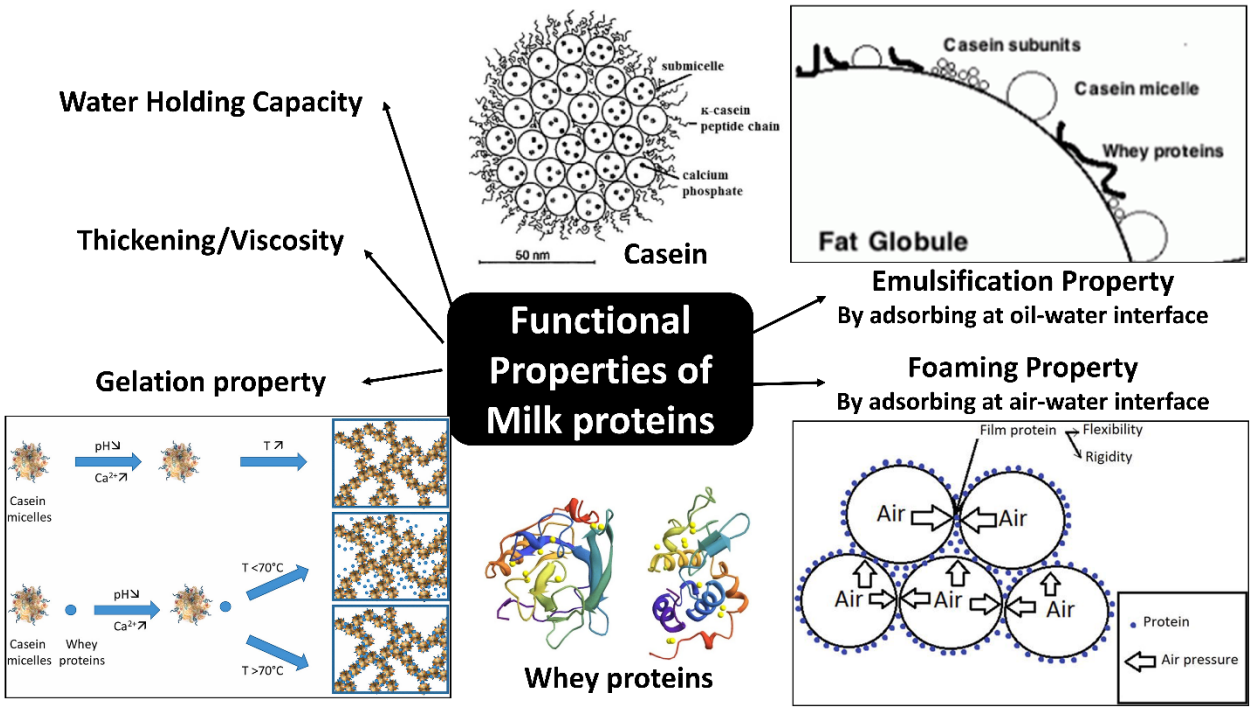

Figure 2.1 Pictorial representation of functionalities of milk proteins (Walstra et al., 2005; Fox et al., 2015a: Lajnaf et al., 2021; Nicolai and Chassenieux, 2021).

Techniques to modify the functionality of proteins

Physical treatments

Thermal processing

In the food industry, thermal processing such as heating cooling, thawing, and freezing are quite common physical processes that have strong effects on different food components and their functionalities. Heating of protein solution results in disruption of protein quaternary structures, unfolding of the protein, protein denaturation, and an increase in protein aggregation

through disulfide, hydrophobic and electrostatic bond formation (Barać et al., 2004). However, these changes depend on the type of proteins, the type of thermal processing and its duration, and also the presence of other constituents. A quite common example of heat-induced functionality modification is heating milk to 90-95°C for 5-10 minutes, which denatures whey proteins and promotes κ-casein-whey protein interaction through disulfide bonds. Therefore, when milk is acidified, whey proteins bound to casein will also take the part in the formation of a three-dimensional close neat gel network (Figure 2.2), which provides a firmer gel with less syneresis, keeping the same milk protein level (Sfakianakis and Tzia, 2014; Lucey et al., 2022). Casein-whey protein interaction also depends on the pH at which they are heated (Figure 2.3). Denaturation of whey proteins leads to the formation of small aggregate on higher heat treatment, therefore pretreatment with higher heating increases the heat stability of skim milk (Huppertz, 2016). Along with traditional thermal processing-induced modifications, there are some novel physical techniques, which are used to improve the functionality of milk proteins.

High-pressure processing

High-pressure processing is a novel technique where the food product is exposed to pressure above 100 MPa in the specifically designed vessel (Figure 2.4A). High-pressure processing can modify the functional properties of food components due to the disruption of hydrophobic bonds and electrostatic interactions (Mirmoghtadaie et al., 2016). Further, extremely high pressure also promotes the formation of new bonds, aggregation, and network formation, leading to the formation of aggregates or gels depending upon protein concentrations (Puppo et al., 2005). Patel and Huppertz, (2014) represented the effect of medium (250 MPa) and high (more than 600 MPa) pressure treatment on casein micelle and whey protein. At 250 MPa, casein micelles swell and β-lactoglobulin denatures, unfolds, and aggregates through disulfide

bonds. The β-lactoglobulin also binds with κ-casein and forms small aggregates. Compared to β-lactoglobulin, α-lactalbumin participates less in aggregation. When pressure is further raised to 600 MPa, αS_2 casein becomes available for thiol interchange reaction, water permeation occurs into micelles and also the dissolution of casein micelles occurs. The β-lactalbumin forms a larger aggregate at a pressure of more than 600 MPa (Figure 2.4B). Disruption of casein micelles was also seen in transmission electron microscopic images by Schrader et al. (1997) when skim milk and skim ultrafiltrate was treated at 400 MPa. This disruption of casein micelle destroys the micellar structure and further increases transmission of light and reduces the turbidity, which was confirmed when caseinates suspensions were treated at 200 MPa, which showed strong reductions in the turbidity (Lee et al., 1996; Anema et al., 1997). These structural changes modify the resultant product structure and characteristics. High-pressure processing of yogurt showed a reduction in post-acidification without affecting an initial number of vital lactic acid bacteria when treated at 200-300 MPa for 10 minutes (Tanaka and Hatanaka, 1992). Johnston et al. (1993) reported improvement in gel rigidity and gel breaking strength of acid set gels when treated at 600 MPa for 15 minutes. High-pressure treatment may lead to exposure to hydrophobic sites, increase crosslinking, and formation of several network strands, leading to improvement in gel strength and reduction in the syneresis of acid gels (Datta and Deeth, 1999). The effect of high-pressure processing is also dependent on the type of protein and the pressure applied and the duration of treatment. For example, among whey proteins, β-Lactoglobulin showed significantly low solubility under high-pressure treatment, however, no significant changes in solubility have been recorded for α-lactalbumin (Van Camp et al., 1997).

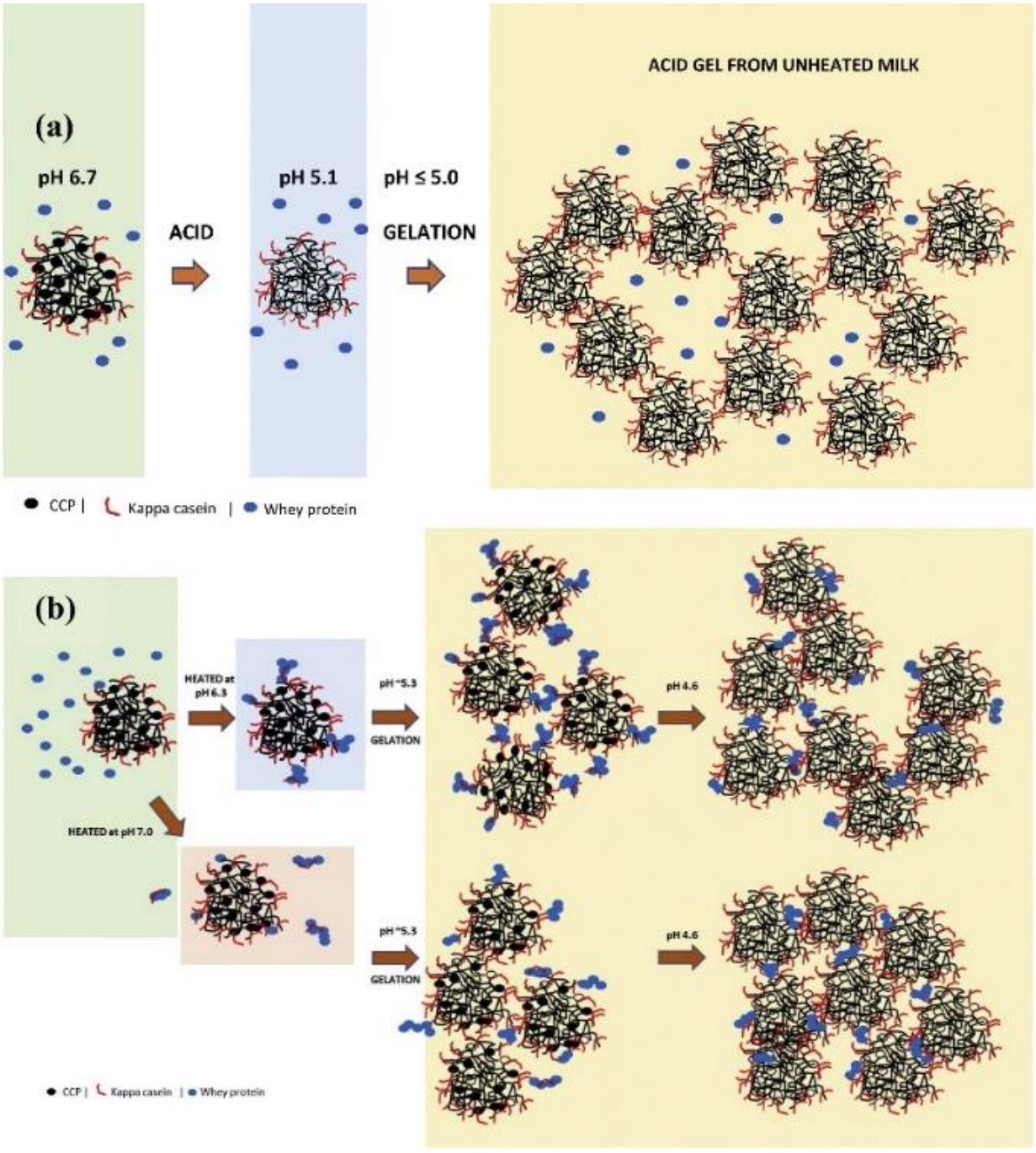

Figure 2.2 Pictorial representation of gelation of unheated (a) and heated milk focusing on casein-whey protein interactions (Lucey et al., 2022).

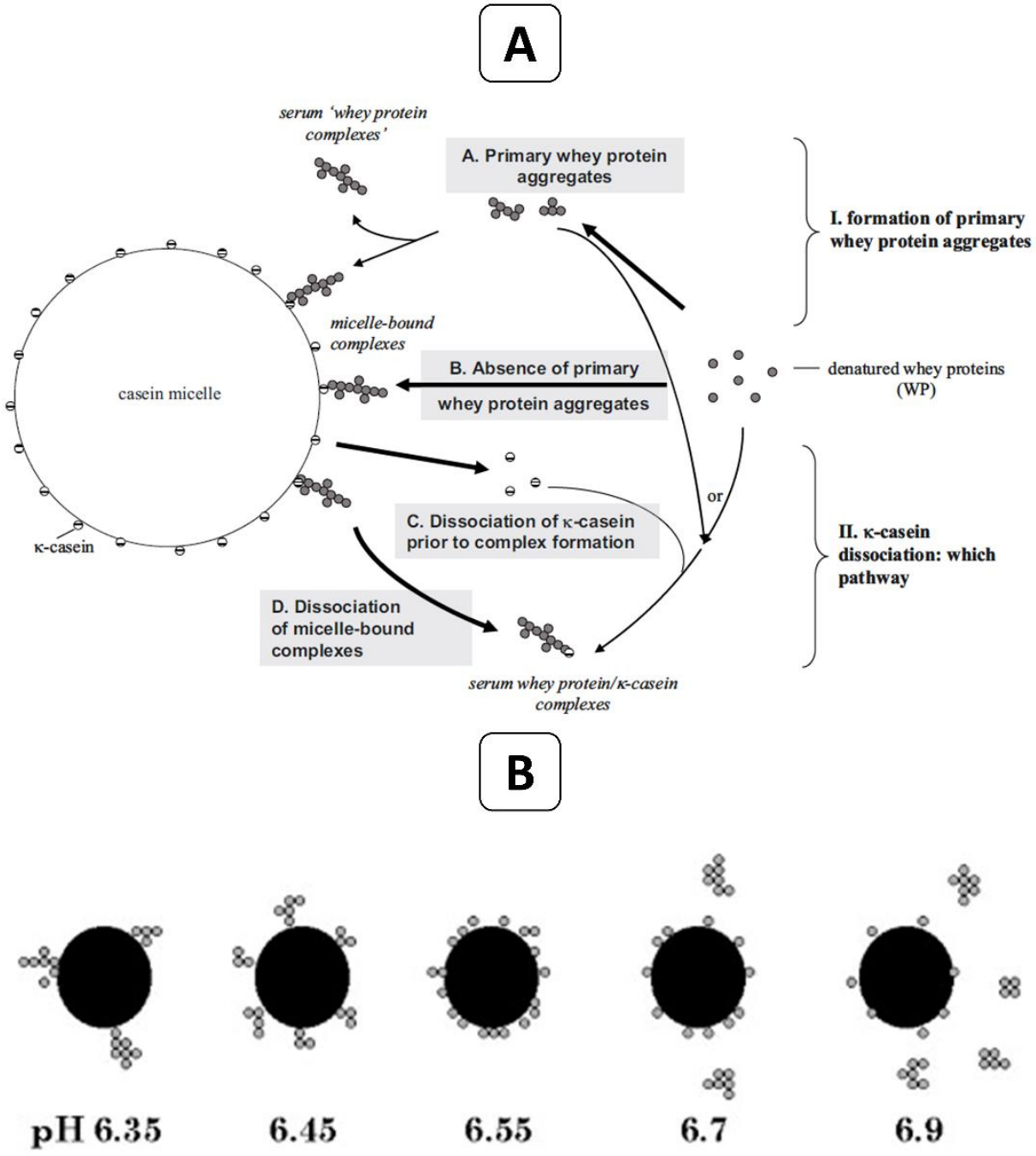

Figure 2.3 Schematic Diagram of heat-induced casein-whey protein interaction (A) and pH-dependent casein-whey protein interactions (B) (Vasbinder and De Kruif, 2003; Donato and Guyomarc'h, 2009; Asaduzzaman et al., 2021).

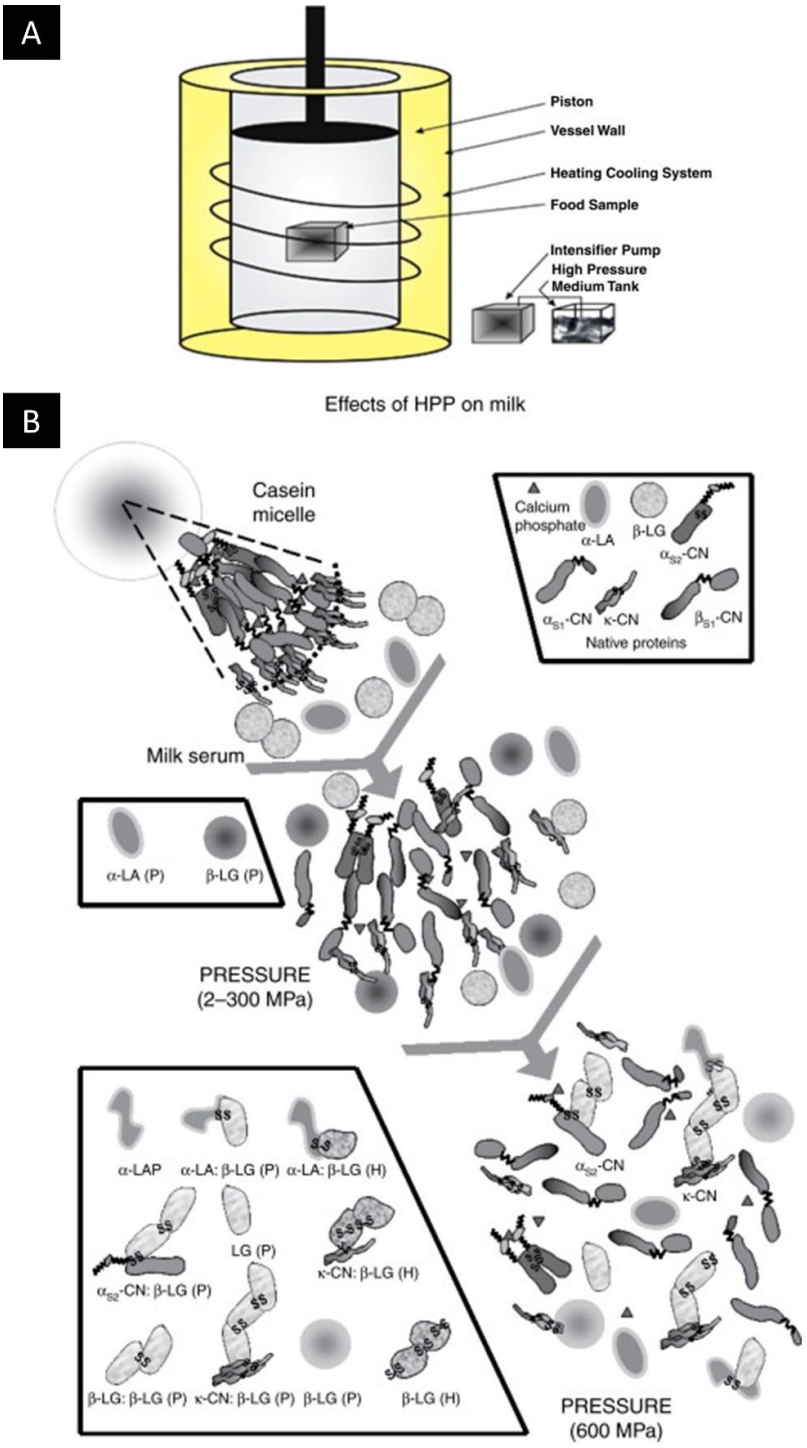

Figure 2.4 Schematic diagram of high-pressure processing equipment (A) Schematic representation of effect of high pressure processing on milk proteins (B) (Patel and Huppertz, 2014) (CN-casein, β-LG- β-lactoglobulin, α-LA-α-lactalbumin).

High-pressure jet processing

High-pressure jet processing is also recently used by many researchers for functional modifications of milk proteins. A schematic diagram of high-pressure jet processing is given in Figure 2.5A. For high-pressure jet processing, milk is continuously pressurized (125 to 500 MPa) and passed through a diamond nozzle with a very small orifice (10-μm-diameter) (Tran et al., 2018). In initial attempts, pasteurized skim milk was processed at pressure from 0 to 500 MPa (Mohan et al., 2016). They found an increase in particle size of casein micelle from 180-220 nm (processed at 0-200 MPa) to a maximum of 404 nm (processed at 400 MPa) then reduction to 285 nm (processed at 500 MPa) (Figure 2.5B). Similarly, Tran et al. (2018) also found an increase in particle size with an increase in pressure to 375 MPa followed by a decrease in particle size at 500 MPa for whole milk (Figure 2.5C). The author suggests that high shear-induced temperature in the high-pressure jet nozzle may have caused dissociation of the casein followed by hydrophobic reaggregation or compaction of dissociated casein proteins into larger micelles, causing increased particle size which could be further confirmed with scanning electron microscopic images of high-pressure jet processed skim milk at different pressure (0-500 MPa) (Figure 2.5D).

Mohan et al. (2016) also reported an increase in viscosity from 2.2 mPa.s (for unprocessed milk) to 4.2 mPa.s for skim milk treated at 500 MPa. Similarly, Tran et al. (2018) also found an increase in viscosity from 2 to 5 mPa.s when whole milk was processed at 375 Mpa. Further, foam expansion was also increased from 80% to 140% when whole milk was processed at more than 125 MPa. These improvements could be due to the dissociation of casein micelles into surface-active casein protein monomers. Hettiarachchi et al. (2018) reported improvement in foam expansion index (75-83%) and emulsification activity index (33-46%)

from skim milk treated at a pressure of 300-500 MPa than the control sample. The increased foamability and emulsifying properties could be due to partial disruption of casein micelles, causing an increase in protein adsorption at the oil-water and air-water interface, and also due to partially heat-induced whey protein denaturation (Harte et al., 2016).

Ultrasound

Ultrasound is also used to modify the functionality of food proteins using low frequency (16-100 kHz) high-intensity waves (typically in the range of 10–1000 W cm^2) (Soria and Villamiel, 2010). The application of ultrasound produces acoustic cavitation that decreases the particle size of proteins by disrupting proteins. At the molecular level, ultrasound effects on hydrophobic and electrostatic interactions such as hydrogen bonds and van der Waals forces, occur among three-dimensional protein networks, which can dissociate protein molecules to generate smaller fragments (Shokri et al., 2022). However, the overall effect on milk proteins is most dependent on the type of frequency used in the processing. Chandrapala et al. (2012) studied the effect of ultrasound (20kHz) on casein micelle integrity, where they found that size of casein micelles was unchanged with a slight increase in soluble whey proteins and a decrease in viscosity, which could be due to breaking up of casein-whey protein aggregates. Denaturation of whey proteins and formation of whey protein-whey protein/ whey protein-casein complexes was seen in the milk (Shanmugam et al., 2012). Madadlou et al. (2009) compared low (35kHz) and high (130kHz), where 130 kHz showed micelle disruption which can be seen by a decrease in particle size and consistency. Ultrasound also opens the buried functional groups and increases solubility (Zhang et al., 2018; Vargas et al., 2021).

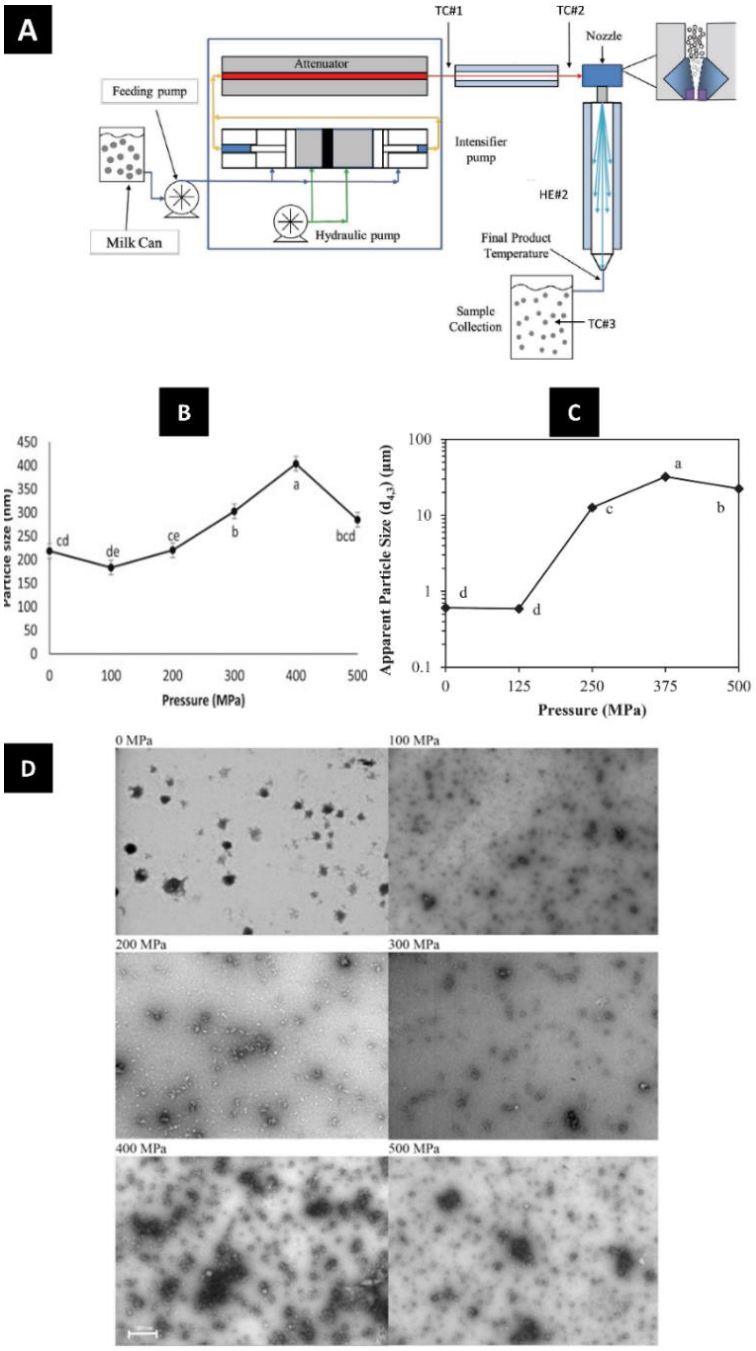

Figure 2.5 Schematic diagram of high-pressure jet processing (A), the particle size distribution of skim milk (B) and whole milk (C) processed with high-pressure jet processing, scanning electron microscopic images of skim milk processed with high-pressure jet processing at different pressure (0-500 MPa) (Mohan et al., 2016; Tran et al., 2018).

Along with solubility, ultrasound also improves interfacial properties such as emulsification and foaming by improving protein absorption at the fluid interface such as the oil-water and air-water interface and decreasing the interfacial tension (Jambrak et al., 2009; Shokri et al., 2022).Further, ultrasound also alters gelation by altering the protein structure, promoting intermolecular interactions such as hydrophobic interactions and disulfide bonding to form a three-dimensional cross-linked protein network (Arzeni et al., 2012). The effect of ultrasound depends on the frequency used and the total exposure. Ultrasound is also used to mix and homogenize samples as well as, it can create micro-nano bubbles that can reduce the viscosity of protein solution and increase the processibility of milk protein concentrates (Babu and Amamcharla, 2022).

Hydrodynamic Cavitation

Like, ultrasound, hydrodynamic cavitation is also a new method to alter the functionality of proteins. The hydrodynamic cavitator is shown in Figure 2.6. In hydrodynamic cavitation, the liquid is passed through constriction, resulting in an increase in the kinematic energy of the liquid at the loss of pressure. Due to this throttling, if pressure around the point of vena contracta goes below the threshold pressure for cavitation, it results in the generation of millions of cavities and bubbles. Consequently, when the liquid jet expands and the pressure recovers, these cavities collapse. When these bubbles collapse, a powerful shockwave is released into the surrounding liquid (Oestergaard, 2016, Li et al., 2018). Similar to ultrasonication, cavitation disrupts protein bonds and leads to a reduction in viscosity of the high protein solutions such as milk protein concentrate, which helped in pumping, atomizing, and spray drying operations (Li et al., 2018). Hydrodynamic cavitation also showed an increase in the solubility of milk protein concentrate (Pathania et al., 2018). Similar to milk protein concentrates, hydrodynamic

cavitation significantly reduced the viscosity of whey protein concentrates solution, which may be due to disruption of protein aggregates and size reduction (Gregersen et al., 2019).

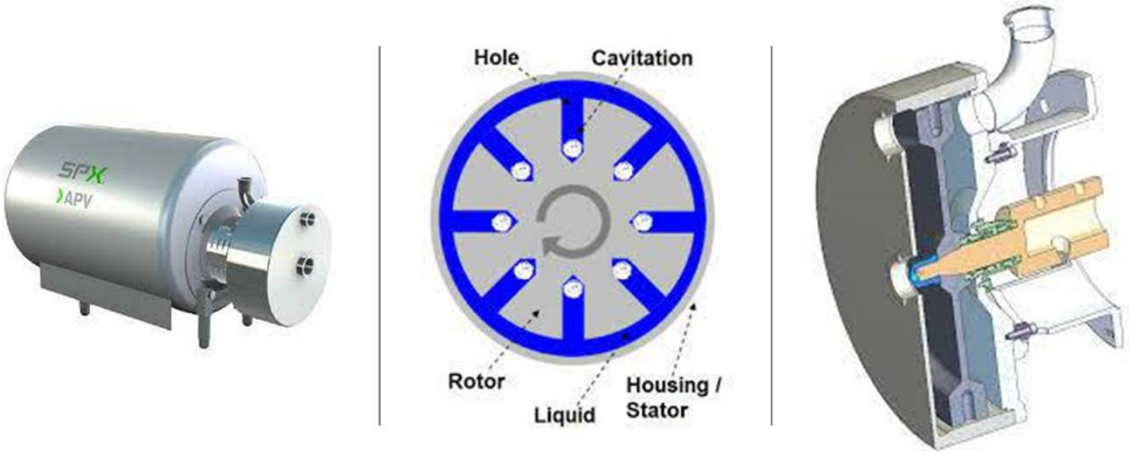

Figure 2.6 Diagram of hydrodynamic cavitator (SPX 2022).

Cold atmospheric plasma

Cold atmospheric plasma processing is a recent popular technique used in food processing as a non-thermal microbial destruction technique, an alternative to thermal treatment (Basak and Annapure, 2022). Plasma is recognized as the fourth state of matter which is divided into thermal plasma and non-thermal/cold plasma. Plasma, with highly ionized species, present in thermodynamic equilibrium with each other is called thermal plasma, where the temperature is raised as high as 10^4 K uniformly across all constituent species. Whereas, in the non-thermal plasma/cold plasma, the temperature of electrons goes extremely high, however, the temperature of ions and unionized species remains around room temperature, following the thermodynamic non-equilibrium between them (Surowsky et al., 2014). Cold plasma produces a wide range of reactive species, therefore identifying and assessing these species is important to understand the interactions between a food component and cold plasma (Sharma and Singh, 2020). A schematic

diagram of cold plasma generation and its effect on protein structure was given in Figure 2.7A. Application of cold plasma disintegrates subunits of quaternary structure and unfolds tertiary structure. These conformational changes in proteins are due to different reactions in the complex plasma chemistry, which is most likely started by Reactive Oxygen Species and UV photons Reactive Oxygen Species produced by the cold plasma. These Reactive Oxygen Species can break peptide bonds, oxidize amino acid side chains, and even cause the formation of cross-linkages between the polypeptide chains (Sharma and Singh, 2020). Due to the structural alteration, bacterial cell wall get destroyed, leading to microbial destruction (Figure 2.7B). However, this alteration in proteins can enhance functionality such as interfacial properties by adsorbing at the oil-water and air-water interface as shown in Figure 2.7C (Ganesan et al., 2021; Basak and Annapure, 2022). Segat et al. (2015) reported changes in the folding pattern of whey proteins (using dynamic light scattering and high-performance liquid chromatography profiles) followed by improvement in the emulsification and foaming capacity of whey proteins when treated with atmospheric pressure cold plasma at 70kV for 15 minutes, due to the unfolding of the protein. However, a further increase in treatment time (30 minutes and 60 minutes) showed a decrease in emulsification and foaming capacity, which may be due to the breakage of the peptide chain into smaller peptides. Sharma and Singh (2022) treated skim milk using cold plasma at 20 kV with frequency (15-25 Hz), they reported an increase in aggregated β-sheet with a simultaneous decrease in random coils of proteins indicating aggregation of proteins upon unfolding of proteins due to cold plasma exposure. Pankaj et al. (2014) reported a decrease in glass transition temperature and increased hydrophilicity when they treated sodium caseinate film using cold plasma (at 60-70 kV for 1-5 minutes). They also documented that cold plasma

disrupts the inter-helical structure of protein molecules without changing the helical configuration, but they reported increased hydrophilicity of sodium caseinate film.

Enzymatic treatments

Enzymatic modifications of food proteins using controlled proteolysis can improve the functional properties over different processing conditions. Therefore, it is important to choose the right proteolytic enzyme, and environmental conditions for the optimum degree of hydrolysis to obtain desired functional properties (Panyam and Kilara, 1996). Hence, understanding of target protein structure, and choosing the right enzyme for the right proteolysis site are important. Endopeptidases work best as they act on a specific site and cleave protein into the desired peptide. As enzyme has their optimum working conditions, it is especially important to control environmental conditions such as pH, temperature, salt concentration, and protein concentration (Panyam and Kilara, 1996) to modify proteins in a controlled manner. Casein and caseinates are less soluble at their isoelectric point- 4.6, and their solubility can be increased by limited hydrolysis using trypsin (Chobert et al., 1988). Denaturation of whey protein also leads to a decrease in solubility, which can partially be restored by hydrolysis using trypsin (Mutilangi et al., 1996). Kneifel and Seiler (1993) reported that hydrolysis of casein with Corolase PN to 2.5 degree of hydrolysis or with bromelain to 5.8% degree of hydrolysis improved the water-holding capacity of casein. Unlike that, hydrolysis of milk proteins with Alcalase or Neutrase gave hydrolysate with relatively low water holding capacity (Mietsch et al., 1989). For gel formation, protein hydrolysis is considered detrimental as hydrolysis increases net charge and repulsion which reduces the gelation ability and strength (Mahmoud, 1994), however, control hydrolysis can improve or control the gel strength.

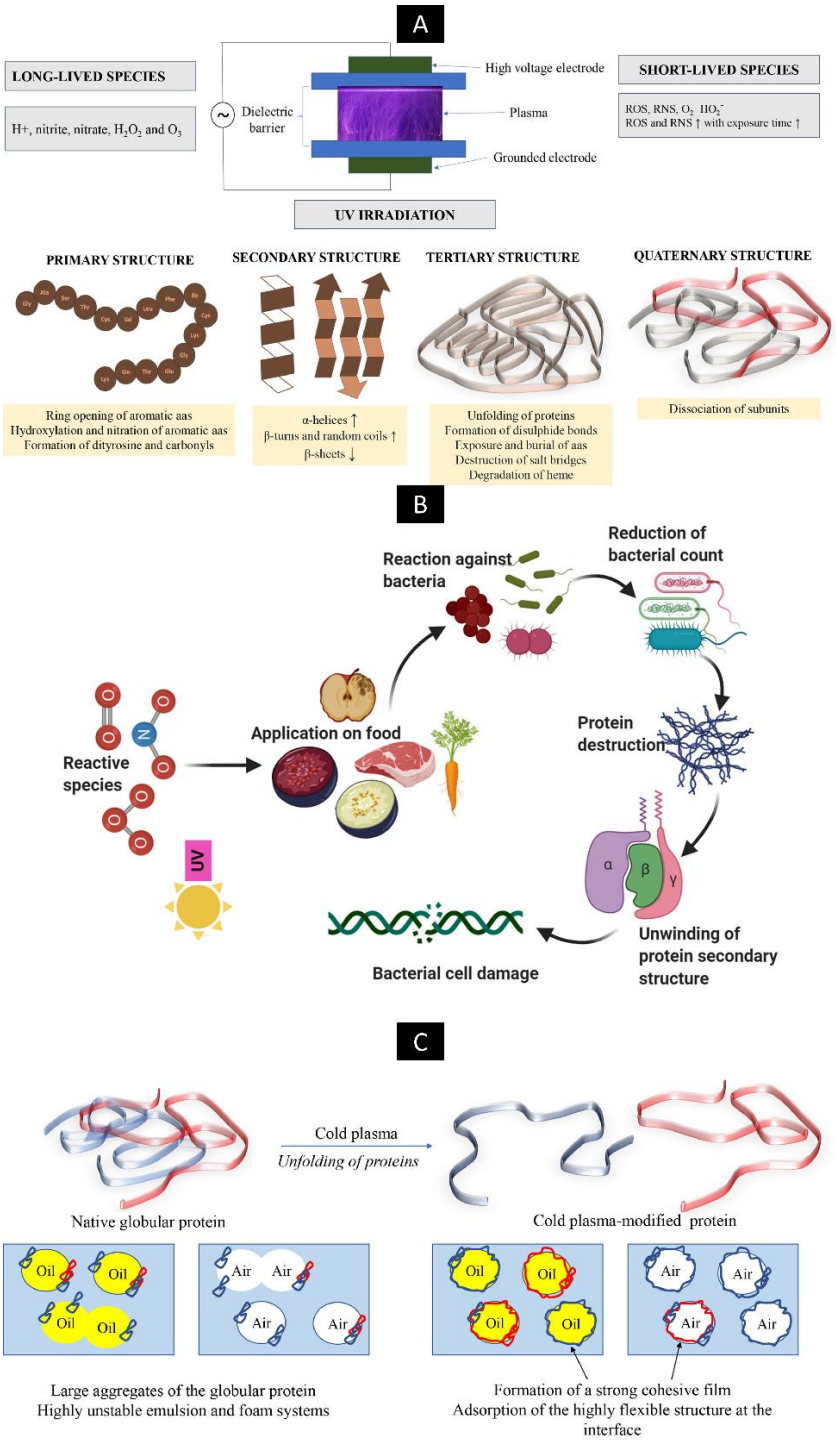

Figure 2.7 Schematic diagram of the cold plasma treatment system and its effect on protein structure (A), mechanism of microbial destruction (B), and mechanism of proteins modification (C) (Ganesan et al., 2021; Basak and Annapure, 2022).

For example, tryptic hydrolysis of whey proteins between 2.3- 6.7% degree of hydrolysis prevented gelation at pH 3.0 and pH 7.0, however, hydrolysis to 2.3 % degree of hydrolysis with a *Bacillus subtilis* protease increased the gelling ability and gel strength at pH 7.0 (Ju et al., 1995). Enzymatic modification can further customize emulsification properties by changing the length of the protein and its hydrophobicity and hydrophilicity based on the resultant peptide from the proteins. Large proteins provide better emulsification properties while small peptides do not. Further, the desorption of protein from the interface leads to the destabilization of emulsion droplets (Haque, 1993). Despite this fact, enzymatic hydrolysis can be beneficial in some conditions, for example, a peptide from αS_1 casein (residue 1-23) showed similar emulsification activity to intact αS_1 casein, but emulsion activity was reduced to half. However, at acidic pH, the peptide of αS_1 casein maintained its emulsification, but intact αS_1 casein did not. Therefore, these peptides can provide emulsification properties better than intact proteins at acidic pH (Shimizu et al., 1984; Panyam and Kilara, 1996). Similar to emulsification, foaming is also interfacial property, which can be fabricated by hydrolysis. The foaming capacity of whey protein was improved with controlled hydrolysis, while foam stability was decreased (Kuehler and Stine, 1974). In the case of casein, hydrolysis of casein using acid fungal protease showed improvement in foaming (Panyam and Kilara, 1996).

Transglutaminase

During hydrolysis, protein, a polypeptide chain is broken down into smaller peptide/amino acids using an enzyme such as protease. Contrary to hydrolysis, those peptides can be joined using enzymes such as ligase. Controlling the state of a protein, chain length and crosslinking can alter protein structure, and thereby protein functionality in terms of viscosity, thickening, and gelling. In the dairy-food industry, transglutaminase is widely used to change

protein functionality. Transglutaminase or glutaminyl-peptide-amine γ-glutamyl transferase (EC 2.3.2.13) forms covalent crosslinks of inter- or intra-molecular ε-(γ-glutamine)-lysine isopeptidic bonds (Kieliszek and Misiewicz, 2014). Due to its crosslinking and bond-making property, transglutaminase is also known as 'meat glue' (Chan and Lim, 2019). Transglutaminase works on deamidation and polymerization mechanisms (Gaspar et al., 2015). Many studies reported the use of transglutaminase in acid gels in different concentrations ranging from (0.1-1.0 U/g) which showed decreased syneresis, increased water holding capacity and viscosity with homogeneous texture, and high storage stability (Bönisch et al., 2007; Gharibzahedi and Chronakis, 2018). The possible mechanism for improvement in gels is shown in Figure 2.8A. Transglutaminase forms intermolecular crosslinking of micellar casein, which stabilizes casein micelles against dissociation or disintegration due to the removal of colloidal calcium phosphate from casein micelles during acidification. Therefore, due to this modified casein micelle structure and micelle-micelle interaction, a transglutaminase-treated gel is altered into a protein gel with a lower mesh size protein network with high mechanical strength and lower water syneresis (Ercili-Cura et al., 2013) which can be seen in confocal microscopic images (Figure 2.8B). Transglutaminase also showed improvement in cheese yield, water holding capacity, and texture in soft-type cheeses, however, it is not common to use in hard-type cheese (Romeih and Walker, 2017). Færgemand et al. (1998) assessed emulsification properties after transglutaminase treatment, and they found that thickening provided by crosslinking reduced the creaming of oil droplets and provided good emulsion stability than not crosslinked ones. Crosslinking ability of transglutaminase is exploited in cheese and ice-cream products to improve texture and rheology (Gharibzahedi et al., 2018). Transglutaminases impart gelation, viscosity, emulsification,

foaming, and water holding capacity, and improvement in functionality, which is well discussed by Gaspar et al. (2015) and Gharibzahedi and Chronakis, (2018) using different reported studies.

Chemical Treatments

In addition to physical and enzymatic methods, several researchers tried different chemical methods such as succinylation, acylation, phosphorylation, glycosylation, and deamidation to change protein functionality. These methods play with the structure of protein and alter its functionality.

Succinylation

Succinylation of lysine is shown in Figure 2.9A, during which the ε-amino group of lysine is attached to the succinyl group of succinic anhydrides, this results in altering the positive charge with a negative charge at lysine amino acid and the hydroxyl group of amino acids. Due to these changes in the charge, protein conformation alters and dissociates, and causes the unfolding of proteins (Agarwal et al., 2020) and possible changes in the functionality of proteins. Shilpashree et al. (2015a) did succinylation of milk protein concentrates which results in improved solubility, foaming capacity and stability, and emulsification activity and stability. Comparable results were seen for the succinylation of sodium caseinates (Shilpashree et al., 2015b). Further, succinylation of milk protein concentrates and caseinate increase zinc retention, therefore complexes of zinc with succinylated milk protein concentrates and sodium caseinate can be used as a carrier of zinc for the food fortification approaches (Shilpashree et al., 2022). Despite these benefits, succinylation of milk affects both the primary and secondary phases of enzymatic coagulation, which hindered the development of an ordered and firm gel network (Vidal et al., 1998; Lieske et al., 2000).

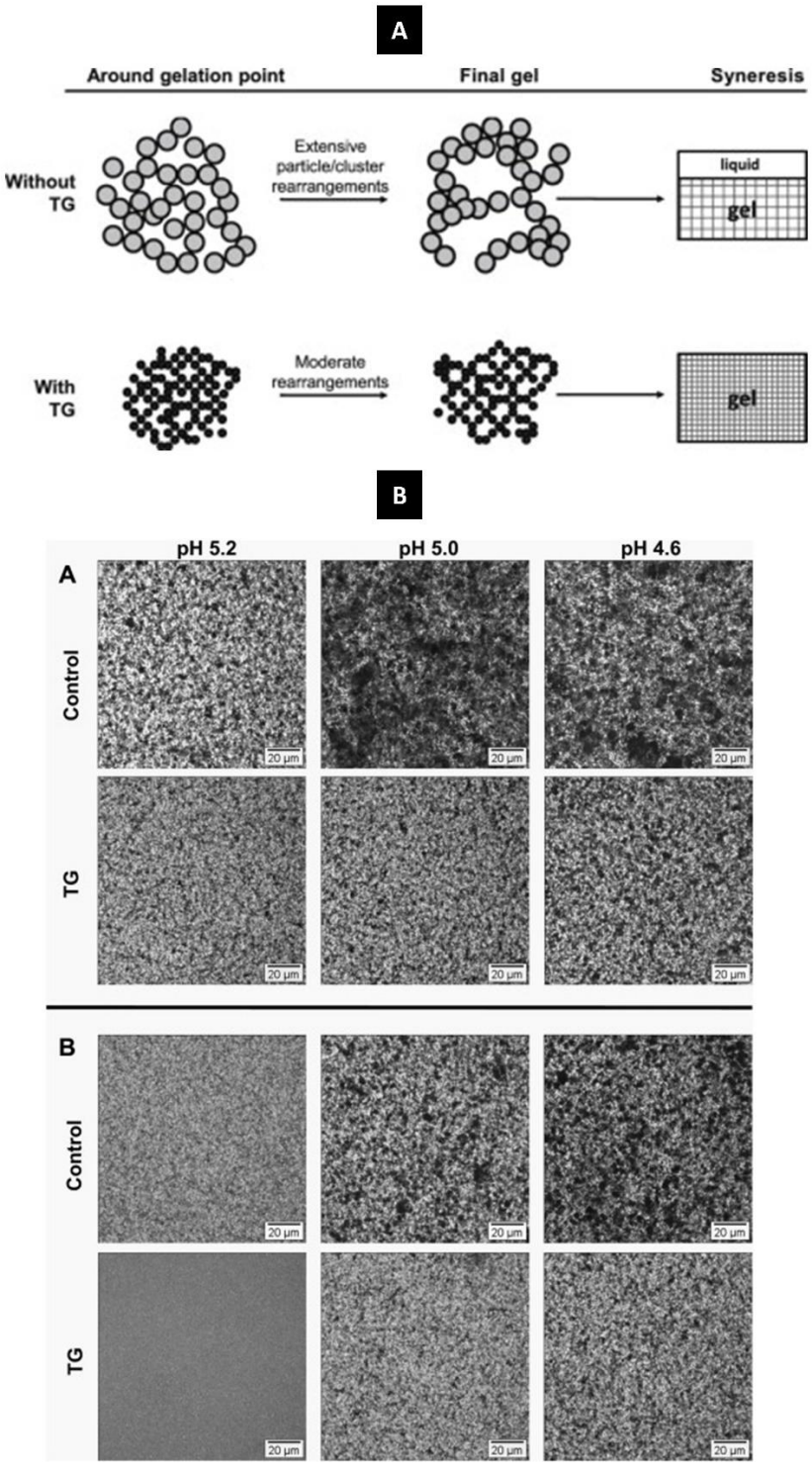

Figure 2.8 Schematic diagram of transglutaminase-induced gelation (A) and confocal images of gels formed by transglutaminase at 40°C and 20°C (B) (Ercili-Cura et al., 2013)

Glycation

Glycation is another way of protein modification where protein is conjugated with sugar (mostly reducing sugar) through the Maillard reaction, which results in an improvement in techno-functional properties such as solubility, heat stability, emulsification, foaming, and gelling (O'Mahony et al., 2017). Grigorovich et al. (2012) reported that sodium caseinate conjugated with maltodextrin with dextrose equivalent (DE) values of 2 or 10 (under dry heating conditions at an initial pH of 7, at 60 °C and 79% RH for 72 h) had improved solubility (~10–80% increase) across the pH range 3.5–5.0, compared with sodium caseinate alone. Zhu et al. (2010) conjugated whey protein isolates with dextran (440 kDa) by heating a solution of 10% whey protein isolates and 30% dextran, at an initial pH of 6.5 at 60 °C for 48 h. They saw higher denaturation temperature and improvements in thermal stability.

Other chemical methods

In another study, whey proteins were conjugated with low acyl gellan gum using the Maillard reaction which results in increased surface hydrophobicity and lower solubility. This modification improved interfacial activity, emulsifying activity (~6%), foaming capacity (~63.64%), and thickening (~24.67 fold) (Nooshkam and Varidi, 2020). ALKaisy and Al-Saadi (2019) studied the effect of acetylation, esterification, and deamidation on the functional properties of camel milk, where they found that as compared to control camel milk caseins, acylated and deamidated camel milk caseins solutions showed higher foaming, while esterification did not show any improvement in foaming properties. However, esterification and deamidation increased the emulsification ability (ALKaisy and Al-Saadi, 2019).

Altering pH is one of the promising methods to improve the functionality of milk protein solutions due to the pH-dependent behavior of milk proteins (casein and whey proteins). Vasbinder and de Kruif (2003) studied the interaction of casein and whey proteins at different

pH in a heated milk system (Figure 2.9B). They found that at a pH of more than 6.6, the interaction between casein and whey protein occurs on casein micelle surface, as well as in serum as whey protein-whey protein interaction (in form of soluble whey protein aggregates), leading to an inhomogeneous coating on casein micelles. However, below pH 6.6, the interaction between casein and whey protein occurs on the micelle surface, leading to a homogeneous coating of casein micelles. In a recent study, Qi et al. (2022) tried exploiting pH-dependent casein-whey protein interaction to alter the rheology and texture of yogurt. They found that reducing the denaturation of whey proteins by decreasing heating temperatures and increasing whey protein binding to casein micelles by decreasing heating pH can help in developing a desirably soft and smooth texture without excessive syneresis for high-protein yogurt. Similarly, Anema (2008) also documented (for acid gels prepared from skim milk heated at pH 6.2–7.1 at 80°C for 30 min) that the whey protein binding to micelles was decreased and the gel firmness was increased with increasing heating pH. So, alteration in heating temperature and pH before fermentation can produce acid gels with a desirable texture.

The approach used in the earlier study is a chemical method with a combination of physical methods (heat and pH). Therefore, combining physicochemical methods can modify protein structure and protein-protein interaction, and produce a protein with desired functionality. Recently, fibrillation is developed as a new method to improve the functionality of milk proteins such as whey proteins, and β-lactoglobulin. In the coming sections, the fibrillation process will be discussed in length.

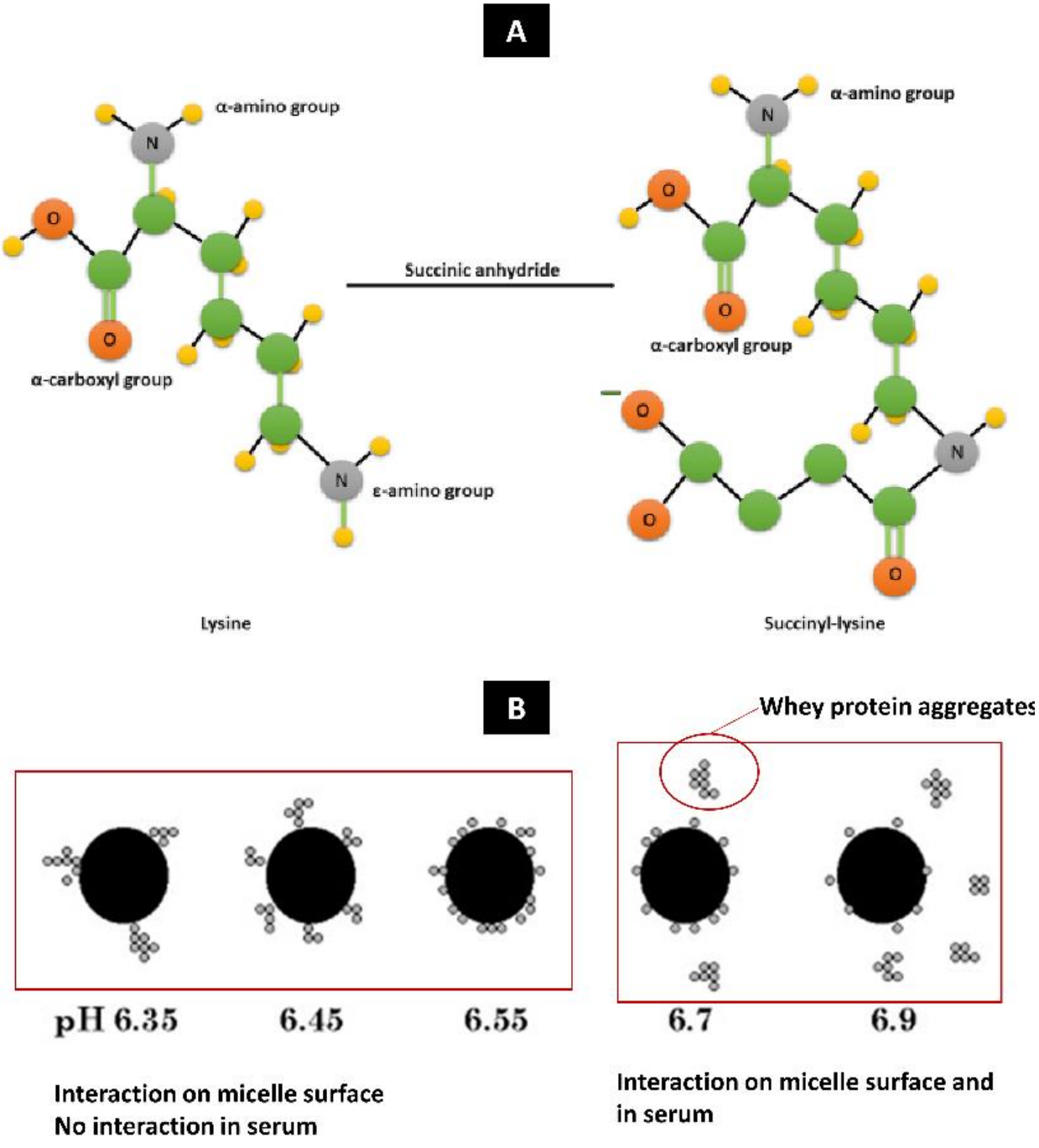

Figure 2.9 Succinylation of lysine (A), a schematic diagram of the interactions between casein micelles and whey proteins occurring in milk at different pH (6.35 to 6.9) at 80°C for 10 min (B). (Vasbinder and De Kruif, 2003; Agarwal et al., 2020).

Fibrillation process

Proteins and peptides have good structural stability; however, they can self-assemble to form protein fibrils through electrostatic forces, hydrophobic interactions, hydrogen bonds, and van der Waals forces under the different conditions of low pHs, low ionic strength, high temperature (80-120°C) and longtime (5-20 h) heating (Loveday et al., 2017; Meng et al., 2022). Protein fibrils are highly ordered and unbranched macromolecular structures with a diameter of a few nanometers to the length of even micrometer-sized (Wang et al., 2020). Due to the high stiffness, high aspect ratio (length: diameter), and collective ordering features of these amyloid fibrils (Cao and Mezzenga, 2019), fibrillation of protein is recognized as an emerging strategy to enhance protein functionality (Mohammadian and Madadlou, 2018; Jansens et al., 2019). Compared with natural food proteins, fibrillated food proteins are biocompatible as well as non-toxic and expand a variety of functional properties, such as thickening, gelling, emulsifying, foaming, antioxidant, and antimicrobial activities (Mohammadian and Madadlou, 2016ab; Meng et al., 2022). These enhanced functionalities are due to the fibrillar structure of protein fibrils.

Structure of fibrils

A structure-related aspect of protein fibrils can be best explained using two different ways, cross β- structure and polymorphism.

Cross β-structure of protein fibrils

The structure and molecular arrangement of protein fibrils mainly depend on the fibrillation conditions such as protein concentration, pH, temperature, salt concentration and type, agitation, seeding of fibril nuclei, and degree of unfolding, under which different variations in structure and morphology may be observed which can be seen in the transmission electron microscopic images and atomic force microscopic images reported in numbers of studies for

milk proteins (Bolder et al., 2006; Bolder et al., 2007a; Loveday et al., 2010; Pedersen et al., 2010; Loveday et al., 2012a). Despite having these structural variabilities, fibrils have distinct similarities at the atomistic length scale, which is a cross β-structure, in which β-sheets are arranged parallel to the fibril axis, while β-strands within the individual sheet are organized perpendicular to the main axis of fibrils (Cao and Mezzenga, 2019). Further, the inter-strand distance (measured with the X-ray diffraction pattern) is approximately 4.8 Å due to N-H.. O=C hydrogen bonds between two sequential peptide backbones, however, inter-sheet distance varies from 6 to 12 Å based on the size of the inner side groups of the cross β-structure and the packing arrangement of groups (Figure 2.10).

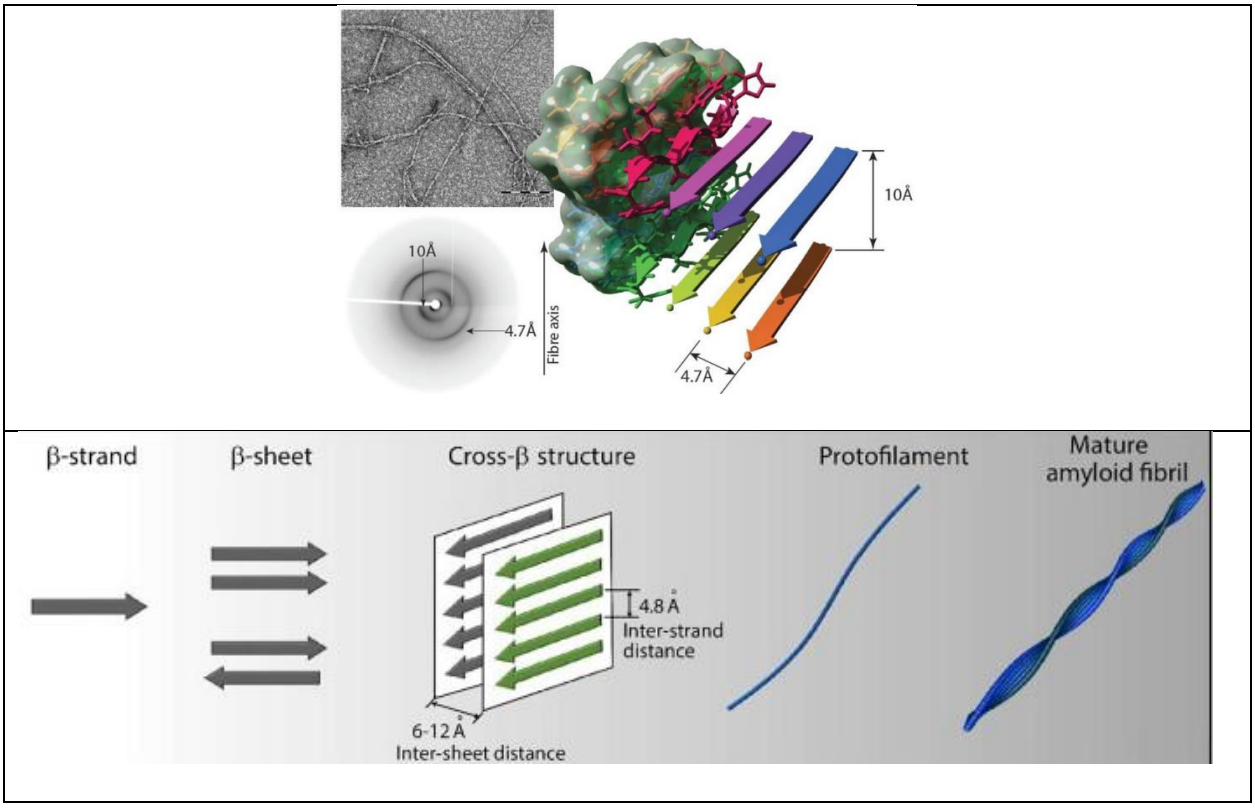

Figure 2.10 Amyloid fibrils β-sheets (antiparallel or parallel arrangement), assembled into a cross-β structure with an inter-strand distance of about 4.8 Å and an inter-sheet distance of 6~12Å. Then, the cross-β structure is extended into protofilaments, and then twisted into multistranded helical mature amyloid fibrils (Cao and Mezzenga, 2019; Jansens et al., 2019).

Polymorphism of protein fibrils

As discussed earlier, fibrils hold a common cross β-structure, however, fibrils made from the same polypeptides can arrange in a different structure. Therefore, the heterogeneity of fibrils is termed polymorphism of protein fibrils which is further divided into structural polymorphism and molecular polymorphism (Otzen, 2013, Adamcik and Mezzenga, 2018). Structural polymorphism comes from the assembly of protofilament, while molecular polymorphism occurs due to differences in the molecular arrangement within a single protofilament. Due to this polymorphism, there can be different morphology of mature fibrils such as twisted ribbon, helical ribbon, nanotube, and crystal polymorphs (Adamcik and Mezzenga, 2018, Cao and Mezzenga, 2019)

Self-assembly behavior and protein fibrillation

Self-assembly of protein is a process of spontaneous formation of ordered structure from a disordered system due to external conditions. Self-assembly is considered a controlled ordered transformation from natural proteins under specific processing conditions such as temperature, ionic strength, pH, and agitation. Self-assembly can occur between proteins or with other molecules such as polysaccharides, phenolic compounds, etc. This self-assembly can transform protein into fractal clusters, flexible chains, and fibrils (Karbasi et al., 2020). Recently, many food-derived globular proteins such as whey proteins, soy proteins, and egg proteins were proved to self-assemble into fibrils through van der Waals force, hydrophobic force, and electrostatic force. The reason for the protein fibril self-assembly behavior is inter- or intra-molecular interactions and coordination effects (Tomadoni et al., 2020). As per the latest studies, the hydrophobic groups inside the protein can be exposed under proper external conditions to

increase the opportunities for contact with protein molecules and facilitate fibrillation (Khalesi, 2021; Meng et al., 2022).

Mechanism of protein fibril formation

There are various mechanism and model have been reported so far for protein fibril formation, however, the nucleated conformation conversion model is widely accepted and contain three stages of fibril formation that includes the initial lag phase, growth phase, and maturity phase (Jansens et al., 2019). The lag phase is the start of the fibril formation phase which includes slow spontaneous nucleation for fibril formation. This phase is slower but primary nucleation is needed for fibril growth. The following phase is the growth phase, where the protein unfolding, conversion of protein, and peptide formation are higher and these converted protein helps to grow the fibril nuclei and produce protofilaments. These protofilaments extend continuously and are converted into mature fibrils, which is known as the fibril maturity phase (Šarić et al., 2016). Extending the fibrillation condition further can break the fibrils and form fibrillar aggregate (Rathod and Amamcharla, 2020). This protein monomer model suggests that protein monomers form fibrillar protein aggregates after denaturation and activation (Bolder et al., 2007b). Whereas some studies have suggested that the peptides formed after proteolysis are essential components of nanofibrils, rather than intact protein monomers, so polypeptide model was proposed which received wide attention (Akkermans et al., 2008a). In intact protein, hydrophobic groups are buried due to the globular structure, therefore, opening the complex protein structure, exposing the functional groups, and breaking big peptide chains to smaller sizes is required to assemble the proteins into fibrils. However, recent studies have shown that both protein monomers, as well as peptides, are the main components of protein fibrils (Wei et al., 2020). Further studies added that secondary nucleation is also one of the

mechanisms of protein fibrillation which is based on adding oligomers to the surface of the primary homogeneous nuclei, formed by the existing polymerization. The protein monomers attach to the surface of the nuclei and begin to continuously elongate to form mature protein fibrils (Yang et al., 2022). It is worth noting that the external mechanical shearing force in this model is particularly important, mainly because fibril disintegration is one of the important indicators in the secondary nucleation process (Bolder et al., 2007a; Cao et al., 2020). Considering all recent findings, in process of fibrils formation, whole protein is unfolded/opened, hydrolyzed to peptides, and converted to monomers under different processing conditions. Monomer and small peptide can serve as nuclei and the other monomer and peptide attached to nuclei and elongate as fibrils (Figure 2.11). The rate of elongation or fibril formation is dependent on how fast the monomer or peptide reaches the nuclei's surface for elongation, which shows the importance of agitation during the process (Bolder et al., 2007a). Deposition of protein monomer and/or peptide forms a long fibril that is converted to mature fibril over a period of time under control assembling of protein monomers/peptide. Uncontrolled assembly of peptides leads to the production of aggregates rather than ordered fibrils (Figure 2.11).

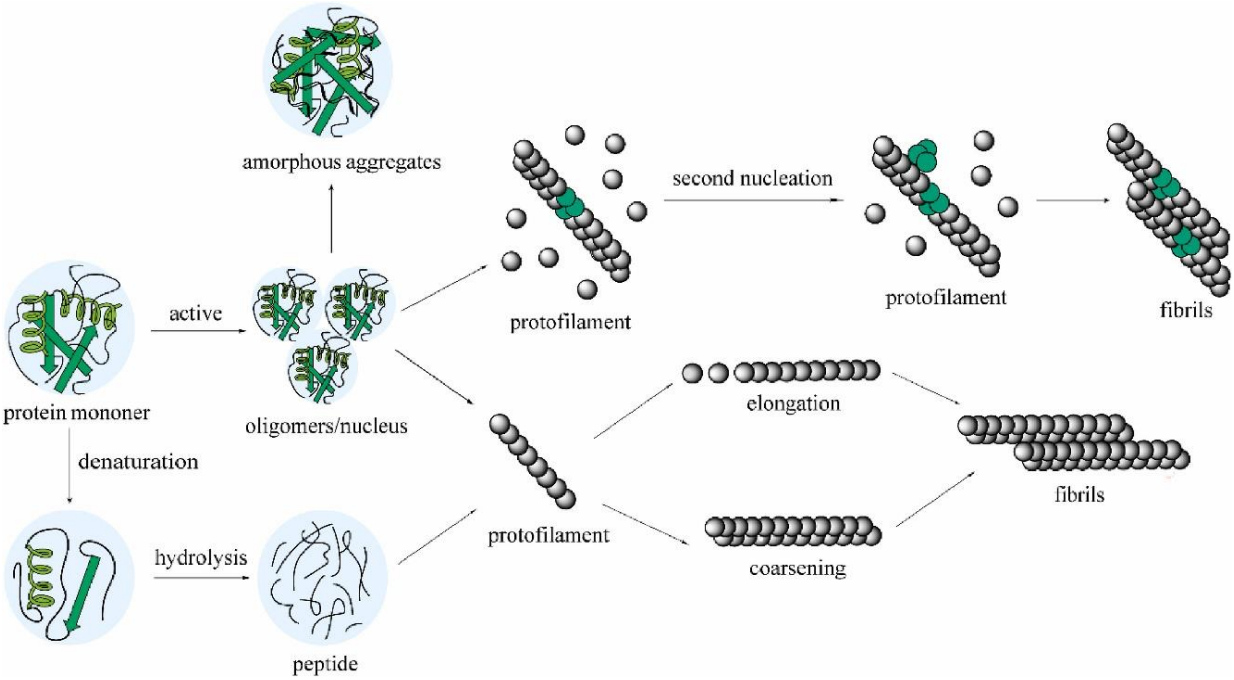

Figure 2.11. Schematic diagram of the fibril formation mechanism of protein fibril (Meng et al., 2022).

Method of protein fibril formation

Numbers of food proteins were tried for fibrillation using different fibrillation techniques which vary mainly in terms of different protein concentrations, pH, temperature, time, and salts. The fibrillation method for milk proteins is listed in Table 2.1.

Table 2.1 Method of fibrillation of dairy proteins

Type of proteins	Source of proteins	Method of fibrillation	Reference
Whey proteins	Whey protein concentrates and isolates	~2 % WPI/WPC at pH 2, 80-120°C for 5-20 h (Most common)	Akkermans et al., 2008b; Loveday et al., 2012ab; Oboroceanu et al., 2014; Mantovani et al., 2018; Zhang et al., 2021
	Whey protein isolates	2 % WPI at pH 2, Heated at 80°C for 24 h with stirring at 200 rpm with the addition of seed fibrils. Seed fibrils were prepared by heating 2% WPI at pH 2 at 80°C for 10h	Bolder et al., 2007ab
	Whey protein isolate	Step 1: Hydrolysis of 4% WPI at 55°C (pH 7.7) for 5 h with Corolase N (Enzyme substrate ratio 1:100) Step 2: pH 2, heating at 85 °C for 5 h at a constant stirring speed (~100 rpm)	Mohammadian and Madadlou, 2016a
	Whey protein isolate	5% (Wt/Wt) WPI solution, pH 2, heated to 110°C in a hydrothermal reaction kettle in an oven for 4 h	Yang et al., 2022
	Whey protein isolate	3% WPI with soybean lecithin (0.05% w/v) at pH 2, heated at 80 °C for 20 h under mild stirring	Mantovani et al., 2016
	Whey protein concentrates	Step 1: Hydrolysis of 7.9% (Wt/Vol) WPC using trypsin, protease A, and protease M at pH 6.7 and pepsin at pH 2 for 30 min with 0.1-0.3% degree of hydrolysis Step 2: Adjusted to 3% protein and pH 2 then Heating at 90°C for 10 h	Gao et al., 2013
β-lactoglobulin	bovine β-lactoglobulin (Sigma-Aldrich)	80~120 °C, pH 2, low salt content	Akkermans et al., 2008a; Loveday et al., 2010; Loveday et al., 2011; Loveday et al., 2012c; Loveday et al., 2017
	bovine β-lactoglobulin (Sigma-Aldrich)	Step 1: hydrolyzed by AspN Endo proteinase at pH 8 and 37 °C; Step 2: adjusting pH to 2	Akkermans et al., 2008c

	bovine β-lactoglobulin (Sigma-Aldrich)	4% β-lactoglobulin, stirring with a magnetic stirrer (250-474 rpm) and heating at 80°C for 24 h at pH-2	Sharma et al., 2014
	bovine β-lactoglobulin (Sigma-Aldrich)	Microwave (Power 4 W) and heating at 80°C for 2-16 h low pH	Hettiarachchi et al., 2012; Zhang et al., 2020
	bovine β-lactoglobulin (Sigma-Aldrich)	Addition of metal (Cu2+, Fe3+) at different concentration then heating at pH-2 (Cu2+ promote fibrillation- Fe3+ hinder fibrillation)	Zappone et al., 2013; Guzzi et al., 2015
	Lyophilized β-lactoglobulin AB (Sigma Chemical Co)	50:50 alcohol (trifluoroethanol, ethanol, methanol, propane-2-ol), water mixture (10 mM phosphate buffer, pH 2 or 7) at 20°C	Gosal et al., 2002; Gosal et al., 2004.
αS_2casein	Purified α_{S2} casein using cation-exchange chromatography	37-50 °C, pH 6.5-7 (Presence of α_{S1} casein inhibits fibril formation of α_{S2} casein)	Thorn et al., 2008
κ-casein	κ-casein (Sigma Chemical Co)	37 °C, pH 7 under physiological condition 20 mM DTT, 37 °C, pH 7 1% κ-casein at pH 2, heated at 90°C for 48 h	Thorn et al., 2005; Koudelka et al., 2012 Pan and Zhong, 2015
β-casein	β-casein (Sigma Chemical Co)	1% β-casein at pH 2, heated at 90°C for 48 h	Pan and Zhong, 2015
Bovine serum albumin	Bovine serum albumin (Sigma Chemical Co)	Heating to 60~90 °C for 10 h, pH 2~3, 0~0.3 M NaCl	Veerman et al., 2003a; Sagis et al., 2004.
	Bovine serum albumin (BioShop)	3 mg/mL in 20 mM HEPES (4-(2-hydroxyethyl)-1-piperazineethanesulfonic acid) (pH 7.8) Probe sonication (20 kHz-30 W, 5-80 cycles at 25°C (Probe sonicator (W 225R) with a standard tapered microtip attached to a 1/2″ disruptor horn)	Stathopulos et al., 2004
Ovalbumin	Pure ovalbumin powder	2-7%, pH 2, 0-50 mM NaCl Heating at 80~90 °C for 1 h,	Veerman et al., 2003b; Sagis et al., 2004; Lara et al., 2012

Whey proteins

Reported studies suggest that fibrillation of whey proteins (beta-lactoglobulin) is done mostly by heating whey protein solution (~2% Wt/Wt) having pH ~2 at 80-120°C for 5-20 h (Akkermans et al., 2008b; Loveday et al., 2012ab; Oboroceanu et al., 2014; Mantovani et al., 2018; Zhang et al., 2021). These processing parameters are most aligned with the mechanism of fibril formation. Loveday et al. (2010) reported that denaturation of β-lactoglobulin starts at 70°C, however for the fibrillation process, controlled denaturation of protein is required. Denaturation unfolds and opens the protein structure, that way, the protein chain is exposed to the external environment. Another important processing step is the reduction of pH to ~2 which is far below the isoelectric point of whey proteins. A reduction in pH will change the charge distribution of functional groups of the protein-peptide chain and further change the native globular structure of whey proteins (Damodaran, 1997). Therefore, a combination of heat and pH change opens the globular structure and changes the charge distribution. Further, heating at low pH leads to the breakdown of proteins into hydrolysate which are building blocks for fibril formation. Akkermans et al. (2008a) have prepared fibril by reducing the pH to pH-2 and heating it at 85°C for 20 h. With gel electrophoresis results, they found that fibrils of β-lactoglobulin were not from intact β-lactoglobulin. For fibrillation, β-lactoglobulin was hydrolyzed into peptides with a molecular weight of 2kDa and 8kDa and then assembled into fibrils. Further, they added that these peptides were obtained due to cleavage of the bonds between aspartic acid residues and any other amino acid or due to the total removal of aspartic acid residues. In another experiment, fibrillation of native whey protein and whey protein isolate (Bolder et al., 2007b) was performed by varying the protein concentration (0.5-5% Wt/Wt) and heating time (0-34 h), keeping pH-2 and heating temperature (80°C) constant. They found that fibrillation of whey

protein increased with protein concentration (>3% Wt/Wt) and heating time which was supported by a sudden increase in the fibril formation in samples with more than 3% protein. The study showed 5% fibril formation for samples with less than 3% protein (Wt/Wt) and 45% fibril formation for samples with more than 5% protein (Wt/Wt). However, gelling of protein solution was experienced when proteins were increased beyond 3%. These experiments were performed in the rested condition in a glass tube without movement of protein solution which allows protein and fibrils to convert the solution into a gel, therefore the effect of mechanical stirring to move liquid, and seeding of already formed fibrils was also studied (Bolder et al., 200a). Results showed a positive effect of stirring on fibril formation, as the rate of fibril formation was faster under stirring conditions. Recalling the mechanism of fibril formation, the continuous stirring of protein solution provides protein hydrolysate and monomer to the nuclei, which accelerate the growth and elongation of fibrils. Unlike stirring, nuclei in the rested solution will form fibrils from the available hydrolysate and monomer, which deplete over time and do not replenish due to the non-movement of the protein solution. However, due to stirring, hydrolysate and monomers are available to nuclei to form elongated fibrils. Therefore, the inclusion of stirring as a processing step for fibrillation was seen in the fibrillation of many proteins, and improvement in fibrillation was confirmed using research techniques such as transmission electron microscopy, atomic force microscopy, and thioflavin T fluorescence value (Pan and Zhong, 2015; Ng et al., 2016; Meng et al., 2022; Wang et al., 2022). In another attempt, seeding of already formed fibrils to the protein solution as nuclei was studied, however, seeding did not show any significant effect on fibril formation (Bolder et al., 2007a).

The fibrillization stopped after continued heating, therefore the duration of heating along with the temperature of heating is also important as heating temperature also affects the

fibrillation process. Hence, the varied temperature range of 70°C to 120°C was studied with a view of fibrillation. They found that higher temperature reduced the fibrillation time but continued heating at higher temperature resulted in a reduction in fibrils that was confirmed with the thioflavin T fluorescence test and transmission electron microscopy. Further, the fibrils formed at a higher temperature (100°C-120 °C) were shorter than the fibrils formed at 80°C (Loveday et al., 2012c). In another study, ionic concentration, and pH of fibrillation were varied for the fibrillation of β-lactoglobulin keeping fibrillation temperature constant at 80°C (Loveday et al., 2010). Faster growth of fibril at lower pH 1.6 than in other pH ranges were seen. Further, the addition of salt also accelerated the formation of the fibril and produced more of a curly worm-like structure. Montovani et al. (2016) used soy lecithin to see the effect on fibrillation, whereas soy lecithin did not show any significant effect on fibrillation, but the presence of soy lecithin helped to retain the shape of the fibrils during pH change from low pH to neutral pH.

Casein

αS_2 casein: For fibrillation, αS_2 casein was incubated at neutral pH (6.5-7) and 37°C which resulted in ribbon-like fibrils, around 12 nm in diameter that seldom formed loops (Thorn et al., 2008). It was observed that fibrillation of αS_2-casein was inhibited by another casein fraction, αS_1-casein, while inhibition from β-casein was less. While Thorn et al. (2005) reported inhibition of fibril formation of κ-casein due to the presence of α and β- casein. Pan and Zhong (2015) studied the fibrillation of all casein fractions. They lowered the pH of casein samples to pH-2 using 1.0 M HCl and then heated it at 90°C for 48 h in a glycerol bath with continuous stirring at 300 rpm with a magnetic stirrer. They observed fibrillation for β and κ-Casein not for α- casein. Further from the rheological aspect, β-casein showed higher viscosity than κ-casein. κ-casein has methionine residue at positions 95 and 106 in the protein sequence. Therefore,

methionine on κ-casein was selectively oxidized to study the role of methionine in fibril formation (Koudelka et al., 2012). Oxidation of native κ-casein was done by dissolving 50 mg of κ-casein in 5 ml of 50 mM phosphate buffer (pH 7.4). 0.1 ml of hydrogen peroxide was added and stirred overnight at 4 °C. Oxidation of methionine increased the rate of fibril formation. Further, the oxidized κ-casein is less prone to inhibition due to β-casein. Hence, it was possible to prepare κ-casein fibril in the casein matrix. Studies shown above were conducted as native individual casein fraction or with another casein fraction, but for the application part, it needs to be studied in the environment of another milk component. Liu et al. (2016) studied the effect on κ-casein fibril formation when other milk components and crowding agents were present. They found no significant effect on calcium and lactose while Heparan sulfate and phosphatidylcholine from milk fat globule membrane interfere with fibril formation.

Most of the reported studies here were performed in the controlled condition in a small-scale laboratory set up, however, for the industrial food product application, these fibrillation conditions need to be further refined to produce fibrillated proteins on large scale. Along with fibrillation conditions, confirmation and characterization of fibrils during and after production is also necessary to standardize the fibrillation process for large-scale production. Therefore, in the coming section, techniques related to confirmation of fibrillation will be discussed.

Common methods for characterization of fibrils

During fibril formation, globular proteins with complex tertiary and quaternary structures are converted into long chain fibrillar forms during which they have structural rearrangements and redistribution of functional groups. The changes in the protein structure are not visible since fibrils are a few nanometers thick and a few microns long, therefore it is difficult to confirm

fibril formation from native protein and it is difficult to know the structural changes. Therefore, the researcher developed techniques to confirm fibril formation and study fibril structure.

Confirmation of fibrils formation

Dye binding method

Dye such as Thioflavin T and Congo red bind to the fibrillar structure and give fluorescence intensity based on their binding with fibrils. In both dyes, Thioflavin T is used by many researchers to confirm the fibrillation of whey proteins (Bolder et al., 2007c; Loveday et al., 2012ac; Farrokhi et al., 2019). The Representative Thioflavin T fluorescence graph is shown in Figure 2.12A. For the Thioflavin T fluorescence value, the sample along with Thioflavin T dye is exited at 440 nm and emission intensity at 482 nm was recorded as an arbitrary unit.

Visual Confirmation

Since fibrils have a size of nanometers, they were observed using transmission electron microscopy using negative stains such as uranyl acetate. Transmission electron microscopy gives an idea about the diameter and length of fibrils as well as it gives information about the morphology of fibrils such as straight, curly, entanglement buddling (Loveday et al., 2010, Loveday et al., 2012ac; Gao et al., 2013; Jiang et al., 2022). An image of the transmission electron microscope and transmission electron microscopic image of whey protein fibrils are shown in Figures 2.12 B and C. Similar to transmission electron microscopy, atomic force microscopy was also used to the size and morphology of fibrils by many researchers (Oboroceanu et al., 2014; Mohammadian and Madadlou, 2016b; Farrokhi et al., 2018; Wang et al., 2020). A representative atomic force microscopic image of whey protein fibril is shown in Figure 2.12D.

Gel electrophoresis

Akkermans et al. (2008a) reported that during fibril formation native protein gets hydrolyzed into 2-8 kDa peptides and rearranged into fibrils. Therefore, protein hydrolysis is also one of the indicators for fibril formation. Hence, researchers used sodium dodecyl sulfate-polyacrylamide gel electrophoresis (SDS-PAGE) to see the peptide formation (Bolder et al., 2007b; Mantovani et al., 2016). Images of gels can quantify (using open-source software such as ImageJ or Gel Doc) the amount of protein converted into fibrils by measuring the intensity of the native protein band. Due to the presence of reducing agent such as β-mercaptoethanol in the sample buffer, protein hydrolysate used in the fibril formation dissociate, and can be quantified using SDS-PAGE.

Change in the structure

As discussed earlier, fibrils have cross β-structure, therefore Fourier transform infrared spectroscopy (FTIR) (Oboroceanu et al., 2011) and circular dichroism spectroscopy (Dave et al., 2014) are mostly used for observing the changes in the secondary structure such changes in β-sheet, α-helix, β-turns. In FTIR, the amide-1 region (1700-1600 cm^{-1}) is observed for changes in secondary structure (Wang et al., 2020).

Change in solution viscosity

Upon fibrillation, an increase in solution viscosity or thickening of the solution is an indicator of fibrillation. This increase in viscosity is measured by a rheometer (cone and plate geometry, cup and bob geometry) using a shear ramp (Loveday et al., 2012abc).

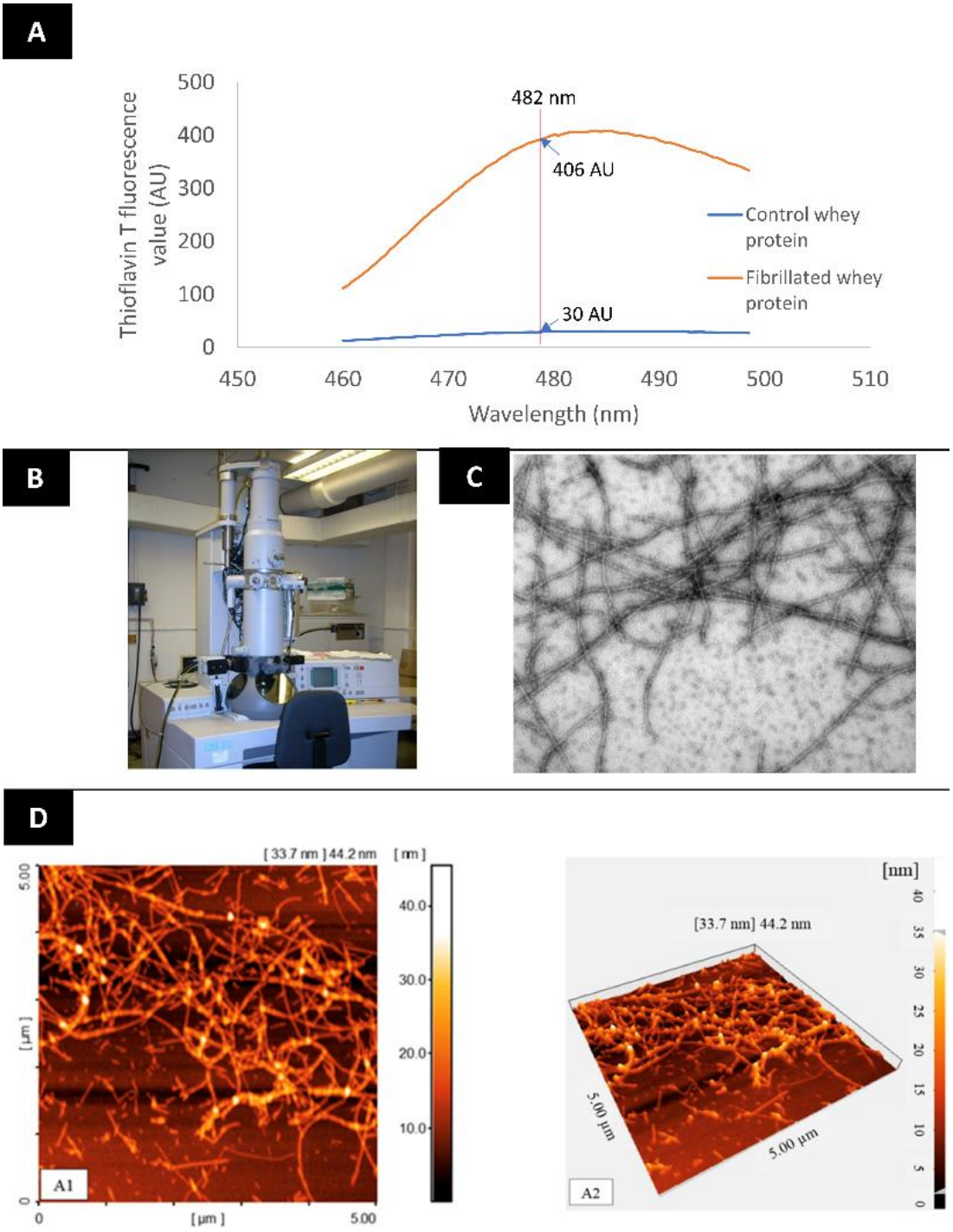

Figure 2.12 Representative Thioflavin T fluorescence graph (A), Transmission electron microscope (B), Transmission electron microscopic image of β-lactoglobulin fibrils (C), representative atomic force microscopic image of whey protein fibrils (D). (Farrokhi et al., 2018)

Functionality and potential application of protein fibrils

Fibrils are known to produce enhanced functionality such as gelling, thickening, emulsification, and foaming as the fibrillar structure has a higher aspect ratio. These functional properties will be discussed in further review.

Viscosity (Thickening) and gelation

As compared to the native globular protein solution, fibrillated protein solution gives a thick solution with higher viscosity (Loveday et al., 2017; Wang et al., 2020; Meng et al., 2022). Unlike globular proteins, fibrils are long string-like structures that entangle with each other. This long string-like fibril structure and entanglement of a fibrillar network, can entrap other substances like water, increase the viscosity and make a thick solution at lower protein content. Increased entanglement further increases the crosslinking and entraps more water, which results in the formation of hydrogels that are responsible for the higher water holding capacity of fibril solution (Farjami et al., 2016). Farjami and co-workers have prepared whey protein fibrils and then converted fibrils into different types of elastic gels by dialysis of different concentrations of calcium chloride solutions, forming gels with zero ash content when dialyzed in distilled water without calcium chloride. They further added that with an increase of calcium chloride, more soft viscoelastic gels with microporous structures and higher water holding capacity could be formed, however the fracture stress and storage modulus of the gel would gradually decrease. This is because the protein fibrils form hydrogen bonds with each other due to the presence of chlorides, and the strongly hydrated calcium ions interacted with the uncharged regions of the protein through site-specific interactions (Farjami et al., 2016). The complex of fibrils with other food constituents can also prepare improved gels. Chen et al. (2020) found a synergistic increase in

gel elasticity when fibrils and potato starch are combined at low pH but not at neutral pH where starch and protein were not compatible.

Bolder et al. (2006) produced whey protein isolates fibrils by heating whey protein isolates solution at pH 2 at 80°C for 10 h, followed by cooling and pH adjustment to pH 7. The pH-adjusted fibrils were gelled with the addition of $CaCl_2$ solution, where they found that β-lactoglobulin fibrils are forming a cold set gel and are responsible for gel strength. Similarly, Farjami et al. (2016) also prepared cold set gels of whey protein isolates fibrils with different concentrations of $CaCl_2$, and they suggested the potential use of these gels for the delivery of drugs sensitive to ions. Mohammadian and Madadlou (2016b) also prepared fibrils from whey protein isolates solution (6%wt/vol) by heating at 85°C for 5 h at pH 2 where they observed higher viscosity than control as well as heat denature whey protein isolates. Then, whey protein fibrils were adjusted to pH 7.5, and converted into gels by mixing with divalent salts ($CaCl_2$, $MnCl_2$, $ZnCl_2$), where gels formed using $ZnCl_2$ showed higher firmness and water holding capacity. Unlike whey protein fibrils, denatured whey protein solution did not form a stable gel with the same salts. This observation showed that fibrils can form stable and firmer gels than non-fibrillated proteins. The above observation suggests that fibrils have good thickening and gelling ability.

Emulsification and foaming properties

Protein fibrils due to their open fibrillar structure can be easily adsorbed on oil droplet surfaces and improve the stability of oil-in-water emulsions (Gao et al., 2017). As compared to unheated native protein monomers, β-lactoglobulin fibrils produced by heat treatment at pH 2.0 created stronger elastic interfaces with a higher rigidity (Jung et al., 2010). Humblet-Hua et al. (2013) also found that compared to native lysozyme- or ovalbumin proteins, fibrils derived from

lysozyme- or ovalbumin proteins could form viscoelastic films at oil-water interfaces with higher dilatational moduli. Peng et al. (2016) studied whey protein fibril emulsions and found that longer fibrils are more effective in stabilizing the emulsions and this stabilization of emulsion is not dependent on the oil volume fraction and temperature. Mantovani et al. (2018) have assessed the potential of whey protein fibrils as an emulsifier at varying pH, and they found that fibril-stabilized emulsions at pH 7 were more stable due to higher viscosity and faster migration of fibrils to interface compared to fibrils at lower pH. Cui et al. (2022) studied the development of pH-responsive emulsion, where they used whey protein isolates fibrils as an emulsifier and stabilizing agent. They found that emulsion prepared with whey protein isolate fibrils were more resistant to coalescence than emulsion formed by whey protein isolate, which could be due to the formation of a more robust interfacial coating around the oil droplets and a strong viscoelastic network in the aqueous phase. Liu et al. (2020) prepared a Pickering emulsion of nanofibrils from glycated whey protein, and they found that glycation enhances the fibril absorption and forms a thicker layer on oil droplets Also, glycated whey protein isolates fibrils to form bigger and more stable oil droplets than whey protein fibrils. Hence, glycation can improve fibrils' emulsification property. In addition, Mantovani et al. (2017) also studied in vitro digestion of oil-in-water emulsions stabilized by whey protein nanofibrils. They found that emulsions are stable under gastric conditions while they were destabilized only under simulated intestinal conditions. Similarly, Ng et al. (2017) prepared palm olein oil oil-in-water emulsion using whey protein fibrils-alginate complex, therefore fibril can be used to develop a potential alternative system to carry lipophilic bioactive compounds. These observations open the possibility of using the emulsification property of fibril to deliver lipophilic drugs into the intestine with released in the stomach.

Along with oil-water interface-based emulsification property, fibrils also showed improved foaming capacity by absorbing at the air-water interface and increasing the solution viscosity. Oboroceanu et al. (2014) found that foam produced by whey protein fibrils has improved foam capacity and foam stability compared to non-fibrillar whey proteins. Further, the foam of fibrillar whey proteins (less than 3% proteins) had comparable foam capacity and stability to egg white protein which is a traditional foaming ingredient in the food industry. Wan et al. (2016) studied the foaming capacity of soy protein fibrils and they found that the foaming behavior was dominated by the small peptides in the fibril system. As compared to pH 2, the fibril mixture at pH 5 and 7 provide much better foam stability and make stable foams even at 0.1 % protein concentration. The presence of fibril clusters and peptide aggregates at pH 5 and 7 may have contributed to foam stability. However, pure fibril showed poor foam stability may be due to an interface with highly pH-responsive adsorption and rheological behavior, and foamability. Zhao et al. (2020) produced a complex of β-lactoglobulin and κ-carrageenan using electrostatic complexion, which showed improved emulsifying and foaming properties.

Antioxidant Property

Mohammadian and Madadlou, (2016a) reported improvement in antioxidant activity upon fibrillation of whey protein isolate as well as whey protein hydrolysate. The complex of curcumin under acidic condition (pH 3.2) with whey protein fibrils improve the solubility of curcumin and improves the antioxidant properties of curcumin (Mohammadian et al., 2019). Wang et al. (2019) used the antioxidant potential of whey protein isolate fibrils and combined it with carvacrol, an antimicrobial agent along with glycerol to make an edible film to coat fresh-cut Cheddar cheese. This edible film has shown lower weight loss and better texture protection for fresh-cut Cheddar cheese. Therefore, this edible film can be used as an alternative to

commercial coatings. Similarly, Feng et al. (2019) prepared an edible coating for chilled beef using whey protein nanofibrils and titanium dioxide nanotubes, which improved lipid peroxidation and antioxidant activity, also retarded microbial growth lowered weight loss, and extend the shelf life of chilled beef. In another study, whey protein fibrils produced using microwave heating were used as an emulsifier and a carrier of lipophilic D- limonene, and emulsion showed an increase in antioxidant and antibacterial activity (Zhang et al., 2020). Guo et al. (2022) also used the antioxidant potential of whey protein isolate fibril in protecting probiotic cultures, as dry probiotic cultures are more prone to oxidative stress. They found improved protection and viability of probiotics when they used whey protein isolate fibrils, which extend the application of whey protein fibrils in the protection of probiotic cultures by reducing oxidative stress.

Carrier of compound or encapsulation

Whey protein fibrils can be used to encapsulate active ingredients as a β-carotene, where whey protein fibrils showed increased encapsulation efficiency from 76.55 to 92.11% compared to non-fibrillated whey proteins (Zhang et al., 2021). Whey protein nanofibrils can be used as a carrier to improve the aqueous solubility of curcumin at acidic conditions (pH 3.2) for expanding its applications in functional beverages and drinks. The complex of curcumin with whey protein fibrils increases the water solubility of curcumin (Mohammadian et al., 2019). Jiang et al. (2022) also used whey protein fibrils Pickering emulsions for the delivery of Nobiletin a lipophilic bioactive compound from citrus fruits. They found that whey protein isolate fibrils-stabilized Pickering emulsions showed excellent long-term stability and were also stable at various pHs (2.0–7.0) and ionic strengths (0–200 mM). Further, in vitro digestion study, this Pickering

emulsion showed an improved extent of lipolysis (from 36% to 49%) and improved bioaccessibility of nobiletin from 21.9% to 62.5%.

The findings on protein fibrils suggest that conversion of native globular proteins such as whey protein into fibrils is beneficial as they can give enhanced functionality in terms of gelation, thickening, emulsification, foaming, antioxidants, and as a carrier. However, there are technical constraints to utilizing the findings of these studies on actual dairy-food industry applications due to some key reasons. Most studies were done at low pH (~2) which is not food pH, also most of the fibrils were made in a controlled lab environment with a capacity of few mL. However, for industrial applications, the process of manufacture should be at least at a pilot scale for practical industrial applications. Therefore, the overall target of the current study was to reveal the answer to the above questions and customize the fibrillation process in such a way that it can be used in the industry to develop fibrillated milk protein ingredients with enhanced functionality. Hence, the current study was formed to develop fibrillated milk protein powders (milk protein concentrates and non-fat dried milk) by selective fibrillation of whey proteins. The study was divided into sub-objectives, first to make fibrillated milk protein concentrates, assessment of functionality, conversion of liquid fibrillated milk protein concentrate ingredients into powder, and assessment for retention of functionality and powder characteristics. As the manufacturing process of membrane-derived ingredients (milk whey proteins and micellar casein) is well established, membrane-derived ingredients are directly used to establish proof of the concept of fibrillation whey protein and subsequent processing. However, in the following study, fibrillated non-fat dried milk was developed using membrane processing and fibrillation at an industrial scale.

References

Adamcik, J., and R. Mezzenga, R. 2018. Amyloid polymorphism in the protein folding and aggregation energy landscape. Angew. Chem. Int. 57:8370-8382.

Agarwal, A., A. K. Pathera, R. Kaushik, N. Kumar, S. B. Dhull, S. Arora, and P. Chawla. 2020. Succinylation of milk proteins: Influence on micronutrient binding and functional indices. Trends in Food Sci. Technol. 97: 254-264.

Akkermans, C., A. J. Van der Goot, P. Venema, E. Van der Linden, and R. M. Boom 2008b. Properties of protein fibrils in whey protein isolate solutions: Microstructure, flow behaviour and gelation. Int. Dairy J. 18:1034-1042.

Akkermans, C., P. Venema, , A. J. van der Goot, R. M. Boom, and E. van der Linden 2008c. Enzyme-induced formation of β-lactoglobulin fibrils by AspN endoproteinase. Food Biophys, 3:390-394.

Akkermans, C., P. Venema, A. J. van der Goot, H. Gruppen, E. J. Bakx, R. M. Boom, and E. van der Linden. 2008a. Peptides are building blocks of heat-induced fibrillar protein aggregates of β-lactoglobulin formed at pH 2. Biomacromolecules, 9:1474-1479.

ALKaisy, Q. H., and J. M. Al-Saadi, 2019. Effect of Acylation, Esterification and Deamidation on Functional Properties of camel Milk caseins. Indian J Public Health, 10:1253.

Anema, S. G. 2008. Effect of milk solids concentration on the gels formed by the acidification of heated pH-adjusted skim milk. Food Chem. 108:110-118.

Anema, S. G. 2017. Storage stability and age gelation of reconstituted ultra-high temperature skim milk. Int. Dairy J. 75:56-67.

Anema, S. G., S. K. Lee, K. Schrader, andW. Buchheim, 1997. Effect of pH on the turbidity of pressure treated calcium caseinate suspensions and skim milk. Milchwissenschaft (Germany).

Arab, M., M. Yousefi, E. Khanniri, M. Azari, V. Ghasemzadeh-Mohammadi, and N. Mollakhalili-Meybodi, 2022. A comprehensive review on yogurt syneresis: effect of processing conditions and added additives. J. Food Sci. Technol. 1-10.

Arzeni, C., K. Martínez, P. Zema, A. Arias, O. E. Pérez, and A. M. R. Pilosof, 2012. Comparative study of high intensity ultrasound effects on food proteins functionality. J. Food Eng. 108:463-472.

Asaduzzaman, M., M. S. Mahomud, and M. E. Haque, 2021. Heat-Induced Interaction of Milk Proteins: Impact on Yoghurt Structure. Int. J. Food Sci. 2021.

Babu, K. S., and J. K. Amamcharla, 2022. Application of micro-and nano-bubbles in spray drying of milk protein concentrates. J. Dairy Sci., 105:3911-3925.

Barać, M., S. Stanojević, S. Jovanović, and M. Pešić, 2004. Soy protein modification: A review. Acta Period. Technol. 35:3-16.

Basak, S., and U. S. Annapure, 2022. Recent trends in the application of cold plasma for the modification of plant proteins-A review. Future Foods, 100119.

Bolder, S. G., H. Hendrickx, L. M. Sagis, and E. Van der Linden, 2006. Ca2+-induced cold-set gelation of whey protein isolate fibrils. Applied rheology, 16:258-264.

Bolder, S. G., L. M. Sagis, P. Venema, and E. van der Linden. 2007a. Effect of stirring and seeding on whey protein fibril formation. J. Agri. Food Chem. 55:5661-5669.

Bolder, S. G., L. M. Sagis, P. Venema, and E. van der Linden, 2007c. Thioflavin T and birefringence assays to determine the conversion of proteins into fibrils. Langmuir, 23:4144-4147.

Bolder, S. G., A. J. Vasbinder, L. M. Sagis, and E. van der Linden, 2007b. Heat-induced whey protein isolate fibrils: Conversion, hydrolysis, and disulphide bond formation. Int. Dairy J. 17:846-853.

Bönisch, M. P., M. Huss, K.Weitl, and U. Kulozik, 2007. Transglutaminase cross-linking of milk proteins and impact on yoghurt gel properties. Int. Dairy J. 17:1360-1371.

Borad, S. G., A. Kumar, and A. K. Singh, 2017. Effect of processing on nutritive values of milk protein. Crit. Rev. Food Sci. Nutr. 57:3690-3702.

Cao, Y., and R. Mezzenga, 2019. Food protein amyloid fibrils: Origin, structure, formation, characterization, applications and health implications. Adv. Colloid Interface Sci., 269, 334-356.

Cao, Y., X. Tang, M. Yuan, and W. Han, 2020. Computational studies of protein aggregation mediated by amyloid: fibril elongation and secondary nucleation. Prog. Mol. Biol. Transl. Sci. 170:461-504.

Carter, B. G., N. Cheng, R. Kapoor, G. H. Meletharayil, and M. A. Drake, 2021. Invited review: Microfiltration-derived casein and whey proteins from milk. J. Dairy Sci. 104:2465-2479.

Chan, S. K., and T. S. Lim, 2019. Bioengineering of microbial transglutaminase for biomedical applications. Appl. Microbiol. Biotechnol. 103:2973-2984.

Chandrapala, J., G. J. O. Martin, B. Zisu, S. E.Kentish, and M. Ashokkumar. 2012. The effect of ultrasound on casein micelle integrity. J. Dairy Sci. 95:6882-6890.

Charoensuk, D., R. G. Brannan, W. Chanasattru, and W. Chaiyasit, 2018. Physicochemical and emulsifying properties of mung bean protein isolate as influenced by succinylation. Int. J. Food Prop. 21:1633-1645.

Chen, D., F. Fang, E. Federici, O. Campanella, and O. G. Jones, 2020. Rheology, microstructure and phase behavior of potato starch-protein fibril mixed gel. Carbohydr. Polym. 239:116247.

Chobert, J. M., C. Bertrand-Harb, and M. G. Nicolas, 1988. Solubility and emulsifying properties of caseins and whey proteins modified enzymically by trypsin. J. Agri. Food Chem. 36:883-892.

Cui, F., D. J. McClements, X. Liu, F. Liu, and T. Ngai. 2022. Development of pH-responsive emulsions stabilized by whey protein fibrils. Food Hydrocol. 122:107067.

Dairy Reporter 2020. The growing importance of clean labels in functional dairy. https://www.dairyreporter.com/Article/2020/07/10/The-growing-importance-of-clean-label-in-functional-dairy?utm_source=copyright&utm_medium=OnSite&utm_campaign=copyright Accessed on 10/25/2022

Damodaran, S. 1997. Food proteins: An overview. Pages 1–24 in Food Proteins and Their Applications. 1st ed. S. Damodaran and A. Paraf, ed. Marcel Dekker, New York, NY.

Darewicz, M., J. Dziuba, and M. Dziuba, 2006. Functional properties and biological activities of bovine casein proteins and peptides. Polish J. Food Nutr. Sci., 15:79.

Datta, N., and H. C. Deeth. 1999. High pressure processing of milk and dairy products. Aust. J. Dairy Technol. 54:41-48.

Dave, A. C., S. M. Loveday, S. G. Anema, T. S. Loo, G. E. Norris, G. B. Jameson, and H. Singh. 2013. β-Lactoglobulin self-assembly: Structural changes in early stages and disulfide bonding in fibrils. J. Agri. Food Chem. 61:7817-7828.

Donato, L., and F. Guyomarc'h. 2009. Formation and properties of the whey protein/$\kappa $-casein complexes in heated skim milk–A review. Dairy Science and Technol. 89:3-29.

Ercili-Cura, D., M. Lille, D. Legland, S. Gaucel, K. Poutanen, R. Partanen, and R. Lantto. 2013. Structural mechanisms leading to improved water retention in acid milk gels by use of transglutaminase. Food Hydrocol. 30:419-427.

Færgemand, M., J. Otte, and K. B. Qvist. 1998. Emulsifying properties of milk proteins cross-linked with microbial transglutaminase. Int. Dairy J. 8:715-723.

Farjami, T., A. Madadlou, and M. Labbafi, 2016. Modulating the textural characteristics of whey protein nanofibril gels with different concentrations of calcium chloride. J. Dairy Res. 83:109-114.

Farrokhi, F., F. Badii, M. R. Ehsani, and M. Hashemi. 2019. Functional and thermal properties of nanofibrillated whey protein isolate as functions of denaturation temperature and solution pH. Colloids and Surf. A: Physicochemical and Engineering Aspects, 583:124002.

Farrokhi, F., M. R. Ehsani, F. Badii, and M. Hashemi, 2018. Structural and thermal properties of nanofibrillated whey protein isolate in the glassy state. LWT, 95:274-281.

Feng, Z., L. Li, Q. Wang, G. Wu, C. Liu, B. Jiang, and J. Xu, 2019. Effect of antioxidant and antimicrobial coating based on whey protein nanofibrils with TiO2 nanotubes on the quality and shelf life of chilled meat. Int. J. Mol. Sci. 20:1184.

Fox, P. F., T. Uniacke-Lowe, P. L. H. McSweeney, and J. A. O'Mahony, 2015a. Salts of milk. In Dairy chemistry and biochemistry (pp. 241-270). Springer, Cham.

Fox, P. F., T. Uniacke-Lowe, P. L. H. McSweeney, and J. A. O'Mahony. 2015b. Milk proteins. In Dairy chemistry and biochemistry (pp. 145-239). Springer, Cham.

Ganesan, A. R., U. Tiwari, P. N. Ezhilarasi, and G. Rajauria, 2021. Application of cold plasma on food matrices: A review on current and future prospects. J. Food Process. Preserv. 45:e15070.

Gao, Y. Z., H. H. Xu, T. T. Ju, and X. H. Zhao. 2013. The effect of limited proteolysis by different proteases on the formation of whey protein fibrils. J. Dairy Sci. 96:7383-7392.

Gao, Z., J. Zhao, Y. Huang, X. Yao, K. Zhang, Y. Fang, K.Nishinari, G. O. Phillips, F. Jiang, and H. Yang, 2017. Edible Pickering emulsion stabilized by protein fibrils. Part 1: Effects of pH and fibrils concentration. LWT-Food Sci. Technol. 76: 1-8.

Gaspar, A. L. C., and S. P. de Góes-Favoni. 2015. Action of microbial transglutaminase (MTGase) in the modification of food proteins: A review. Food Chem. 171:315-322.

Gharibzahedi, S. M. T., and I. S. Chronakis, I. S. 2018. Crosslinking of milk proteins by microbial transglutaminase: Utilization in functional yogurt products. Food Chem. 245: 620-632.

Gharibzahedi, S. M. T., M. Koubaa, F. J. Barba, R. Greiner, S. George, and S. Roohinejad. 2018. Recent advances in the application of microbial transglutaminase crosslinking in cheese and ice cream products: A review. Int. J. Biol. Macromol. 107:2364-2374.

Gosal, W. S., A. H. Clark, and S. B. Ross-Murphy. 2004. Fibrillar β-lactoglobulin gels: Part 1. Fibril formation and structure. Biomacromolecules, 5:2408-2419.

Gosal, W. S., A. H. Clark, P. D. Pudney, and S. B. Ross-Murphy. 2002. Novel amyloid fibrillar networks derived from a globular protein: β-lactoglobulin. Langmuir, 18:7174-7181.

Gregersen, S. B., L. Wiking, K. B. Bertelsen, J. Tangsanthatkun, B. Pedersen, K. R. Poulsen, U. Andersen, and M. Hammershøj. 2019. Viscosity reduction in concentrated protein solutions by hydrodynamic cavitation. Int. Dairy J. 97: 1-4.

Grigorovich, N. V., D. V. Moiseenko, A. S. Antipova, M. S. Anokhina, L. E. Belyakova, Y. N. Polikarpov, N. Korica, M. G. Semenova, and Baranov, B. A. 2012. Structural and thermodynamic features of covalent conjugates of sodium caseinate with maltodextrins underlying their functionality. Food Funct. 3:283-289.

Gunasekaran, S., and O. Solar. 2012. Heat-induced casein-whey protein interactions. *Food proteins and peptides. Chemistry, functionality, interactions, and commercialization*, 199-228.

Guo, Q., T. Li, C. Yuan, L. Liang, M. G. Gänzle, and M. Zhao, 2022. Effects of protein fibrillation and antioxidants on probiotic survival during ambient storage. Food Chem. 389:133117.

Guzzi, R., B. Rizzuti, C. Labate, B. Zappone, and M. P. De Santo. 2015. Ferric ions inhibit the amyloid fibrillation of β-lactoglobulin at high temperature. Biomacromolecules, 16:1794-1801.

Hammam, A. R., S. L. Beckman, and L. E. Metzger. 2022. Production and storage stability of concentrated micellar casein. J. Dairy Sci. 105:1084-1098.

Haque, Z. U. 1993. Influence of milk peptides in determining the functionality of milk proteins: a review. J. Dairy Sci. 76:311-320.

Harte, F. M., M. C. Martinez, and M. S. Mohan. 2019. U.S. Patent No. 10,390,543. Washington, DC: U.S. Patent and Trademark Office.

Hettiarachchi, C. A., M. Corzo-Martínez, M. S. Mohan, and F. M. Harte. 2018. Enhanced foaming and emulsifying properties of high-pressure-jet-processed skim milk. Int. Dairy J. 87:60-66.

Hettiarachchi, C. A., L. D. Melton, J. A. Gerrard, and S. M. Loveday. 2012. Formation of β-lactoglobulin nanofibrils by microwave heating gives a peptide composition different from conventional heating. Biomacromolecules, 13:2868-2880.

Humblet-Hua, N. P. K., E. van der Linden, and L. M. Sagis. 2013. Surface rheological properties of liquid–liquid interfaces stabilized by protein fibrillar aggregates and protein–polysaccharide complexes. Soft Matter, 9:2154-2165.

Huppertz, T. 2016. Heat stability of milk. In *Advanced dairy chemistry* (pp. 179-196). Springer, New York, NY.

Jambrak, A. R., V. Lelas, T. J. Mason, G. Krešić, and M. Badanjak. 2009. Physical properties of ultrasound treated soy proteins. J. Food Eng. 93:386-393.

Jansens, K. J., I. Rombouts, C. Grootaert, K. Brijs, J. Van Camp, P. Van der Meeren, F. Rousseau, J. Schymkowitz, and Delcour. 2019. Rational design of amyloid-like fibrillary structures for tailoring food protein techno-functionality and their potential health implications. Compr. Rev. Food Sci, 18:84-105.

Jiang, F., C. Chen, X. Wang, W. Huang, W. Jin, and Q. Huang. 2022. Effect of Fibril Entanglement on Pickering Emulsions Stabilized by Whey Protein Fibrils for Nobiletin Delivery. Foods, 11:1626.

Johnston, D. E., B. A. Austin, and R. J. Murphy. 1993. Properties of acid-set gels prepared from high pressure treated skim milk. Milchwissenschaft, 48:206-209.

Ju, Z. Y., J. Otte, J. S. Madsen, and K. B. Qvist. 1995. Effects of limited proteolysis on gelation and gel properties of whey protein isolate. J. Dairy Sci. 78:2119-2128.

Jung, J. M., D. Z. Gunes, and R. Mezzenga. 2010. Interfacial activity and interfacial shear rheology of native β-lactoglobulin monomers and their heat-induced fibers. Langmuir, 26:15366-15375.

Karbasi, M., A. Sánchez-Ferrer, J. Adamcik, G. Askari, A. Madadlou, and R. Mezzenga. 2021. Covalent β-lactoglobulin-maltodextrin amyloid fibril conjugate prepared by the Maillard reaction. Food Chem. 342:128388.

Kethireddipalli, P., A. R. Hill, and D. G. Dalgleish, 2010. Protein interactions in heat-treated milk and effect on rennet coagulation. Int. Dairy J. 20:838-843.

Khalesi, H., C. Sun, J. He, W. Lu, and Y. Fang. 2021. The role of amyloid fibrils in the modification of whey protein isolate gels with the form of stranded and particulate microstructures. Food Res. Int. 140:109856.

Kieliszek, M., and A. Misiewicz. 2014. Microbial transglutaminase and its application in the food industry. A review. Folia Microbiol. 59:241-250.

Kneifel, W., and A. Seiler. 1993. Water-holding properties of milk protein products-A review. Food Struct. 12:3.

Koudelka, T., F. C. Dehle, I. F. Musgrave, P. Hoffmann, and J. A. Carver. 2012. Methionine oxidation enhances κ-casein amyloid fibril formation. J. Agri. Food Chem. 60:4144-4155.

Kuehler, C. A., and C. M. Stine. 1974. Effect of enzymatic hydrolysis on some functional properties of whey protein. J. Food Sci. 39:379-382.

Lajnaf, R., H. Attia, and M. A. Ayadi. 2021. Promising Food Ingredients: Milk Proteins. In *Bovine Science-Challenges and Advances*. IntechOpen.

Lara, C., S. Gourdin-Bertin, J. Adamcik, S. Bolisetty, and R. Mezzenga. 2012. Self-assembly of ovalbumin into amyloid and non-amyloid fibrils. Biomacromolecules, 13:4213-4221.

Lee, S. K., S. G. Anema, K. Schrader, and W. Buchheim. 1996. Effect of high hydrostatic pressure on Ca-caseinate systems. Milchwissenschaft (Germany).

Li, K., M. W. Woo, H. Patel, L. Metzger, and C. Selomulya. (2018). Improvement of rheological and functional properties of milk protein concentrate by hydrodynamic cavitation. J. Food Eng. 221:106-113.

Lieske, B., G. Konrad, and W. Faber. 2000. Effects of succinylation on the renneting properties of raw milk. Milchwissenschaft, 55:71-74.

Lindmark Månsson, H. 2008. Fatty acids in bovine milk fat. Food Nutr. Res. 52:1821.

Liu, G., W. Li, X. Qin, and Q. Zhong. 2020. Pickering emulsions stabilized by amphiphilic anisotropic nanofibrils of glycated whey proteins. Food Hydrocol. 101:105503.

Loveday, S. M., S. G. Anema, H. Singh. 2017. β-Lactoglobulin nanofibrils: The long and the short of it. Int. Dairy J. 67:35-45.

Loveday, S. M., J. Su, M. A. Rao, S. G. Anema, and H. Singh. 2012a. Whey protein nanofibrils: The environment–morphology–functionality relationship in lyophilization, rehydration, and seeding. J. Agric. Food Chem. 60:5229-5236.

Loveday, S. M., J. Su, M. A. Rao, S. G. Anema, and H. Singh. 2012b. Whey protein nanofibrils: Kinetic, rheological and morphological effects of group IA and IIA cations. Int. Dairy J. 26:133-140.

Loveday, S. M., X. L. Wang, M. A. Rao, S. G. Anema, and H. Singh. 2012c. β-Lactoglobulin nanofibrils: Effect of temperature on fibril formation kinetics, fibril morphology and the rheological properties of fibril dispersions. Food Hydrocol. 27: 242-249.

Loveday, S. M., X. L. Wang, M. A. Rao, S. G. Anema, and H. Singh, H. 2011. Effect of pH, NaCl, CaCl2 and temperature on self-assembly of β-lactoglobulin into nanofibrils: A central composite design study. J. Agric. Food Chem. 59:8467-8474.

Loveday, S. M., X. L. Wang, M. A. Rao, S. G. Anema, L. K. Creamer, and H. Singh. 2010. Tuning the properties of β-lactoglobulin nanofibrils with pH, NaCl and CaCl2. Int. Dairy J. 20:571-579.

Lu, N., J. Wang, Z. Chen, X. Zhang, C. Chen, and S. Wang. 2021. The effect of adding phospholipids before homogenization on the properties of milk fat globules. LWT, 146:111659.

Lucey, J. A., D. J. Wilbanks, and D. S. Horne. 2022. Impact of heat treatment of milk on acid gelation. Int. Dairy J. 125:105222.

Madadlou, A., M. E. Mousavi, Z. Emam-Djomeh, M. Ehsani, and D. Sheehan. 2009. Comparison of pH-dependent sonodisruption of re-assembled casein micelles by 35 and 130 kHz ultrasounds. J. Food Eng. 95:505-509.

Mahmoud, M. I. (1994). Physicochemical and functional properties of protein hydrosylates in nutritional products. Food Technol. 48:89-95.

Mantovani, R. A., G. de Figueiredo Furtado, F. M. Netto, R. L. Cunha. 2018. Assessing the potential of whey protein fibril as emulsifier. J. Food Eng. 223:99-108.

Mantovani, R. A., J. Fattori, M. Michelon, and R. L. Cunha. 2016. Formation and pH-stability of whey protein fibrils in the presence of lecithin. Food Hydrocol. 60:288-298.

Mantovani, R. A., A. C. Pinheiro, A. A. Vicente, and R. L. Cunha. 2017. In vitro digestion of oil-in-water emulsions stabilized by whey protein nanofibrils. Food Res. Int. 99:790-798.

Meng, Y., Z. Wei, and C. Xue. 2022. Protein fibrils from different food sources: A review of fibrillation conditions, properties, applications and research trends. Trends Food Sci. Technol. 121:59-75.

Mietsch, F., J. Fehér, and A. Halasz. 1989. Investigation of functional properties of partially hydrolyzed proteins. Food/Nahrung, 33:9-15.

Mirmoghtadaie, L., S. S. Aliabadi, and S. M. Hosseini. 2016. Recent approaches in physical modification of protein functionality. Food Chem. 199:619-627.

Mohammadian, M., and A. Madadlou. 2016a. Characterization of fibrillated antioxidant whey protein hydrolysate and comparison with fibrillated protein solution. Food Hydrocol. 52:221-230.

Mohammadian, M., and A. Madadlou. 2016b. Cold-set hydrogels made of whey protein nanofibrils with different divalent cations. Int. J. Biol. Macromol. 89:499-506.

Mohammadian, M., and A. Madadlou. 2018. Technological functionality and biological properties of food protein nanofibrils formed by heating at acidic condition. Trends Food Sci. Technol. 75:115-128.

Mohammadian, M., M. Salami, S. Momen, F. Alavi, Z. Emam-Djomeh, and A. A. Moosavi-Movahedi. 2019. Enhancing the aqueous solubility of curcumin at acidic condition through the complexation with whey protein nanofibrils. Food Hydrocol. 87:902-914.

Mohan, M. S., R. Ye, and F. Harte. 2016. Initial study on high pressure jet processing using a modified waterjet on physicochemical and rennet coagulation properties of pasteurized skim milk. Int. Dairy J. 55:52-58.

Munialo, C. D., A. H. Martin, E. Van Der Linden, and H. H. De Jongh. 2014. Fibril formation from pea protein and subsequent gel formation. J. Agric. Food Chem. 62:2418-2427.

Mutilangi, W. A. M., D. Panyam, and A. Kilara. 1996. Functional properties of hydrolysates from proteolysis of heat-denatured whey protein isolate. J. Food Sci. 61:270-275.

Ng, S. K., K. L. Nyam, O. M. Lai, I. A. Nehdi, G. H. Chong, and C. P. Tan. 2017. Development of a palm olein oil-in-water (o/w) emulsion stabilized by a whey protein isolate nanofibrils-alginate complex. LWT-Food Sci.Technol. 82:311-317.

Ng, S. K., K. L. Nyam, I. A. Nehdi, G. H. Chong, O. M. Lai, and C. P. Tan. 2016. Impact of stirring speed on β-lactoglobulin fibril formation. Food Sci. Biotechnol. 25:15-21.

Nicolai, T., and C. Chassenieux. 2021. Heat-induced gelation of casein micelles. Food Hydrocol. 118:106755.

Nooshkam, M., and M. Varidi, M. 2020. Whey protein isolate-low acyl gellan gum Maillard-based conjugates with tailored technological functionality and antioxidant activity. Int. Dairy J. 109:104783.

Oboroceanu, D., L. Wang, A. Kroes-Nijboer, A. Brodkorb, P. Venema, E. Magner, and M. A. Auty. 2011. The effect of high pressure microfluidization on the structure and length distribution of whey protein fibrils. Int. Dairy J. 21:823-830.

Oboroceanu, D., L. Wang, E. Magner, and M. A. Auty. 2014. Fibrillization of whey proteins improves foaming capacity and foam stability at low protein concentrations. J. Food Eng. 121:102-111.

Oestergaard, B. 2016. Hydrodynamic cavitation helps dairy powder processing. SPX Flow Technology, USA.

O'Mahony, J. A., K. P. Drapala, E. M. Mulcahy, and D. M. Mulvihill. 2017. Controlled glycation of milk proteins and peptides: Functional properties. Int. Dairy J. 67:16-34.

Otzen, D. E. (Ed.). 2013. Amyloid fibrils and prefibrillar aggregates: molecular and biological properties. John Wiley & Sons. (Weinheim: Wiley-VCH).

Pan, K., and Q. Zhong. 2015. Amyloid-like fibrils formed from intrinsically disordered caseins: physicochemical and nanomechanical properties. Soft Matter 11:5898-5904.

Pankaj, S. K., C. Bueno-Ferrer, N. N. Misra, L. O'Neill, B. K. Tiwari, P. Bourke, and P. Cullen. 2014. Physicochemical characterization of plasma-treated sodium caseinate film. Food Res. Int. 66:438-444.

Panyam, D., and A. Kilara. 1996. Enhancing the functionality of food proteins by enzymatic modification. Trends Food Sci. Technol. 7:120-125.

Patel, H. A., and T. Huppertz. 2014. Effects of high-pressure processing on structure and interactions of milk proteins. In Milk proteins (pp. 243-267). Academic Press.

Pathania, S., Q. T. Ho, S. A. Hogan, N. McCarthy, and J. T. Tobin. 2018. Applications of hydrodynamic cavitation for instant rehydration of high protein milk powders. J. Food Eng. 225:18-25.

Pedersen, J. S., C. B. Andersen, and D. E. Otzen. 2010. Amyloid structure–one but not the same: the many levels of fibrillar polymorphism. FEBS J. 277:4591-4601.

Peng, J., J. R. Simon, P. Venema, and E. Van Der Linden. 2016. Protein fibrils induce emulsion stabilization. Langmuir, 32:2164-2174.

Power, O. M., V. Maidannyk, D. J. McSweeney, M. A. Fenelon, J. A. O'Mahony, and N. A. McCarthy. 2020. Water sorption and hydration properties of high protein milk powders are influenced by enzymatic crosslinking and calcium chelation. Powder Technol. 364:680-688.

Puppo, M. C., F. Speroni, N. Chapleau, M. de Lamballerie, M. C. Añón, and M. Anton. 2005. Effect of high-pressure treatment on emulsifying properties of soybean proteins. Food Hydrocol., 19:289-296.

Qi, X., D. Liu, J. Yuan, J. M. Regenstein, and P. Zhou. 2022. Effects of heating temperatures and pH of skim milk fortified with milk protein concentrate on the texture and microstructure of high-protein yoghurts. Int. Dairy J. 131:105395.

Rathod, G., and J. Amamcharla. 2020. Effect of Stirring and Static Heating on Fibrilization of Milk Whey Protein: A Processing Approach. Kansas Agricultural Experiment Station Research Reports, 7:2.

Romeih, E., and G. Walker. 2017. Recent advances on microbial transglutaminase and dairy application. Trends Food Sci. Technol. 62:133-140.

Sagis, L. M., C. Veerman, and E. van der Linden. 2004. Mesoscopic properties of semiflexible amyloid fibrils. Langmuir 20:924-927.

Salunke, P., C. Marella, and L. E. Metzger. 2021. Microfiltration and ultrafiltration process to produce micellar casein and milk protein concentrates with 80% crude protein content: Partitioning of various protein fractions and constituents. Dairy 2:367-384.

Šarić, A., T. C. Michaels, A. Zaccone, T. P. Knowles, and D. Frenkel. 2016. Kinetics of spontaneous filament nucleation via oligomers: Insights from theory and simulation. J. Chem. Phys. 145:211926.

Schrader, K., W. Buchheim, and C. V. Morr. 1997. High pressure effects on the colloidal calcium phosphate and the structural integrity of micellar casein in milk. Part 1. High pressure dissolution of colloidal calcium phosphate in heated milk systems. Food/Nahrung, 41:133-138.

Segat, A., N. N. Misra, P. J. Cullen, and N. Innocente. 2015. Atmospheric pressure cold plasma (ACP) treatment of whey protein isolate model solution. Innov Food Sci Emerg Technol, 29:247-254.

Sfakianakis, P., and C. Tzia. 2014. Conventional and innovative processing of milk for yogurt manufacture; development of texture and flavor: a review. Foods, 3:176-193.

Shanmugam, A., J. Chandrapala, and M. Ashokkumar. 2012. The effect of ultrasound on the physical and functional properties of skim milk. Innov Food Sci Emerg Technol. 16:251-258.

Sharma, R. K., K. Furusawa, A. Fukui, and N. Sasaki. 2014. Effects of a flow field on amyloid fibrillogenesis in a β-lactoglobulin solution. Int. J. Biol. Macromol. 70:490-497.

Sharma, S. (2020). Cold plasma treatment of dairy proteins in relation to functionality enhancement. Trends Food Sci Technol. 102:30-36.

Sharma, S., and R. K. Singh. 2022. Effect of atmospheric pressure cold plasma treatment time and composition of feed gas on properties of skim milk. LWT 154:112747.

Shen, Y., S. Hong, G. Singh, K. Koppel, and Y. Li. 2022. Improving functional properties of pea protein through “green” modifications using enzymes and polysaccharides. Food Chem. 385:132687.

Shilpashree, B. G., S. Arora, P. Chawla, and V. Sharma. 2022. A comparison of zinc interactions with succinylated milk protein concentrate and sodium caseinate. LWT, 157:113116.

Shilpashree, B. G., S. Arora, P. Chawla, and S. K. Tomar. 2015. Effect of succinylation on physicochemical and functional properties of milk protein concentrate. Food Res. Int. 72:223-230.

Shilpashree, B. G., S. Arora, P. Chawla, R. Vakkalagadda, and A. Sharma. 2015. Succinylation of sodium caseinate and its effect on physicochemical and functional properties of protein. LWT-Food Sci. Technol. 64:1270-1277.

Shimizu, M., S. W. Lee, S. Kaminogawa, and K. Yamauchi. 1984. Emulsifying properties of an N-terminal peptide obtained from the peptic hydrolyzate of αs1-casein. J. Food Science, 49:1117-1120.

Shokri, S., F. Javanmardi, M. Mohammadi, and A. M. Khaneghah. 2022. Effects of ultrasound on the techno-functional properties of milk proteins: A systematic review. Ultrason. Sonochem. 83:105938.

Silva, M., B. Zisu, and J. Chandrapala. 2020. Interfacial and emulsification properties of sono-emulsified grape seed oil emulsions stabilized with milk proteins. Food Chem. 309:125758.

Sim, S. Y., X. Y. Hua, and C. J. Henry. 2020. A novel approach to structure plant-based yogurts using high pressure processing. Foods 9:1126.

Soria, A. C., and M. Villamiel. 2010. Effect of ultrasound on the technological properties and bioactivity of food: a review. Trends Food Sci. Technol. 21:323-331.

Speroni, F., V. Beaumal, M. de Lamballerie, M. Anton, M. C. Añón, and M.C. Puppo. 2009. Gelation of soybean proteins induced by sequential high-pressure and thermal treatments. Food Hydrocol. 23:1433-1442.

SPX. 2022. SPX flow cavitator operating manual. https://www.spxflow.com/assets/original/APV-Mixers-Cavitator-456424-IOM-GB.pdf. Accessed on 08/09/2022

Stathopulos, P. B., G. A. Scholz, Y. M. Hwang, J. A. Rumfeldt, J. R. Lepock, and E. M. Meiering. 2004. Sonication of proteins causes formation of aggregates that resemble amyloid. Protein Sci. 13:3017-3027.

Surowsky, B., A. Fischer, O. Schlueter, and D. Knorr. 2013. Cold plasma effects on enzyme activity in a model food system. Innov Food Sci Emerg Technol. 19:146-152.

Tanaka, T., and K. Hatanaka. 1992. Application of hydrostatic pressure to yoghurt to prevent its after-acidification. Nippon Shokuhin Kogyo Gakkaishi, 39:173-177.

Thorn, D. C., H. Ecroyd, M. Sunde, S. Poon, and J. A. Carver. 2008. Amyloid fibril formation by bovine milk αs2-casein occurs under physiological conditions yet is prevented by its natural counterpart, αs1-casein. Biochem. 47:3926-3936.

Thorn, D. C., S. Meehan, M. Sunde, A. Rekas, S. L. Gras, C. E. MacPhee, C. M. Dobson, M. R. Wilson, and J. A. Carver. 2005. Amyloid fibril formation by bovine milk κ-casein and its inhibition by the molecular chaperones αS-and β-casein. Biochem. 44:17027-17036.

Tomadoni, B., C. Capello, G. A. Valencia, and T. J. Gutiérrez. 2020. Self-assembled proteins for food applications: A review. Trends Food Sci. Technol. 101:1-16.

Tran, M., R. Roberts, T. L. Felix, and F. M. Harte. 2018. Effect of high-pressure-jet processing on the viscosity and foaming properties of pasteurized whole milk. J Dairy Sci. 101:3887-3899.

Van Camp, J., W. Messens, J. Clément, and A. Huyghebaert. 1997. Influence of pH and calcium chloride on the high-pressure-induced aggregation of a whey protein concentrate. J. Agric. Food Chem. 45:1600-1607.

Vargas, S. A., R. J. Delgado-Macuil, H. Ruiz-Espinosa, M. Rojas-López, and G. G. Amador-Espejo. 2021. High-intensity ultrasound pretreatment influence on whey protein isolate and its use on complex coacervation with kappa carrageenan: Evaluation of selected functional properties. Ultrason. Sonochem. 70:105340.

Vasbinder, A. J., and C. G. De Kruif. 2003. Casein–whey protein interactions in heated milk: the influence of pH. Int. Dairy J. 13:669-677.

Veerman, C., G. de Schiffart, L. M. Sagis, and E. van der Linden. 2003b. Irreversible self-assembly of ovalbumin into fibrils and the resulting network rheology. Int. J Biol. Macromol. 33:121-127.

Veerman, C., L. M. Sagis, J. Heck, and E. van der Linden. 2003a. Mesostructure of fibrillar bovine serum albumin gels. Int. J Biol. Macromol. 31:139-146.

Vidal, V., E. Gastaldi, E. Lefebvre-Cases, A. Lagaude, S. Marchesseau, B. T. de la Fuente, and J. L. Cuq. 1998. Effect of succinylation on the rennet coagulation of milk. J. Dairy Sci. 81:69-75.

Walstra, P., J. T. Wouters, and T. J. Geurts. 2005. Milk components. Pages 17–108 in Dairy Science and Technology. 2nd ed. CRC press, Boca Raton, FL.

Wan, Z., X. Yang, and L. M. Sagis. 2016. Contribution of long fibrils and peptides to surface and foaming behavior of soy protein fibril system. Langmuir, 32:8092-8101.

Wang, Q., H. Yu, B. Tian, B. Jiang, J. Xu, D. Li, Z. Feng and C. Liu. 2019. Novel edible coating with antioxidant and antimicrobial activities based on whey protein isolate nanofibrils and carvacrol and its application on fresh-cut cheese. Coatings, 9:583.

Wang, Y. R., Q. Yang, Y. N. Du, and H. Q. Chen. 2022. Evaluation of the impact of stirring on the formation, structural changes and rheological properties of ovalbumin fibrils. Food Hydrocol, 128:107615.

Wang, Y., Y. Shen, G. Qi, Y. Li, X. S. Sun, D. Qiu, and Y. Li. 2020. Formation and physicochemical properties of amyloid fibrils from soy protein. Int. J. Biol. Macromol. 149:609-616.

Wei, Z., Y. Chen, W. Wijaya, Y. Cheng, J. Xiao, and Q. Huang. 2020. Hydrogels assembled from ovotransferrin fibrils and xanthan gum as dihydromyricetin delivery vehicles. Food Funct, 11:1478-1488.

Wei, Z., J. Cheng, and Q. Huang. 2019. Food-grade Pickering emulsions stabilized by ovotransferrin fibrils. Food Hydrocol. 94:592-602.

Xia, W., H. Zhang, J. Chen, H. Hu, F. Rasulov, D. Bi, X. Houng and S. Pan. (2017). Formation of amyloid fibrils from soy protein hydrolysate: Effects of selective proteolysis on β-conglycinin. Food Res. Int. 100:268-276.

Yang, X., M. Xie, C. Guan, R. Guo, C. Ma, H. Xu, and M. Shao. 2022. Effect of CaCl2 on 2 heat-induced whey protein concentrate fibrillation pathways: Spontaneous and nuclear induction. J. Dairy Sci. 105:5573-5586.

Yang, Y., Q. Jiao, L. Wang, Y. Zhang, B. Jiang, D. Li, Z. Feng and C. Liu. 2022. Preparation and evaluation of a novel high internal phase Pickering emulsion based on whey protein isolate nanofibrils derived by hydrothermal method. Food Hydrocol. 123:107180.

Zappone, B., M. P. De Santo, C. Labate, B. Rizzuti, and R. Guzzi. 2013. Catalytic activity of copper ions in the amyloid fibrillation of β-lactoglobulin. Soft Matter. 9:2412-2419.

Zhang, C., Y. Fu, Z. Li, T. Li, Y. Shi, H. Xie, Y. Li, H. Su, and Z. Li. 2021. Application of whey protein isolate fibrils in encapsulation and protection of β-carotene. Food Chem. 346:128963.

Zhang, R., X. Pang, J. Lu, L. Liu, S. Zhang, and J. Lv. 2018. Effect of high intensity ultrasound pretreatment on functional and structural properties of micellar casein concentrates. Ultrason. Sonochem. 47:10-16.

Zhang, Y., S. Liang, J. Zhang, Y. Chi, B. Tian, L. Li, B. Jiang, D. Li, Z. Feng, and C. Liu. 2020. Preparation of whey protein isolate nanofibrils by microwave heating and its application as carriers of lipophilic bioactive substances. LWT 125:109213.

Zhao, M., J. Hu, H. Zhang, K. Nishinari, and Y. Fang. 2020. Electrostatic complexation of β-lactoglobulin aggregates with κ-carrageenan and the resulting emulsifying and foaming properties. J. Dairy Sci. 103:8709-8720.

Zhao, X., X. Fan, X. Shao, M. Cheng, C. Wang, H. Jiang, X. Zhang and J. Wang. 2022. Modifying the physicochemical properties, solubility and foaming capacity of milk proteins by ultrasound-assisted alkaline pH-shifting treatment. Ultrason. Sonochem. 88:106089.

Zhu, D. A. N., S. Damodaran, and J. A. Lucey. 2010. Physicochemical and emulsifying properties of whey protein isolate (WPI)− dextran conjugates produced in aqueous solution. J. Agric. Food Chem. 58:2988-2994.

Chapter 3 - Process development for a novel milk protein concentrate with whey proteins as fibrils[1]

Abstract

Milk protein concentrate (MPC) is a preferred ingredient to provide nutritional and functional benefits in various dairy and food products. Altering the protein configuration and protein-protein interactions in MPC can provide a novel functionality and may open doors for new applications. The fibrillation process converts the globular structure of whey proteins to fibrils and consequently increases viscosity and water-holding capacity compared with the native protein structure. The objective of the current work was to selectively convert the whey proteins in MPC as fibrils. For this purpose, a simulated control model MPC was prepared by combining solutions of micellar casein concentrate (MCC) and milk whey protein isolate (mWPI) to give casein and whey protein in an 80:20 ratio. The mWPI solution was converted to fibrils by heating at low pH, neutralized, and combined with MCC solution similar to control model MPC and termed "fibrillated model MPC." Thioflavin T fluorescence value, transmission electron microscopy, and gel electrophoresis confirmed the fibril formation and their survival after neutralization and mixing with MCC. Further, the fibrillated mWPI showed significantly higher viscosity and consistency coefficient than nonfibrillated mWPI. Similarly, fibrillated model MPC showed significantly higher viscosity and consistency coefficient compared with control model MPC. Hence, the fibrillated model MPC can be used as ingredient to increase viscosity. Heat

[1] Rathod, G., and J.K. Amamcharla. 2021. Process development for a novel milk protein concentrate with whey proteins as fibrils. J. Dairy Sci. 104:4094–4107.

coagulation time was found to be significantly higher for control model MPC compared with fibrillated model MPC.

Keywords: Whey protein fibrils, fibrillated model milk protein concentrate, viscosity

Introduction

Protein is a unique food component that contributes to the nutrition, taste, and texture of foods. Most food proteins are globular in form and are usually found in secondary, tertiary, and quaternary structures (Damodaran, 1997). During processing, proteins generally undergo structural changes including formation of flexible strands, long and short fibrils, aggregates, and nano-microparticles, depending on the processing conditions such as pH, temperature, ionic strength, and presence of other food constituents (Moayedzadeh et al., 2015). Conversion of globular food proteins into protein fibrils changes the native structure of proteins and opens up an avenue for new product formulation with enhanced functionality, texture, and surface properties. Therefore, researchers are working on the conversion of globular proteins into fibrils to enhance absorption and nutrition, reduce allergenicity, improve overall food structure, and develop new food analogs (Kroes-Nijboer et al., 2012a; Teodorowicz et al., 2017; Hu et al., 2019). Lassé et al. (2016) studied the digestibility and toxicity of fibrils derived from various plant and animal proteins, including whey proteins, and reported no potential health risks from amyloid-like whey protein fibrils in foods at concentrations up to 0.25 mg/ mL. Several researchers have reported the development of fibrils from various food proteins and protein blends to harness the benefits of fibrillar proteins (Mohammadian and Madadlou, 2018). Methods of fibril formation are well reported for plant proteins, such as soy (Xia et al., 2017), pea (Munialo et al., 2014), wheat (Ridgley et al., 2012), maize (An et al., 2016), and rice proteins (Zhang and Huang, 2014) and animal proteins, such as egg proteins (Lara et al., 2012). They

studied the effect of different processing conditions such as pH, processing temperature, ionic strength, and addition of additives such as lecithin (Mantovani et al., 2016) to develop protein fibrils. Milk proteins, including casein (Koudelka et al., 2012; Pan and Zhong, 2015) and whey proteins, were also extensively studied for fibril formation in the last 2 decades.

Milk proteins are composed of 2 principal proteins, caseins and whey proteins, and whey proteins are the most studied protein for fibril formation. The globular structure of whey proteins undergoes changes upon heating (>75°C) at lower pH. Upon heating at lower pH, whey proteins are hydrolyzed and rearrange themselves as fibrils (Kroes-Nijboer et al., 2012b). Most researchers used a combination of low pH (1.8–3) and temperature (75–120°C), and the combination of solution pH 2 and heating at 80°C for 20 h led to the formation of mature fibrils from whey protein isolate (WPI) and pure β-LG (Loveday et al., 2010, 2012a,b). Most researchers have worked on isolated protein fractions of whey proteins such as β-LG, α-LA, and BSA, among which they found β-LG is the most responsible for the formation of the fibril (Bolder et al., 2006, 2007b; Akkermans et al., 2008). Whey protein isolate is one of the concentrated sources of whey proteins, which is usually manufactured from cheese whey. Bolder et al. (2007b) studied fibrils formation from WPI, but there was no reported study on fibril formation of milk whey proteins (mWP). Unlike WPI, mWP isolate (mWPI) is produced by membrane separation; hence, it is a purer source of whey proteins and thereby, a pure source of fibrillated mWPI.

Fibrillation of proteins is known to improve functionality such as gelling, foaming, and emulsification (Oboroceanu et al., 2014; Zhang et al.,2014; Gao et al., 2017; Wang et al., 2020). Whey protein fibrils can physically entangle to form nanohydrogels at low protein concentrations (Ramos et al., 2017). Further, fibrillated WPI showed an increase in viscosity (Paximada et al.,

2016; Loveday et al., 2017) and water holding capacity (Farrokhi et al., 2019) compared with the native proteins at the same protein concentration. Due to increased viscosity and surface activity, fibrils can be used as a foam stabilizer by slowing foam drainage. Fibrils can be easily absorbed at the oil–water interface to form a stable emulsion (Kroes-Nijboer et al., 2012a). Veerman (2006) reported a higher viscosity in yogurt prepared from skim milk added with fibrillated whey proteins than the control yogurt manufactured with unmodified whey proteins. Hence, fibrillation can provide multipoint modifications, which make it the preferred choice for modification of MPC over other conventional methods. Mixing fibrillated mWPI with micellar casein in the same ratio in the milk system can give a mixture that resembles milk protein concentrate (MPC), which can be used as a gelling, foaming, and emulsifying agent. The developed functional ingredient may have potential to eliminate the need for synthetic non-dairy-based ingredients completely or partially. Hence, the present study was planned to convert mWPI into fibrils and mix with micellar casein to develop fibrillated model MPC.

Materials and methods

Experimental Approach

Two lots of mWPI [4.3% moisture, 91.6% true protein (87.6% whey protein and 12.4% casein), 1.4% lactose, and 2.1% ash] and one lot of micellar casein concentrate [MCC; 5.76% moisture, 85.5% true protein (7.6% whey protein and 92.4% casein)] were procured from a commercial supplier as powders. In phase 1 of the study, fibrillated mWPI was manufactured from reconstituted mWPI solutions, characterized in terms of chemical and physical properties, and compared with nonfibrillated mWPI solutions. Also, experiments were carried out to understand the effect of pH on the stability of fibrillated mWPI. In phase 2 of the study, a

simulated model MPC was prepared by mixing fibrillated mWPI with reconstituted MCC to achieve the same ratio of caseins to whey proteins as in milk. The fibrillated model MPC were also characterized in terms of chemical, physical, and functional properties and compared with control and nonfibrillated model MPC. A detailed experimental approach is provided in Figure 3.1. Chemicals used in the analysis were of analytical grade.

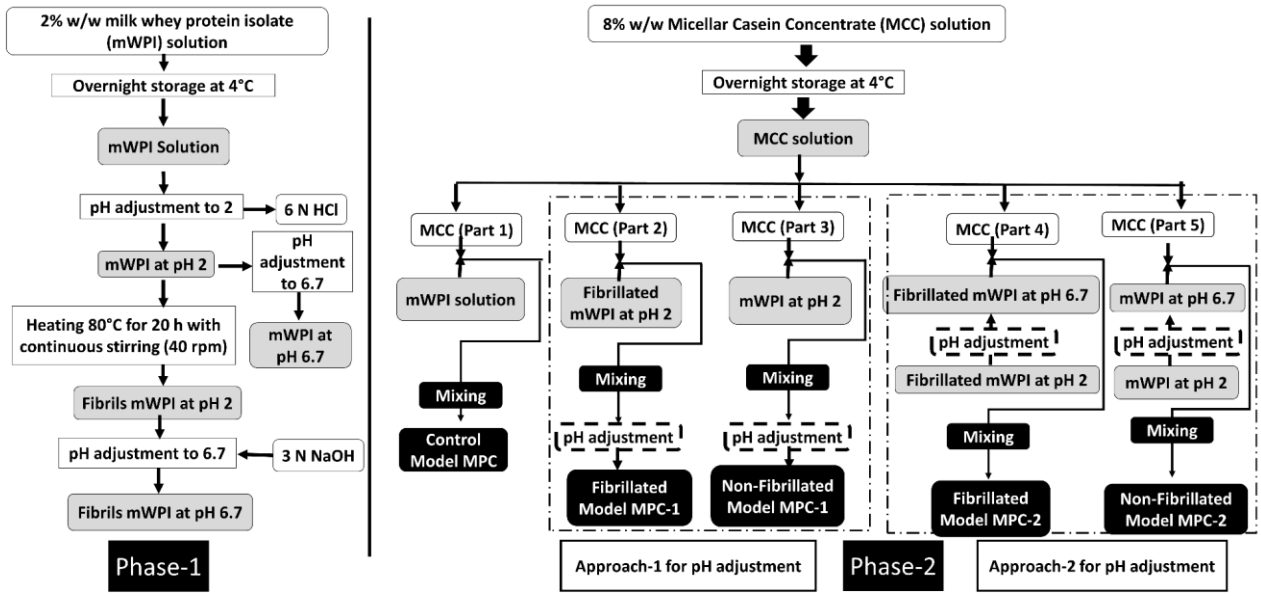

Figure 3.1 Process flow diagram of milk whey protein isolate (mWPI) fibrils and fibrillated model milk protein concentrate (MPC).

Phase-1. Fibrillation of mWPI

The mWPI powders were rehydrated to 2% (wt/ wt) solution on a protein basis with distilled water and stored overnight at 4°C to ensure complete hydration. The pH of mWPI solution was adjusted to 2 using 6 N HCl and stored overnight at 4°C. The pH-adjusted mWPI solutions were heated at 80°C for 20 h in a glass container using a temperature-controlled circulatory water bath (Cole Parmer, Vernon Hills, IL) under gentle continuous stirring (40 rpm)

using a magnetic stirrer. The glass container was sealed to ensure no moisture loss during heating. A thermocouple (RDXL4SD 4 Channel, Omega Engineering Inc., Norwalk, CT) was used to continuously monitor and record the temperature during the heating process. At the end of heating, the fibrillated mWPI solution was cooled to 4°C using an ice water bath and stored refrigerated until further analysis. To understand the effect of change in pH on the stability of fibrillated mWPI, the pH of the fibrillated mWPI solution was adjusted back to 6.7 using 3 N NaOH under gentle stirring. A representative sample was drawn from various stages including initial rehydrated mWPI solution, pH 2 adjusted mWPI solution, pH 6.7 adjusted mWPI solution, fibrillated mWPI solution at pH 2, and fibrillated mWPI solution at pH 6.7 to understand the stability, aggregation behavior, and functionality of mWPI fibrils. Fibrillated mWPI solution at pH 6.7 was stored overnight at refrigerated temperatures for further analysis and use

Confirmation of mWPI Fibrils

Thioflavin T (Th T) fluorescence value.

Thioflavin T (ThT) fluorescence value of samples was determined using the method described by Loveday et al., (2010). For the assay, a 48-μL sample was added to 4 mL of ThT fluorescence working solution; the mixture was vortexed for 15 s using a mini vortex mixer (Fisher Scientific, Waltham, MA) and held at room temperature for 1 min before measuring in spectrofluorometer (LS-55; Perkin Elmer, Waltham, MA). Excitation wavelength was fixed at 440 nm with a slit width of 10 nm, and excitation wavelength was scanned from 460 to 500 nm with a slit width of 5 nm. Fluorescence intensity recorded at 482 nm wavelength was taken as ThT fluorescence value. The ThT fluorescence value of the ThT working solution was taken as blank and subtracted from all the measurements. For each sample, the triplicate analysis was carried out and the scans were averaged to improve the signal-to-noise ratio.

Transmission electron microscopy.

Samples were prepared for transmission electron microscopy (TEM) by diluting the protein solutions to 0.05% (wt/wt) protein using deionized pH 2 water, where the pH of deionized water was adjusted with 6 N HCl and mounted on Formvar/carbon-coated 200-mesh copper grids (Electron Microscopy Sciences, Fort Washington, PA), as mentioned by Sun et al., (2008). Grids were viewed by TEM at 100 kV (CM100 TEM, FEI Company, Hillsboro, OR), and images were captured using a digital camera (model C8484, Hamamatsu, Bridgewater, NJ) and AMT software (Advanced Microscopy Techniques, Chazy, NY). The length and width of the mWPI fibrils were measured and analyzed using ImageJ software (ImageJ, National Institutes of Health, Bethesda, MD).

Gel electrophoresis.

Samples for gel electrophoresis were diluted to 0.5% protein content and vortexed. The diluted samples were analyzed with 3 different gel electrophoresis techniques such as native PAGE (Mantovani et al., 2017), nonreducing SDS-PAGE, and reducing SDS-PAGE (Mohammadian and Madadlou, 2016; Sanchez Alan et al., 2017) with some modification.

Characterization of mWPI fibrils

Rheology.

Continuous rotational flow data were collected at 20°C using a stress-strain-controlled rheometer (MCR-92 Anton Paar, Vernon Hills, IL) fitted with a 50-mm diameter stainless steel cone with 1° angle and 101-μm gap (Loveday et al., 2012b) at a varied shear rate from 0.01 s^{-1} to 200 s^{-1} at 20°C. Along with viscosity, the consistency coefficient and flow behavior index were also calculated using the power-law model:

$$\tau = K\dot{\Upsilon}^{\eta}$$

Where τ=shear stress

Ÿ=shear strain

K=consistency coefficient

η=flow behavior index

Electrical conductivity.

The conductivity of the samples was measured using a portable conductivity meter (Accumet, Fisher Scientific, Waltham, MA). The probe was dipped in the samples placed in plastic tubes at room temperature and kept until the conductivity meter was stabilized at one value.

Phase-2. Model MPC

In phase 2 of the study, model MPC was prepared by mixing equal proportions of MCC reconstituted to 8% protein and mWPI reconstituted to 2% protein using a magnetic stirrer (50 rpm). Consequently, the model MPC contained 5% protein and casein-to-whey protein ratio similar to MPC and served as control. Similarly, fibrillated model MPC was also prepared using a fibrillated mWPI solution in place of mWPI solution. Mixing of fibrillated mWPI (at pH 2) with reconstituted MCC (at pH 6.7) was carried out in 2 approaches. In approach 1, fibrillated mWPI (at pH 2) was mixed with reconstituted MCC (at pH 6.7) in equal proportions, and the pH of the final mixture was then adjusted to 6.7 using 3 N NaOH and termed “fibrillated model MPC-1.” In approach 2, the pH of the fibrillated mWPI (pH = 2) was adjusted to 6.7 using 3 N NaOH and subsequently mixed with the reconstituted MCC solution in equal proportions and

named as fibrillated model MPC-2. The details about the process are given in Figure 3.1. The next day, mWPI fibrils were mixed with MCC after pH adjustment and stored at 4°C and the analysis was completed within the next 2 to 3 d.

For comparison and better understanding of the effect of fibrillation and pH change on proteins, nonfibrillated model MPC-1 and nonfibrillated model MPC-2 were also prepared using a similar approach using nonfibrillated mWPI solutions and reconstituted MCC solutions. The samples were analyzed for ThT fluorescence value, TEM, gel electrophoresis, rheology, heat coagulation time, and color value. The whole experiment was replicated with 2 different lots of mWPI.

Confirmation of mWPI fibrils

Confirmation of mWPI fibrils in model MPC was done by Th T fluorescence value, TEM, and gel electrophoresis as described in phase-1.

Characterization of control and fibrillated model MPC for functional properties

Rheology of the model MPC were measured as described in the first part of the study.

Heat coagulation time.

Four milliliters of the sample were placed in heat-resistant screw-cap test tubes (8 mL, 17 mm × 63 mm; DWK Life Science, Millville, NJ). The test tubes were inserted on the stainless steel rack. The rack along with tubes was immersed in an oil bath (Narang Scientific Works Pvt. Ltd., New Delhi, India) maintained at 140°C and placed on the rocker. Heat coagulation time was noted as the time elapsed between dipping the samples in the hot oil bath and the onset of first visible clots/flakes. (Crowley et al., 2014; Meena et al., 2016).

Color.

The color analysis was performed by following the method described by Rathod and Kairam (2018). Approximately 15 to 20 mL of liquid samples was poured on a glass Petri plate and placed on a white platform. Then the samples were scanned using Mini Scan XE plus (Hunter Color Lab, Reston, VA) for L* (lightness), a* (red-green color), and b* (yellow-blue color) values. Total color was determined using following equation:

$$Total\ color = \sqrt{((L*)^2 + (a*)^2 + (b*)^2)}$$

Statistical Analysis

Statistical analysis was performed using Excel (Microsoft Corp., Redmond, WA), one-way ANOVA, and subsequent Duncan's multiple range test using SPSS for Windows version 20 (IBM Corp., Armonk, NY).

Results and discussion

Phase-1: Fibrillation of mWPI

Th T fluorescence value

Thioflavin T fluorescence values of control, nonfibrillated, and fibrillated mWPI solutions are shown in Table 3.1. The ThT fluorescence value of reconstituted mWPI solution (control) at pH 6.67 was 12.0 ± 1.5 arbitrary units (AU). A similar low ThT values were reported by Loveday et al. (2012a; 2012b) for solutions prepared from WPI and β-LG. Further, the reduction of pH of mWPI solution to 2 did not significantly ($P > 0.05$) influence the ThT fluorescence value and was found to be 16.6 ± 3.9 AU. On the other hand, heating (80°C for 20 h) of mWPI at pH 2 significantly ($P < 0.05$) increased the ThT fluorescence value to 355.4 ± 71.4 AU. Loveday et al. (2012b) also reported a significant increase in ThT fluorescence value

upon heating of β-LG at low pH. Thioflavin T is a fluorescent dye that specifically binds to amyloid fibrils and can be used as an indicator for the detection and quantification of amyloid fibrils (Bolder et al., 2007a; Koudelka et al., 2012; Pan and Zhong, 2015). In the current study, a significant increase in ThT fluorescence value of mWPI solutions after heating can be attributed to the formation of mWPI fibrils.

To understand the stability and sensitivity of fibrillated mWPI on pH, the pH of the fibrillated mWPI solution was adjusted to pH 6.7 and stored overnight at refrigerated temperature. There was no pH change observed in fibrillated mWPI after overnight storage. However, neutralization resulted in a significant ($P < 0.05$) decrease in ThT fluorescence value to 207.5 ± 6.7 AU. A significant ($P < 0.05$) drop in ThT value after pH adjustment may be due to the loss of fibrillar structure as ThT dye specifically binds to the amyloid fibrils. Fibril aggregation could be a possible reason for the loss of fibrillar structure, which showed a significant ($P < 0.05$) decrease in ThT fluorescence value of fibrillated mWPI at pH 6.7, but it was significantly ($P < 0.05$) higher than the control and nonfibrillated mWPI solutions. This observation showed that the fibrillar structures were present due to which ThT fluorescence value of the fibrils after pH adjustment was significantly ($P < 0.05$) higher than the nonfibrillated samples. Mantovani et al., (2016) has also reported a decrease in ThT fluorescence value for fibrils solution of WPI upon pH change from 3 to 7. The above observations show that fibrils exist even after pH adjustment back to 6.7. Further visual confirmation is needed from TEM and gel electrophoresis to ensure fibrils formation and its viability after pH change.

Table 3.1 Th T value, rheology, and conductivity of non-fibrillated and fibrillated milk whey protein isolate (mWPI) solution.

Name of sample	ThT	Apparent viscosity (mPaS) (at $100S^{-1}$)	Consistency Coefficient (K) (PaS^n)	Flow behavior index (η)	Conductivity mS
mWPI#(pH-6.7)	12.0±1.5[a]	1.13±0.04 [a]	0.0017±0.0010 [a]	0.94±0.10 [c]	0.37±0.03 [a]
mWPI(pH-2)	16.6±3.9 [a]	1.14±0.03 [a]	0.0012±0.0001 [a]	0.99±0.02 [c]	5.81±0.07 [c]
mWPI(pH-adjusted back to 6.7 from 2)	17.9±0.8 [a]	1.10±0.03 [a]	0.0013±0.0001 [a]	0.97±0.01 [c]	4.45±0.05 [b]
F_mWPI* (pH-2)	355.4±71.4 [b]	6.23±0.94 [b]	0.0348±0.0038 [b]	0.63±0.01 [b]	5.64±0.19 [c]
F_mWPI (pH-adjusted back to 6.7 from 2)	207.5±6.7 [c]	19.39±12.38 [c]	0.5766±0.5800 [c]	0.38±0.18 [a]	4.65±0.10 [b]

[a-c] Mean within a column with different superscripts differ ($P<0.05$) n=4

#mWPI denotes 2% w/w milk whey protein isolate solution, *F_mWPI indicates Fibrillated mWPI solution

TEM

The TEM images of fibrillated mWPI solution at pH 2 are shown in Figure 3.2A. A long mature mWPI fibril having a diameter ranging between 8 and 14 nm is evident from the TEM images (Figures 3.2A and 3.2B). Further, separate string-like individual fibrils at pH 2 can be seen in Figure 3.2A. A similar fibrillar structure was seen for whey protein fibrils (Loveday et al., 2012a) and β-LG fibrils (Loveday et al., 2012b). The TEM images of fibrillated mWPI confirmed the formation of the fibrils and showed a uniform distribution without any large aggregates.

However, neutralization of fibrillated mWPI to 6.7 showed a decrease in the number of individual fibrils, overall fibril density, and its distribution (Figures 3.2C and 3.2D). The TEM image at lower magnification showed that, unlike the continuous fibrils network seen at pH 2 (Figure 3.2A), a cluster of fibrils was seen when the pH was adjusted to 6.7 (Figure 3.2C). Higher magnification image (Figure 3.2D) showed that some fibrils interacted with adjacent fibrils and entangled like a rope, and thereby formed a cluster and aggregates. A similar fibril aggregation was reported in a previous study on whey protein fibrils (Mantovani et al., 2016) where the authors observed a mixture of fibrils and aggregates at pH 7. Whey proteins form aggregates at their isoelectric pH (4.5) as the net charge on proteins became zero (Damodaran, 1997). Further, Kroes-Nijboer et al. (2012b) reported that only 46% of total proteins were converted into fibrils. The rest was nonfibrillated protein. Further, they separated the fibril containing solution into fibrillated and nonfibrillated parts and adjusted their pH to 5 and 8. They found that at pH 5, which is closer to the isoelectric point of whey protein, fibrils were shrunken together, whereas the nonfibrillated part yielded aggregates. When pH was changed to 8, fibrils regained their structure with some aggregation, but most of the nonfibrillar parts were seen in aggregated form. In the present study, it was also observed that some of the individual mWPI fibrils turned into a cluster of fibrils, and some of them returned to their shape after pH adjustment. Therefore, the number of intact fibrils was decreased, which can be correlated with a decrease in ThT fluorescence value after pH adjustment.

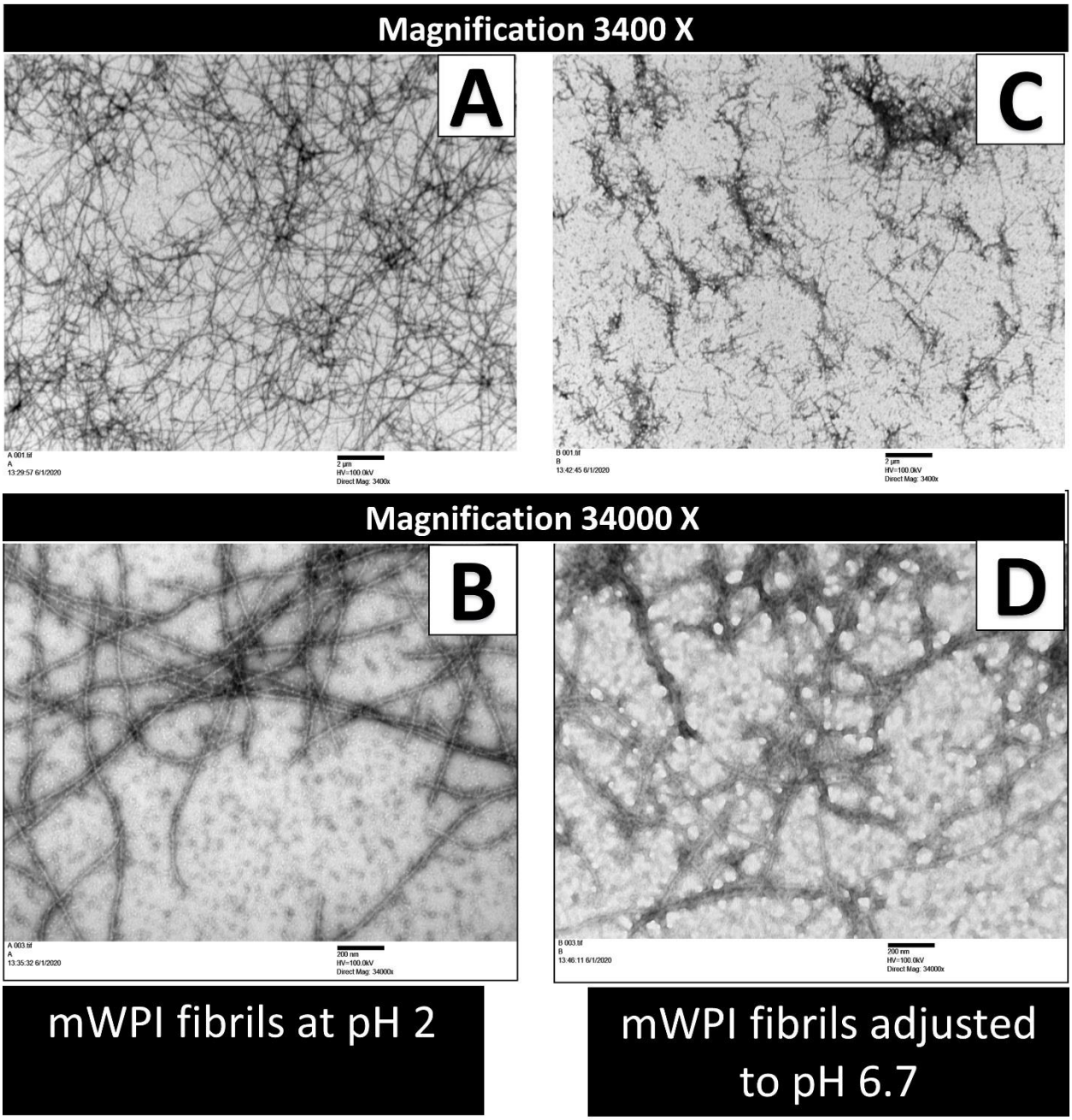

Figure 3.2 TEM images of milk whey protein isolates (mWPI) fibrils before (A and B) and after (C and D) pH adjustment**.**

Gel electrophoresis

Individual protein fractions of mWPI can be seen in the native PAGE gel (Figure 3.3A, lane 1). When whey proteins are subjected to fibrillation process, they showed a continuous spread across the gel band (Figure 3.3A, lane 3). A similar pattern for gel electrophoresis of fibrils was reported for whey proteins by Mantovani et al. (2017) and for soy protein fibrils by Wang et al. (2020). The gel band pattern suggests that spread was due to fibrils that were not separated during native PAGE. As the fibrillar structure is interlinked together, and consequently difficult to separate into a particular band, a uniform spread was observed. However, a small band can be seen near the end of separating gel (Figure 3.3A, lane 3), which could be due to small peptides formed by hydrolysis of whey proteins owing to heating at a lower pH for a longer time. These results confirm the fibril formation as explained by ThT fluorescence value and TEM images. Nonheated mWPI samples showed a clear separation of protein fractions (Figure 3.3A, lane 2).

When the pH of fibrillated mWPI was readjusted to 6.7, almost a similar type of spread pattern can be seen (Figure 3.3A, lane 4), which showed the presence of fibrils in the sample. However, the intensity of the spread was lower than fibrillated mWPI at pH 2 (Figure 3.3A, lane 3). Further, the intensity of a small band, seen near the end of separating gel (Figure 3.3A, lane 4) was decreased after pH adjustment to 6.7. These results show that there could be some aggregation due to pH change from 2 to 6.7 as proteins pass through their isoelectric point (4.5). When a similar pH readjustment was done to nonfibrillar mWPI solution, the gel pattern was almost similar to mWPI solution with the absence of small peptide band and persistent band at high molecular weight side (Figure 3.3A, lane 2). This shows that a part of proteins formed aggregates that were not regained their structure back after pH readjustment.

Nonreducing (Figure 3.3B) and reducing SDS-PAGE (Figure 3.3C) showed a clear band of α-LA and β-LG, and their position was marked with respect to marker bands on the ladder (Figures 3.3B and 3.3C, lane 6) based on their molecular weight, 14.2 and 18.4 kDa, respectively (Arunkumar and Etzel, 2013). When mWPI solution was subjected to the fibrillation process, β-LG completely disappeared, whereas many small molecular weight fractions (<10 kDa) were seen below the band of α-LA (Figures 3.3B and 3.3C, lane 3). These small molecular weight fractions could be formed from fibrils due to the action of dissociating agents SDS and β-mercaptoethanol. The disappearance of the β-LG band and rise in small molecular weight fraction indicated that β-LG was converted to fibrils and α-LA remained unchanged after fibril formation. A similar observation has been reported that the β-LG was responsible for fibrils formation, not α-LA, and BSA (Bolder et al., 2006). Akkermans et al. (2008) found that β-LG was hydrolyzed into peptides with molecular weight of 2 and 8 kDa in the initial stages and subsequently rearranged as fibrils during heating. Further, they added that these peptides were mainly obtained due to cleavage of the bonds between aspartic acid residues and any other amino acids or due to the total removal of aspartic acid residues.

The pH adjustment of fibrillated mWPI to 6.7 did not show any marked changes in the gel pattern (Figures 3.3B and 3.3C, lane 4). These may be due to the dissociation of aggregates that were formed due to pH change into smaller peptide upon the action of the dissociating agent. Hence, a considerable difference from fibrillated mWPI at pH 2 was not seen.

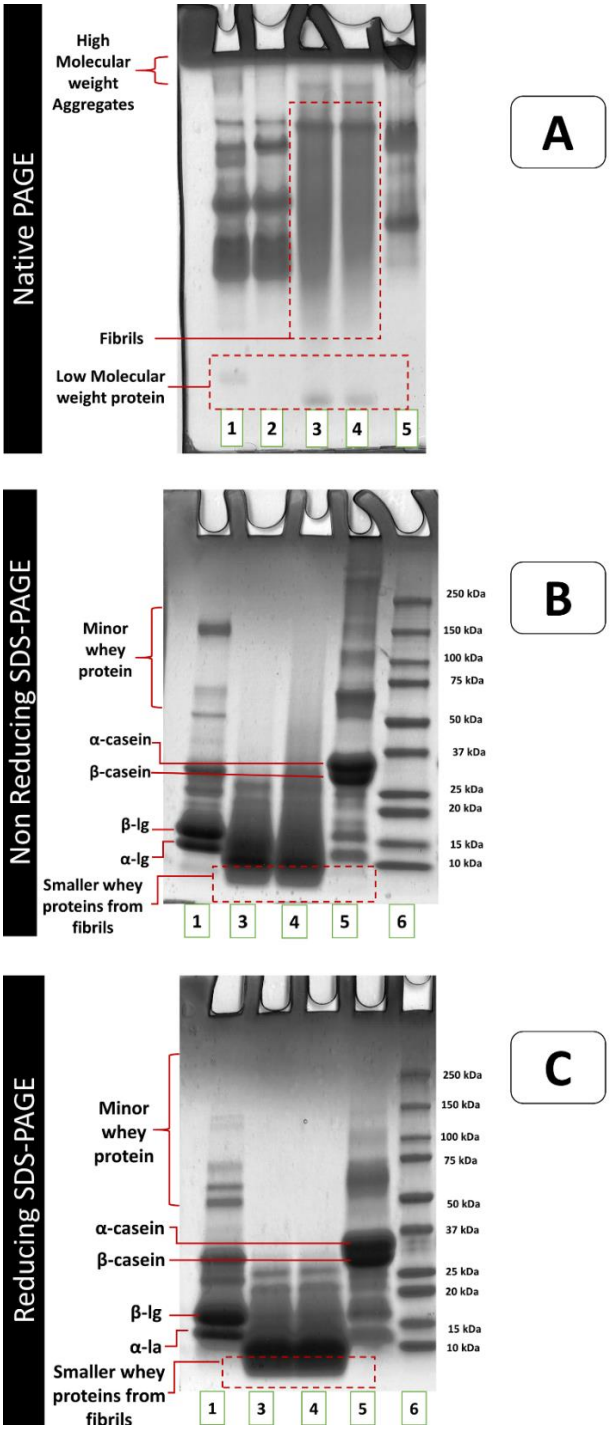

Figure 3.3 Gel electrophoresis of milk whey protein isolate (mWPI) fibrils and micellar casein concentrate (MCC). 1)-2% mWPI solution at pH 6.67, 2)-2% mWPI solution at pH 2 adjusted to pH 6.7, 3)-2% Fibrillated mWP solution at pH-2, 4)-2% mWP fibrils solution at pH 2 adjusted to pH 6.7, 5)-8% MCC solution, L-ladder (10-250kDa)).

Rheology

Table 3.1 shows the rheological properties of control, nonfibrillated and fibrillated mWPI solution. The mWPI solution showed apparent viscosity of 1.13 ± 0.04 mPa·s at 100 s−1. Further, the consistency coefficient (K) and flow behavior index (η) was reported to be 0.0017 ± 0.0010 Pa·sn and 0.94 ± 0.10, respectively. Results showed that the mWPI solution has non-Newtonian shear thinning behavior, but the values were still nearer to the value of the Newtonian fluid. This is because mWPI is in true solution in water (Walstra et al., 2005) and without any modification, mWPI solution behaves the same as the water. However, apparent viscosity and consistency coefficient were increased significantly ($P < 0.05$) to 6.23 ± 0.94 mPa·s at 100 s−1, and 0.0348 ± 0.0038 Pa·sn, respectively for fibrillated mWPI solutions. However, flow behavior index was reduced significantly ($P < 0.05$) to 0.63 ± 0.01 for fibrillated mWPI solutions. The fibrillated mWPI showed a shear thinning behavior and higher viscosity than mWPI solution. Fibrillation of mWPI resulted in conversion of globular structured proteins to the fibrillar structure proteins, which formed a network as seen in the TEM images (Figure 3.2A), that may have resulted in more water holding and thereby increased viscosity. Paximada et al. (2016) reported that fibrillar structure held water in its network and increased water holding capacity with an increase in the number of bacterial cellulose fibrils. Due to this water entrapment and fibrillar network, the viscosity of bacterial cellulose fibrils solution was increased with an increase in the number of fibrils. Similarly, fibrillated mWPI have higher viscosity than the control and nonfibrillated mWPI samples. Similarly, a rise in the viscosity and shear thinning behavior upon fibril formation was also seen by Loveday et al. (2012b) for β-LG fibrils and Zhang et al. (2014) for rice bran albumin fibrils.

When mWPI fibrils were adjusted back to pH 6.7, a significant ($P < 0.05$) increase in viscosity and consistency coefficient was seen. However, the flow behavior index decreased further (Table 3.1). The pH adjustment resulted in an entanglement of fibrils that could be seen in TEM image (Figure 3.2D). Due to fibril-fibril aggregation and network formation, the viscosity and consistency coefficient of fibrillated mWPI at pH 6.7 was significantly ($P < 0.05$) higher than the control, as well as the fibrillated mWPI at pH 2. However, when nonfibrillated mWPI solution was subjected to pH change to 2 and 6.7, nonsignificant ($P > 0.05$) change concerning apparent viscosity, consistency coefficient, and flow behavior was seen. Hence, pH adjustment did not show any significant effect on the rheology of nonfibrillated mWPI but has a significant effect on fibrillated mWPI.

Electrical conductivity

Table 3.1 shows electrical conductivity of control, nonfibrillated, and fibrillated mWPI solutions. Electrical conductivity of mWPI solution was 0.37 ± 0.03 μS·cm−1 (Table 3.1). Mucchetti et al. (1994) also reported 0.214 μS·cm−1 for 0.78% whey proteins solution. They added that the electrical conductivity of the solution was mainly contributed by the soluble salt available in the solution. Milk sugar lactose is not conductive, whereas milk fat decreases the conductivity. Protein and peptide have a minor effect on electrical conductivity. The mWPI contains 93% protein and a very low amount of salt, which could be the reason behind lower conductivity of mWPI solution. When mWPI solution was adjusted to pH 2 using 6 N HCL, the electrical conductivity of the solution increased drastically to 5.81 μS·cm−1 as the addition of acid to the solution may have increased the conductivity. Fibrillar mWPI solution at pH 2 showed a nonsignificant decrease in conductivity as compared with nonfibrillar mWPI solution at pH 2.

When pH of the mWPI solution (at pH 2) and fibrillated mWPI (at pH 2) were adjusted to 6.7, further decrease ($P < 0.05$) was seen. Hence, it could be said that fibrillation and pH adjustment both play a significant role in changing the electrical conductivity but the specific reason for decrease after neutralization of both the samples is still not fully known.

Phase-2: Model MPC

Th T fluorescence value

Table 3.2 shows the ThT fluorescence value of control, nonfibrillated, and fibrillated model MPC. The ThT fluorescence value of control model MPC was 279.6 ± 102.3 AU. Fibrillated model MPC-1 prepared from approach 1, which was prepared by mixing mWPI fibrils at pH 2, and MCC solution and subsequent pH adjustment to 6.7, has a ThT fluorescence value of 475.7 ± 92.9 AU, which is significantly higher than control and nonfibrillated model MPC. Similarly, fibrillated model MPC-2 prepared from approach 2, which was prepared by mixing pH-adjusted mWPI fibril (pH 6.7) with MCC solution, has ThT fluorescence value of 390.0 ± 88.9, which is significantly ($P < 0.05$) different from the control and nonfibrillated model MPC. Higher ThT fluorescence value of both the fibrillated model MPC showed that fibrils were present in the solution even after mixing.

However, the fibrillated model MPC were significantly ($P < 0.05$) different from each other, showing that the method of mixing has a marked effect on survival of fibrils after mixing. As approach 1 gave a significantly ($P < 0.05$) higher ThT fluorescence value, it could be said that higher number of fibrils may have survived in approach 1. The possible reason could be due to the buffering capacity of casein, and the total proportion of casein in the fibrillated model MPC. Casein showed a maximum buffering capacity at pH ~5.0 upon acidification due to solubilization of colloidal calcium phosphate (Seibel et al., 2015). Due to the 80% share of casein in the

solution, casein dominated in the overall behavior of the solution. Further, when mWPI fibrils were mixed with MCC solution, the final pH of the mixture obtained was around 5.7 ± 0.1, due to which lesser quantity of alkali was required to bring pH to 6.7. Further, mixing in approach 1 resulted in a quick increase in pH through the pH 4.5, an isoelectric pH of whey proteins, due to which proteins may have not got enough time to form aggregates. This could be a possible reason for the survival of fibrils and thereby higher ThT fluorescence value. Loveday et al. (2017) has also reported that rapid pH change would not allow fibrils to assemble and can improve the stability of fibrils against pH change. Nonfibrillated model MPC samples from approach 1 and approach 2 were not significantly ($P > 0.05$) different from each other and control model MPC. This result depicts that the overall effect on ThT fluorescence value is due to the mWPI fibrils which are in connection with earlier reported studies in phase-1.

Table 3.2 Th T value, rheology, heat coagulation time, and color value of control and fibrillated, and non-fibrillated model milk protein concentrate (MPC).

	Name of the sample	Thioflavin T fluorescence value (AU)	Viscosity (mPaS) (at $100S^{-1}$)	Consistency Coefficient (K)	Flow behavior index (η)	Particle Size (nm)	Heat coagulation time (s)	Color Value			
								L*	a*	b*	Total color
Control	model MPC	279.6±102.3 [a]	14.7±2.7 [b]	0.096±0.027 [a]	0.60± 0.02 [bc]	295.9± 35.4 [a]	73.0±2.0 [d]	74.62± 3.50 [c]	-2.47± 0.13 [a]	3.74±0 .07 [c]	74.75± 3.49[c]
Approach-1	Fibrillated model MPC-1	475.7±92.9 [c]	31.1±6.9 [c]	0.328±0.089 [b]	0.49± 0.05 [ab]	289.517 ±24.9 [a]	26.3±3.1 [a]	63.91± 2.53 [a]	-1.36± 0.04 [e]	3.89±0 .18 [d]	64.91± 1.57[a]
	Non-Fibrillated model MPC-1	296.4±74.3 [a]	11.0±0.6 [a]	0.100±0.074 [a]	0.56± 0.12 [bc]	275.850 ±39.1 [a]	40.7±3.1 [b]	62.73± 2.96 [a]	-2.00± 0.13 [c]	3.02±0 .12 [a]	62.83± 2.96[a]
	Fibrillated model MPC-2	390.0±88.9 [b]	37.7±8.8 [d]	0.689±0.277 [c]	0.38± 0.04 [a]	546.0± 519.4 [a]	59.7±2.5 [c]	69.08± 2.37 [b]	-1.57± 0.06 [d]	3.42±0 .09 [b]	69.18± 2.37[b]
Approach-2	Non-Fibrillated model MPC-2	325.1±63.9 [a]	14.0±2.6 [b]	0.075±0.032 [a]	0.65± 0.05 [c]	276.5± 48.1 [a]	78.7±1.5 [e]	69.73± 3.04 [b]	-2.22± 0.08 [b]	3.68±0 .09 [c]	69.87± 3.04[b]

[a-e] Mean within a column with different superscript different ($P<0.05$) n=4

TEM

In TEM image in Figure 3.4, mWPI fibrils can be seen in fibrillated model MPC produced by approaches 1 and 2. A bunch of aggregated fibrils can be seen around micellar casein, showing a possible interaction of mWPI fibrils with casein in approach 1 (Figures 3.4A and 4B). However, mWPI fibrils seen in approach 2 (Figures 3.4C and 3.4D) were clearer and longer than those of approach 1 and more similar to the pH-adjusted mWPI fibrils of phase 1 (Figure 3.2C and 3.2D), showing no interaction with casein in the fibrillated model MPC solution. Very thin clustered fibrils can be seen in the background, which shows that not all the fibrils were affected by the pH change. At lower magnification, approach 1 (Figure 3.4A) showed a distributed cluster against the continuous matrix of proteins in approach 2 (Figure 3.4C).

In approach 1, fibrillated mWPI solution (pH 2) and MCC solution (~pH 6.7) has higher pH difference and therefore micellar casein was exposed to a low pH environment. However, the pH of the mixture was 5.7 ± 0.1 which was finally adjusted to 6.7. The sudden change in pH may have promoted interactions between micellar casein and fibrillated mWPI, and fibril-fibrils interaction. This could result in altered casein structure and increased clustering, as seen in Figures 3.4A and 3.4B. Lucey et al. (1996) also reported a similar clustering of casein micelles when casein was acidified to pH 6 and 5.5 and neutralized back to pH 6.6. However, in approach 2, both the solutions were near to 6.7, and mixing did not cause any change in pH to micellar casein. Hence, both MCC and fibrillated mWPI were able to maintain their distinct identity and formed a continuous network without any further interaction or clusters in approach 2.

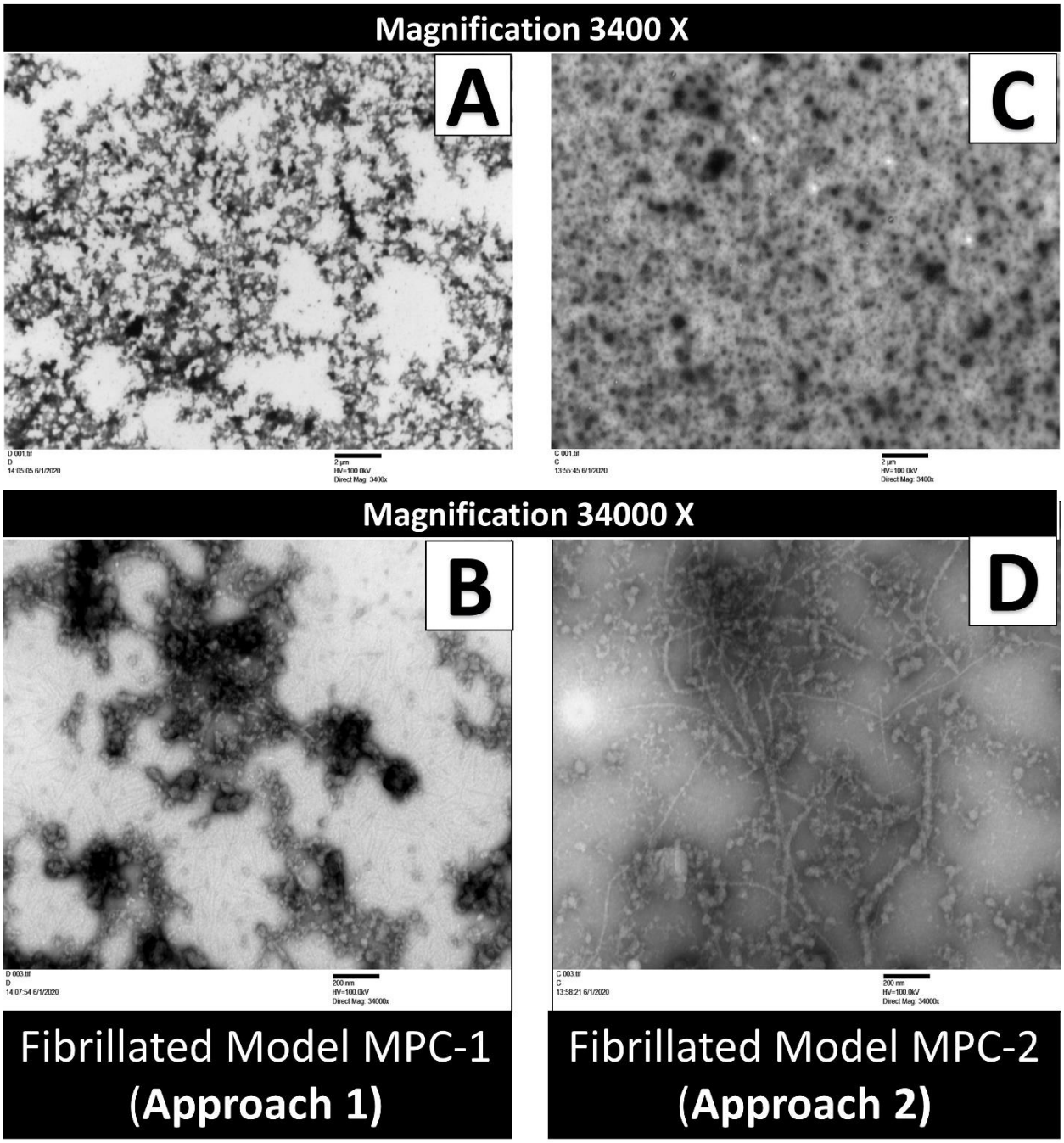

Figure 3.4 TEM images of fibrillated model milk protein concentrate (MPC) with two approaches. i. (A&B)- approach-1-pH adjustment to 6.7 done after mixing milk whey protein isolate (mWPI) fibril and micellar casein concentrate (MCC) solution. ii. (C&D)- approach-2-pH of adjustment of mWPI fibrils to 6.7 before mixing with MCC solution.

Gel electrophoresis

Native PAGE image (Figure 3.5A) shows thick bands at the entry of stacking gel, corresponding to high-molecular-mass protein aggregates, which were not able to penetrate the gel for all model MPC except for the control model MPC. Aggregates probably formed due to whey protein interaction within themselves and with caseins via noncovalent, or covalent interactions (Grewal et al., 2017). Control model MPC showed a separate band for protein fractions (Figure 3.5A, lane 7). In contrast to that, both fibrillated model MPC (Figure 3.5A, lane 9 and 11) showed a similar spreader band as mWPI fibril band (Figure 3.3A, lane 3) of phase 1 of the study, which confirmed the presence of fibrils in both the samples. However, in approach 1, the fibrillated model MPC showed more uniform spread rather than approach 2, which suggests that approach 1 may have more intact fibrils than the approach 2. Further, nonfibrillated model MPC from both approaches showed almost similar bands as control model MPC, which indicated that both approaches of mixing and pH adjustment did not have a marked effect for a nonfibrillated model MPC.

Similar to phase 1, images of nonreducing (Figure 3.5B) and reducing (Figure 3.5C) SDS-PAGE showed a reduction in the gel band of β-LG in fibrillated model MPC in both the approaches, which was due to the conversion of β-LG to fibrils. But still, β-LG was seen in the fibrillated model MPC because MCC has some part of β-LG in its composition (Figures 3.5B and 3.5C, lane 5) as contaminant. Further, fibrillated model MPC-1 showed the lighter β-LG band (Figures 3.5B and 5C, lane 11) than fibrillated model MPC-2 (Figures 3.5B and 3.5C, lane 9) as β-LG present in the MCC was exposed to sudden pH change during mixing with fibrillated mWPI and further suffered pH change from 5.7 to 6.7 in approach 1. However, the same harsh pH change has not occurred in approach 2 where pH of both the solution was adjusted to 6.7.

Unlike fibrillated model MPC, control model MPC and nonfibrillated MPC from both approaches has almost similar bands with no marked difference in gel pattern.

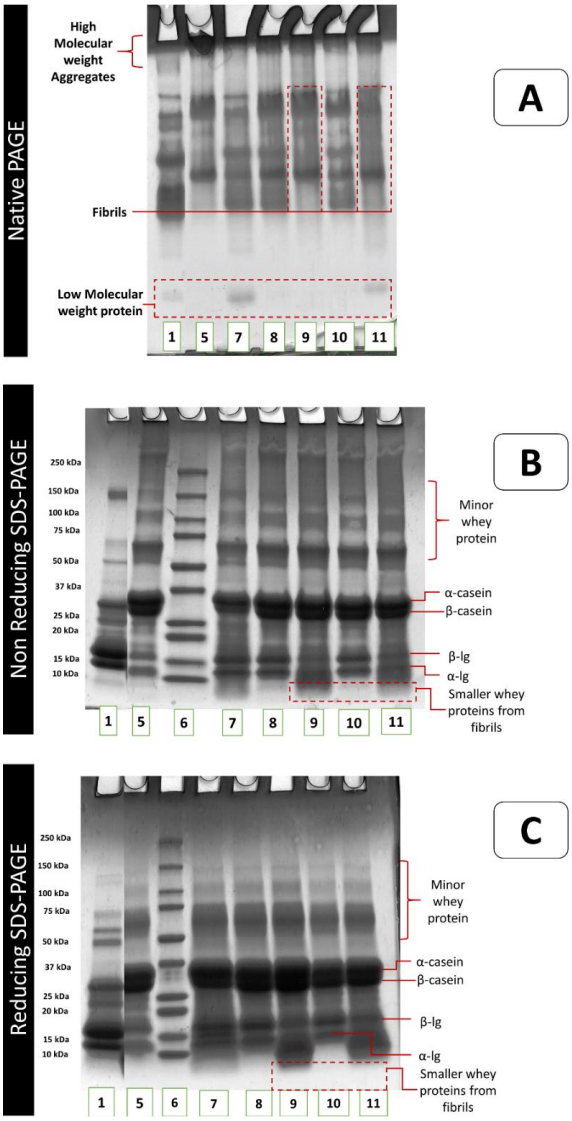

Figure 3.5 Gel electrophoresis of model milk protein concentrate (MPC. 1)-2% milk whey protein isolate (mWPI) solution at pH 6.67, 5)-8% micellar casein concentrate (MCC) solution, 6)-ladder (10-250kDa), 7)-control model milk protein concentrate (MPC), 8)-non-fibrillated model MPC (Approach-2), 9)-fibrillated model MPC (Approach-2), 10)-non-fibrillated model MPC (Approach-1), 11)-fibrillated model MPC (Approach-1).

Rheology

Table 3.2 shows the rheological parameters of control, nonfibrillated, and fibrillated model MPC. Apparent viscosity of the control model MPC was 14.7 ± 2.7 mPa·s at 100 s−1 (Table 3.2). Further, the apparent viscosity of the fibrillated model MPC-1 (31.1 ± 6.9 mPa·s) was significantly ($P < 0.05$) lower than the fibrillated model MPC-2 (37.7 ± 8.8 mPa·s) but significantly ($P < 0.05$) higher than the control model MPC and nonfibrillated model MPC-1 and 2. In case of nonfibrillated model MPC, apparent viscosity of model MPC-1 was significantly ($P < 0.05$) lower than model MPC-2 and control model MPC. These results showed that the approach of mixing had a significant effect on apparent viscosity and the fibrillated model MPC have higher apparent viscosity than nonfibrillated model MPC. Conversion of globular to fibrillar structure is well known to produce higher viscosity in animal and plant-based proteins including β-LG (Loveday et al., 2012b), rice bran albumin (Zhang et al., 2014), and soy protein (Wang et al., 2020). Following a similar trend, fibrillated model MPC showed a higher viscosity due to the presence of whey proteins in fibrillar structure.

In approach 1, due to the pH difference between fibrillated mWPI and MCC solution, some of mWPI fibrils may have interacted with MCC, and not all the fibrils were cross-linked with each other (Figures 3.4A and 3.4B). However, a similar interaction was not seen in approach 2 (Figures 3.4C and 3.4D). Hence, the viscosity of the fibrillated model MPC-2 was a cumulative viscosity of 2 solutions. Similar supportive results can be seen in phase 1, where pH-adjusted mWPI fibrils showed a higher viscosity then all other samples. Hence, mixing and pH adjustment both had a considerable effect on apparent viscosity.

The consistency coefficient of the control model MPC was 0.096 ± 0.027 Pa·sn whereas fibrillated model MPC-1 and 2 have consistency coefficient of 0.328 ± 0.089 $Pa \cdot S^n$ and 0.689 ±

0.277 Pa·S^n, respectively, that are significantly ($P< 0.05$) different with each other and significantly ($P < 0.05$) higher than that of control and nonfibrillated model MPC. Hence, it could be said that fibril containing samples had a higher consistency coefficient where approach 2 gave the highest value. All the samples showed a non-Newtonian shear thinning behavior (Table 3.2), where fibrillated model MPC have a lower flow behavior index than the nonfibrillated model MPC with lowest in approach 2. Hence, it could be said that the presence of fibrils has a marked effect on flow behavior.

Heat Coagulation Time

Table 3.2 shows the heat coagulation time of control, nonfibrillated, and fibrillated model MPC. The results given in Table 3.2 showed that both presence of fibrils and the approach of mixing have a significant ($P < 0.05$) effect on heat coagulation time. Fibrillated model MPC-2 showed significantly ($P < 0.05$) higher heat coagulation time than fibrillated model MPC-1 and the heat coagulation time of fibrillated model MPC was significantly ($P < 0.05$) lower than nonfibrillated model MPC. Hence, it can be said that fibrillation reduced heat coagulation time, and when pH adjustment was done before mixing, it can give higher heat coagulation time.

When globular proteins are converted to fibrillar protein, it opens up more hydrophobic groups. That reduces overall repulsion, resulting in faster heat coagulation during heating at 140°C, which could be the possible reason of lesser heat coagulation time of the fibrillated model MPCs in both approaches. During the pH adjustment process, these proteins are passed through their respective isoelectric points, at which they tend to form aggregates that could be reversible or nonreversible, that affect heat stability.

Any change in pH affects the structure of protein and functional properties including heat stability. In approach 1, pH of casein micelles was briefly exposed to pH 5.7 ± 0.1 resulting in a partial removal of colloidal calcium phosphate (CCP) and consequently an increase in ionic calcium concentration. The mixture was then neutralized to pH 6.7. Ezeh and Lewis (2011) observed an increase in ionic calcium of skim milk when skim milk was acidified to pH 5.7 and subsequently neutralized back to pH 6.7 and concluded that restoration of CCP did not restored to its original concentration after neutralization. Sinaga et al. (2017) also reported any alteration to casein structure within range of pH 6.0 to 7.0 was reversible, beyond that structural changes were irreversible specifically the particle size. On the other hand, Lucey et al. (1996) found that acidification of skim milk to pH > 5.5 followed by neutralization back to pH 6.6 hardly influenced the buffering capacity of skim milk suggesting reformation of CCP upon neutralization. Crowley et al. (2014) reported a drop in heat stability of MPC when pH was lowered below 6.8 due to an increase in calcium ion activity. After observing the changes due to acidification and neutralization in skim milk systems from the literature and TEM images (Figures 3.4A and 3.4B) from the present study which showed aggregates of fibrils and caseins, it is evident that the acidification and neutralization affected the casein in approach 1 leading to a reduction in heat coagulation time of the mixture. On the other hand, in approach 2, casein was not exposed to any pH alteration and also did not show any clusters in TEM images (Figures 3.4C and 3.4D) leading to a higher heat coagulation time compared with approach 1.

Color

Table 3.2 shows the color value of control, nonfibrillated, and fibrillated model MPC. Among all the samples, control samples showed the highest L* value (74.62 ± 3.50). Significantly ($P < 0.05$) higher L* value was reported for approach 2 than approach 1. However,

fibrillated model MPC in both approaches were not significantly different from nonfibrillated model MPC, but all the fibrillated and nonfibrillated model MPC were significantly ($P < 0.05$) different than the control sample. So, lightness value was affected by both the method of mixing and pH adjustment, but not by fibrillation. However, a* and b* values were significantly different ($P < 0.05$) for all the samples, which suggests that a* and b* values have been affected by methods of mixing, pH adjustment, and fibrillation. Both fibrillated model MPC were different ($P < 0.05$) from each other and from the control model MPC. Total color value was highest for control model MPC. Total color was significantly ($P < 0.05$) higher for approach 2 than approach 1. However, there was no significant difference between fibrillated and nonfibrillated MPC. Hence, similar to L* value, total color value was also affected by method of mixing and pH adjustment but not by fibril formation. So, all the color value was significantly affected by treatments.

We observed that due to prolonged heating, fibrillated mWPI solution was darker in color than nonfibrillated mWPI solutions due to which reduction in L* value can be seen in the fibrillated mWPI and subsequently in fibrillated MPC from both approaches. The reduction in L* values after prolonged heating (80°C for 20 h) of mWPI solution could be attributed to Maillard browning (Dave et al., 2014; Wei and Huang, 2019) and protein oxidation (Dave et al., 2013). Hu et al., (2019) reported browning of WPI fibrils solutions upon heating at 80°C for 20 h. Keppler et al. (2019) studied oxidation of β-LG at pH 2 and 3.5 after heating to 90°C for 72 h, and reported that tyrosine oxidation peaked at 5 h of heating time. However, tryptophan oxidation and carbonyls continued to increase during 72 h of heating. Further, during pH adjustment, the fibrillated mWPI sample becomes translucent with some whitish color. This could be the possible reason for the higher L* value of samples of approach 2.

Conclusion

Among milk proteins, whey proteins are the most suitable proteins for fibril formation and consequently modify rheological properties of resultant fibril containing proteins solutions. To harness the functional benefits of fibrils, reconstituted mWPI solution was heated at low pH which showed fibrillar structure in TEM and higher ThT fluorescence value, and increased viscosity and consistency coefficient than the nonfibrillated mWPI. The mWPI fibrils survived the pH adjustment and mixing with MCC, which was confirmed by higher ThT fluorescence value, TEM, and gel electrophoresis images of mWPI fibrils and fibrillated model MPC. Fibrillated model MPC-2, which was prepared by combining pH-adjusted mWPI fibrils (pH-6.7) and MCC solution, showed higher viscosity, heat coagulation time, and uniform spread in TEM images than fibrillated model MPC-1, which was prepared by mixing mWPI fibrils (pH 2) and MCC solution with subsequent pH adjustment to 6.7. However fibrillated model MPC-1 showed higher ThT fluorescence value and uniform distribution of across gel band. Hence, it could be said that whey protein in MPC can be modified as fibrils, which can give higher viscosity and can be used in dairy and food products for texture modification. Further research is necessary to evaluate the survivability of the developed fibrillated model MPC during subsequent spray drying to produce powdered form for its widespread application in dairy and food formulations. In addition, further studies are also needed to evaluate the new fibril containing MPC in terms of toxicological and protein oxidation before it is used as an ingredient.

Acknowledgments

We are highly thankful to the National Dairy Council and Midwest Dairy Foods Research Center (St. Paul, MN) for their financial support. This project was conducted under Kansas State

Research and Extension contribution number 20-356-J. This work was partially supported by the USDA National Institute of Food and Agriculture (Washington, DC) Hatch project 1014344.

References

Akkermans, C., P. Venema, A. J. van der Goot, H. Gruppen, E. J. Bakx, R. M. Boom, and E. van der Linden. 2008. Peptides are building blocks of heat-induced fibrillar protein aggregates of β-lactoglobulin formed at pH 2. Biomacromolecules 9:1474–1479. https://doi.org/10.1021/bm7014224.

An, B., X. Wu, M. Li, Y. Chen, F. Li, X. Yan, J. Wang, C. Li, and C. Brennan. 2016. Hydrophobicity-modulating self-assembled morphologies of α-zein in aqueous ethanol. Int. J. Food Sci. Technol. 51:2621–2629. https://doi.org/10.1111/ijfs.13248.

Arunkumar, A., and M. R. Etzel. 2013. Fractionation of α-lactalbumin from β-lactoglobulin using positively charged tangential flow ultrafiltration membranes. Separ. Purif. Tech. 105:121–128. https://doi.org/10.1016/j.seppur.2012.12.018.

Bolder, S. G., H. Hendrickx, L. M. C. Sagis, and E. van der Linden. 2006. Fibril assemblies in aqueous whey protein mixtures. J. Agric. Food Chem. 54:4229–4234. https://doi.org/10.1021/jf060606s.

Bolder, S. G., L. M. C. Sagis, P. Venema, and E. van der Linden. 2007a. Effect of stirring and seeding on whey protein fibril formation. J. Agric. Food Chem. 55:5661–5669. https://doi.org/10.1021/jf063351r.

Bolder, S. G., A. J. Vasbinder, L. M. C. Sagis, and E. van der Linden. 2007b. Heat-induced whey protein isolate fibrils: Conversion, hydrolysis, and disulphide bond formation. Int. Dairy J. 17:846–853. https://doi.org/10.1016/j.idairyj.2006.10.002.

Crowley, S. V., M. Megemont, I. Gazi, A. L. Kelly, T. Huppertz, and J. A. O'Mahony. 2014. Heat stability of reconstituted milk protein concentrate powders. Int. Dairy J. 37:104–110. https://doi.org/10.1016/j.idairyj.2014.03.005.

Damodaran, S. 1997. Food proteins: An overview. Pages 1–24 in Food Proteins and Their Applications. 1st ed. S. Damodaran and A. Paraf, ed. Marcel Dekker, New York, NY.

Dave, A. C., S. M. Loveday, S. G. Anema, G. B. Jameson, and H. Singh. 2014. Glycation as a tool to probe the mechanism of β-lactoglobulin nanofibril self-assembly. J. Agric. Food Chem. 62:3269–3278. https://doi.org/10.1021/jf405441g.

Dave, A. C., S. M. Loveday, S. G. Anema, T. S. Loo, G. E. Norris, G. B. Jameson, and H. Singh. 2013. β-Lactoglobulin self-assembly: Structural changes in early stages and disulfide bonding in fibrils. J. Agric. Food Chem. 61:7817–7828. https://doi.org/10.1021/jf401084f.

Ezeh, V. N., and M. J. Lewis. 2011. Milk reversibility following reduction and restoration of pH. Int. J. Dairy Technol. 64:179–187. https://doi.org/10.1111/j.1471-0307.2010.00649.x.

Farrokhi, F., F. Badii, M. R. Ehsani, and M. Hashemi. 2019. Functional and thermal properties of nanofibrillated whey protein isolate as functions of denaturation temperature and solution pH. Colloids Surf. A Physicochem. Eng. Asp. 583:124002. https://doi.org/10.1016/j.colsurfa.2019.124002.

Gao, Z., J. Zhao, Y. Huang, X. Yao, K. Zhang, Y. Fang, K. Nishinari, G. O. Phillips, F. Jiang, and H. Yang. 2017. Edible pickering emulsion stabilized by protein fibrils. Part 1: Effects of pH and fibrils concentration. LWT Food Sci. Technol. 76:1–8. https://doi.org/10.1016/j.lwt.2016.10.038.

Grewal, M. K., J. Chandrapala, O. Donkor, V. Apostolopoulos, and T. Vasiljevic. 2017. Electrophoretic characterization of protein interactions suggesting limited feasibility of

accelerated shelf-life testing of ultra-high temperature milk. J. Dairy Sci. 100:76–88. https://doi.org/10.3168/jds.2016-11278.

Hu, Y., C. He, M. W. Woo, H. Xiong, J. Hu, and Q. Zhao. 2019. Formation of fibrils derived from whey protein isolate: Structural characteristics and protease resistance. Food Funct. 10:8106–8115. https://doi.org/10.1039/C9FO00961B.

Keppler, J. K., T. R. Heyn, P. M. Meissner, K. Schrader, and K. Schwarz. 2019. Protein oxidation during temperature-induced amyloid aggregation of beta-lactoglobulin. Food Chem. 289:223–231. https://doi.org/10.1016/j.foodchem.2019.02.114.

Koudelka, T., F. C. Dehle, I. F. Musgrave, P. Hoffmann, and J. A. Carver. 2012. Methionine oxidation enhances κ-casein amyloid fibril formation. J. Agric. Food Chem. 60:4144–4155. https://doi.org/10.1021/jf205168t.

Kroes-Nijboer, A., H. Sawalha, P. Venema, A. Bot, E. Flöter, R. den Adel, W. G. Bouwman, and E. van der Linden. 2012b. Stability of aqueous food grade fibrillar systems against pH change. Faraday Discuss. 158:125–138. https://doi.org/10.1039/c2fd20031g.

Kroes-Nijboer, A., P. Venema, and E. van der Linden. 2012a. Fibrillar structures in food. Food Funct. 3:221–227. https://doi.org/10.1039/C1FO10163C.

Lara, C., S. Gourdin-Bertin, J. Adamcik, S. Bolisetty, and R. Mezzenga. 2012. Self-assembly of ovalbumin into amyloid and nonamyloid fibrils. Biomacromolecules 13:4213–4221. https://doi.org/10.1021/bm301481v.

Lassé, M., D. Ulluwishewa, J. Healy, D. Thompson, A. Miller, N. Roy, K. Chitcholtan, and J. A. Gerrard. 2016. Evaluation of protease resistance and toxicity of amyloid-like food fibrils from whey, soy, kidney bean, and egg white. Food Chem. 192:491–498. https://doi.org/10.1016/j.foodchem.2015.07.044.

Loveday, S. M., S. G. Anema, and H. Singh. 2017. β-Lactoglobulin nanofibrils: The long and the short of it. Int. Dairy J. 67:35–45. https://doi.org/10.1016/j.idairyj.2016.09.011.

Loveday, S. M., J. Su, M. A. Rao, S. G. Anema, and H. Singh. 2012a. Whey protein nanofibrils: The environment–morphology–functionality relationship in lyophilization, rehydration, and seeding. J. Agric. Food Chem. 60:5229–5236. https://doi.org/10.1021/jf300367k.

Loveday, S. M., X. L. Wang, M. A. Rao, S. G. Anema, L. K. Creamer, and H. Singh. 2010. Tuning the properties of β-lactoglobulin nanofibrils with pH, NaCl and CaCl2. Int. Dairy J. 20:571–579. https://doi.org/10.1016/j.idairyj.2010.02.014.

Loveday, S. M., X. L. Wang, M. A. Rao, S. G. Anema, and H. Singh. 2012b. β-Lactoglobulin nanofibrils: Effect of temperature on fibril formation kinetics, fibril morphology and the rheological properties of fibril dispersions. Food Hydrocoll. 27:242–249. https://doi.org/10.1016/j.foodhyd.2011.07.001.

Lucey, J. A., C. Gorry, B. O'Kennedy, M. Kalab, R. Tan-Kinita, and P. F. Fox. 1996. Effect of acidification and neutralization of milk on some physico-chemical properties of casein micelles. Int. Dairy J. 6:257–272. https://doi.org/10.1016/0958-6946(95)00014-3.

Mantovani, R. A., J. Fattori, M. Michelon, and R. L. Cunha. 2016. Formation and pH-stability of whey protein fibrils in the presence of lecithin. Food Hydrocoll. 60:288–298. https://doi.org/10.1016/j.foodhyd.2016.03.039.

Mantovani, R. A., A. C. Pinheiro, A. A. Vicente, and R. L. Cunha. 2017. In vitro digestion of oil-in-water emulsions stabilized by whey protein nanofibrils. Food Res. Int. 99:790–798. https://doi.org/10.1016/j.foodres.2017.06.049.

Meena, G. S., A. K. Singh, S. Borad, and N. R. Panjagari. 2016. Effect of concentration, homogenization and stabilizing salts on heat stability and rheological properties of cow

skim milk ultrafiltered retentate. J. Food Sci. Technol. 53:3960–3968. https://doi.org/10.1007/s13197-016-2388-4.

Moayedzadeh, S., A. Madadlou, and A. Khosrowshahi Asl. 2015. Formation mechanisms, handling and digestibility of food protein nanofibrils. Trends Food Sci. Technol. 45:50–59. https://doi.org/10.1016/j.tifs.2015.05.005.

Mohammadian, M., and A. Madadlou. 2016. Characterization of fibrillated antioxidant whey protein hydrolysate and comparison with fibrillated protein solution. Food Hydrocoll. 52:221–230. https://doi.org/10.1016/j.foodhyd.2015.06.022.

Mohammadian, M., and A. Madadlou. 2018. Technological functionality and biological properties of food protein nanofibrils formed by heating at acidic condition. Trends Food Sci. Technol. 75:115–128. https://doi.org/10.1016/j.tifs.2018.03.013.

Mucchetti, G., M. Gatti, and E. Neviani. 1994. Electrical conductivity changes in milk caused by acidification: determining factors. J. Dairy Sci. 77:940–944. https://doi.org/10.3168/jds.S0022-0302(94)77029-6.

Munialo, C. D., A. H. Martin, E. van der Linden, and H. H. de Jongh. 2014. Fibril formation from pea protein and subsequent gel formation. J. Agric. Food Chem. 62:2418–2427. https://doi.org/10.1021/jf4055215.

Oboroceanu, D., L. Wang, E. Magner, and M. A. Auty. 2014. Fibrillization of whey proteins improves foaming capacity and foam stability at low protein concentrations. J. Food Eng. 121:102–111. https://doi.org/10.1016/j.jfoodeng.2013.08.023.

Pan, K., and Q. Zhong. 2015. Amyloid-like fibrils formed from intrinsically disordered caseins: Physicochemical and nanomechanical properties. Soft Matter 11:5898–5904. https://doi.org/10.1039/C5SM01037C.

Paximada, P., E. A. Dimitrakopoulou, E. Tsouko, A. A. Koutinas, C. Fasseas, and I. G. Mandala. 2016. Structural modification of bacterial cellulose fibrils under ultrasonic irradiation. Carbohydr. Polym. 150:5–12. https://doi.org/10.1016/j.carbpol.2016.04.125.

Ramos, O. L., R. N. Pereira, A. Martins, R. Rodrigues, C. Fuciños, J. A. Teixeira, L. Pastrana, F. X. Malcata, and A. A. Vicente. 2017. Design of whey protein nanostructures for incorporation and release of nutraceutical compounds in food. Crit. Rev. Food Sci. Nutr. 57:1377–1393. https://doi.org/10.1080/10408398.2014.993749.

Rathod, G., and N. Kairam. 2018. Preparation of omega 3 rich oral supplement using dairy and non-dairy based ingredients. J. Food Sci. Technol. 55:760–766. https://doi.org/10.1007/s13197-017-2988-7.

Ridgley, D. M., E. C. Claunch, and J. R. Barone. 2012. The effect of processing on large, self-assembled amyloid fibers. Soft Matter 8:10298–10306. https://doi.org/10.1039/c2sm26496j.

Sanchez Alan, K., L. Wang, and K. Schmidt. 2017. Heat stability of radio frequency dielectric heat treated low heat and high heat nonfat dry milk. Int. Dairy J. 74:21–26. https://doi.org/10.1016/j.idairyj.2017.05.003.

Seibel, J. R., M. S. Molitor, and J. A. Lucey. 2015. Properties of casein concentrates containing various levels of beta-casein. Int. J. Dairy Technol. 68:24–29. https://doi.org/10.1111/1471-0307.12170.

Sinaga, H., N. Bansal, and B. Bhandari. 2017. Effects of milk pH alteration on casein micelle size and gelation properties of milk. Int. J. Food Prop. 20:179–197. https://doi.org/10.1080/10942912.2016.1152480.

Sun, X. S., D. Wang, L. Zhang, X. Mo, L. Zhu, and D. Bolye. 2008. Morphology and phase separation of hydrophobic clusters of soy globular protein polymers. Macromol. Biosci. 8:295–303. https://doi.org/10.1002/mabi.200700235.

Teodorowicz, M., J. Van Neerven, and H. Savelkoul. 2017. Food processing: The influence of the Maillard reaction on immunogenicity and allergenicity of food proteins. Nutrients 9:835. https://doi.org/10.3390/nu9080835.

Veerman, C. 2006. Method for improving the functional properties of a globular protein, protein thus prepared, use thereof and products containing the protein. U.S. Patent Application 10/536,713. Patent no. PCT/EPO3/13678.

Walstra, P., J. T. Wouters, and T. J. Geurts. 2005. Milk components. Pages 17–108 in Dairy Science and Technology. 2nd ed. CRC press, Boca Raton, FL.

Wang, Y., Y. Shen, G. Qi, Y. Li, X. S. Sun, D. Qiu, and Y. Li. 2020. Formation and physicochemical properties of amyloid fibrils from soy protein. Int. J. Biol. Macromol. 149:609–616. https://doi.org/10.1016/j.ijbiomac.2020.01.258.

Wei, Z., and Q. Huang. 2019. Modification of ovotransferrin by Maillard reaction: Consequences for structure, fibrillation and emulsifying property of fibrils. Food Hydrocol. 97:105186. https://doi.org/10.1016/j.foodhyd.2019.105186.

Xia, W., H. Zhang, J. Chen, H. Hu, F. Rasulov, D. Bi, X. Huang, and S. Pan. 2017. Formation of amyloid fibrils from soy protein hydrolysate: Effects of selective proteolysis on β-conglycinin. Food Res. Int. 100:268–276. https://doi.org/10.1016/j.foodres.2017.08.059.

Zhang, Y. H., and L. H. Huang. 2014. Effect of heat-induced formation of rice bran protein fibrils on morphological structure and physicochemical properties in solutions and gels. Food Sci. Biotechnol. 23:1417–1423. https://doi.org/10.1007/s10068-014-0194-1.

Zhang, Y. H., L. H. Huang, and Z. C. Wei. 2014. Effects of additional fibrils on structural and rheological properties of rice bran albumin solution and gel. Eur. Food Res. Technol. 239:971–978. https://doi.org/10.1007/s00217-014-2294-9.

Chapter 4 - Acid gelation properties of fibrillated model milk protein concentrate[2]

Abstract

Whey proteins in milk are globular proteins that can be converted into fibrils to enhance functional properties such as gelation, emulsification, and foaming. A model fibrillated milk protein concentrate (MPC) was developed by mixing micellar casein concentrate (MCC) with fibrillated milk whey proteins. Similarly, a control model MPC was obtained by mixing MCC with milk whey proteins. The resulting fibrillated model MPC and control model MPC contained 5% protein and a ratio of casein to whey proteins similar to milk. The objective of the current study was to understand the rheological characteristics of fibrillated and control model MPC during acid gelation, using Förster resonance energy transfer (FRET) to assess small amplitude oscillation and casein–whey protein interaction. The results from the FRET index images showed greater interactions between caseins and whey proteins in fibrillated model MPC compared with the moderate and uniform interactions in control model MPC gels. Rheological study showed that the maximum storage modulus of acid gel of fibrillated model MPC was 546.9 ± 15.5 Pa, which was significantly higher than acid gel made from control model MPC (336.9 ± 11.3 Pa), indicating that fibrillated model MPC produced a firmer gel. Therefore, it can be concluded that acid gel produced from fibrillated model MPC was stronger than control model MPC. Selective fibrillation of the whey protein fraction in MPC can be used to improve gelation characteristics of acid gel type products.

[2] Rathod, G., D.L. Boyle, and J.K. Amamcharla. 2022. Acid gelation properties of fibrillated model milk protein concentrate dispersions. J. Dairy Sci. 105:4925–4937

Keywords: Fibrillated whey proteins, acid gelation, Förster resonance energy transfer (FRET), protein interactions

Introduction

Major milk proteins are composed of caseins and whey proteins. In milk, casein micelles are present in a colloidal state and stabilized by surface (zeta) potential and steric stabilization due to protruding κ-CN hairs (Fox et al., 2015). When the pH of milk is reduced to 4.6 by gradual acidification, the surface potential on the casein micelles is diminished and casein micelles form a 3-dimensional network that entraps other constituents and consequently creates a homogeneous gel matrix (Donato et al., 2007). Acid gel properties such as firmness and mechanical strength are important for overall product quality and consumer acceptability (Peng et al., 2009). Acid gelation properties are best measured by rheological parameters such as storage modulus and complex viscosity (Lucey et al., 1997).

Currently, several processes are used extensively to improve the quality and stability of acid gels. Among them, the heating of milk before acid gelation is a common practice because it denatures whey proteins, allowing more water to be bound and the formation of a firm gel (Lucey et al., 1997; Anema et al., 2004; Lee and Lucey, 2004). Therefore, milk is heated to 90 to 95°C before acid gelation to denature whey proteins and to promote casein and whey protein interactions, specifically between κ-CN and β-LG (Gunasekaran and Solar, 2012). Casein–whey protein interactions during heating and acid gelation can be studied using the Förster resonance energy transfer (FRET) technique (Sahoo, 2011; Okamoto and Sako, 2017). Another approach to improving gelation characteristics is to incorporate additional milk proteins such milk protein concentrates and isolates and whey protein concentrates and isolate, as proteins are mainly responsible for the gel formation (Modler et al., 1983: Marafon et al., 2011; Karam et al., 2013).

However, these additions contribute to increased costs. Hence, addition of gums and texture modifiers such as guar gum and low methoxyl pectin is another cost-effective method to improve acid gelation properties and gel strength (Baba et al., 2018; Khubber et al., 2021). The addition of gums and texture modifier improves gel by forming a dense network, which increases viscosity, water holding, and overall gel strength.

Converting globular proteins into fibrils has the potential to improve acid gelation characteristics because the fibrillar form has a good network-forming ability (Loveday et al., 2017). Most commonly, fibrils are prepared by heating an acidified protein solution to 80°C at pH 2 for 5 to 20 h. Unlike native globular proteins, fibrils have a high aspect ratio, with a length of a few micrometers and a diameter of a few nanometers. The conversion of native globular proteins such as whey proteins opens the protein structure and exposes more reactive groups that favor protein-protein interactions, enabling the formation of a close-knit acid gel (Loveday et al., 2012; Munialo et al., 2014; Mohammadian and Madadlou, 2016). In a previous study (Rathod and Amamcharla, 2021), milk whey protein isolates (mWPI) were converted into fibrillated mWPI, and a novel fibrillated model milk protein concentrate (MPC) was subsequently developed by selective fibrillation of whey proteins, followed by mixing with micellar casein concentrate (MCC) to achieve a ratio of caseins to whey proteins similar to milk. The fibrillated model MPC showed a higher viscosity and consistency compared with the control model MPC. In the current study, fibrillated model MPC was used for gelation studies along with control model MPC. The objective was to understand the rheological characteristics during acid gelation of the newly developed fibrillated model MPC. Further, the FRET technique was also used to understand the interactions between caseins and fibrillated whey proteins.

Material and Methods

No animals were used in this study, and ethical approval for the use of animals was thus deemed unnecessary.

Experimental Approach

Two lots of mWPI [4.3% moisture, 91.6% true protein (87.6% whey protein and 12.4% casein), 1.4% lactose, and 2.1% ash] and 1 lot of MCC [5.76% moisture, 85.5% true protein (7.6% whey protein and 92.4% casein)] were procured from a commercial supplier as powders. A simulated control model MPC was prepared by mixing reconstituted mWPI (2% protein) with reconstituted MCC (8% protein) to achieve a similar ratio of caseins to whey proteins as in milk. The fibrillated model MPC was likewise prepared by mixing pH-adjusted fibrillated mWPI (2% protein) with reconstituted MCC (8% protein) as described by Rathod and Amamcharla (2021). Control and fibrillated model MPC dispersions were heat treated and subsequently acidified to form a gel. Next, FRET analysis was carried out to understand protein-protein interactions between casein and whey proteins in control and fibrillated model MPC. Further, rheological properties of control and fibrillated model MPC were analyzed and compared. The experiment was replicated twice, using 2 independent lots of mWPI.

Preparation and characterization of simulated control and fibrillated model MPCs

Simulated control and fibrillated model MPC were prepared following the protocol described by Rathod and Amamcharla (2021). Initially, mWPI powders were reconstituted to 2% (wt/wt) solution on a protein basis using distilled water and stored overnight at 4°C to ensure complete rehydration. The following day, the mWPI solution was divided into 2 equal parts. One part was used as a control without any further treatment, while the pH of the second part was adjusted to 2.0 using 6 N hydrochloric acid and stored overnight at 4°C. The pH-adjusted mWPI

solution was heated to 80°C and maintained at 80°C for 20 h under continuous gentle stirring using a magnetic stirrer to fibrillate the whey proteins, followed by immediate cooling to 4°C. Subsequently, the fibrillated mWPI solution was neutralized back to pH 6.7 using 3 N sodium hydroxide under gentle stirring to produce pH-adjusted fibrillated mWPI.

Simultaneously, MCC powder was also reconstituted to 8% (wt/wt) on a protein basis using distilled water at 50°C. Mixing was performed using an overhead stirrer (Caframo) at 750 rpm for the first 15 min, followed by continuous stirring at 500 rpm for an additional 30 min. The MCC dispersion was stored overnight at 4°C and then divided into 2 equal parts the following day. The first part of the reconstituted MCC was mixed with nonfibrillated mWPI using a magnetic stirrer (50 rpm), resulting in control model MPC with 5% (wt/ wt) protein and a casein-to-whey protein ratio similar to milk. Similarly, fibrillated model MPC was also prepared by mixing pH-adjusted fibrillated mWPI solution and the second part of the reconstituted MCC, resulting in fibrillated model MPC with 5% (wt/wt) protein similar to control model MPC. Sodium azide was added at the rate of 0.02% (wt/wt) in both types of MPC and stored in the refrigerator.

Confirmation of the presence of fibrils in model MPCs

Both the model MPCs dispersions were characterized in terms of thioflavin T fluorescence value, transmission electron microscopy, and viscosity using the respective methods as described by Rathod and Amamcharla (2021) to confirm the presence of fibrils.

Acid-base titration curve.

Acid-base titration profiles of control and fibrillated model MPC were constructed by using the method described by Meletharayil et al. (2015). Briefly, both control and fibrillated

MPC samples were titrated from their initial pH of 6.7 to pH 3.0 by adding 0.2 mL of 0.5 N hydrochloric acid in increments under constant stirring. The pH was recorded after each 0.2 mL incremental addition of hydrochloric acid. Once the pH reached 3.0, the same sample was back-titrated to pH 7.0 by 0.2-mL incremental additions of 0.5 N sodium hydroxide under constant stirring. The pH was also recorded after each 0.2-mL addition of sodium hydroxide. The pH was recorded using an Accumet AP110 portable pH meter (Fisher Scientific). Similarly, the acid-base titration curves of nonfibrillated mWPI and fibrillated mWPI solutions were constructed through incremental addition of 0.1 mL instead of 0.2 mL of acid and base for acidification and neutralization, respectively. Samples were analyzed in triplicate using 2 independent lots, and results were averaged.

FRET (Förster resonance energy transfer) microscopy

The FRET technique is widely used in biomedical and molecular biology to understand intermolecular or intramolecular interactions. The technique is based on the nonradiative (dipole-dipole) energy transfer from a donor fluorescent dye to an acceptor fluorescent dye that is bound to a molecule or molecules of interest (Hochreiter et al., 2019) when the donor and acceptor dyes are in close proximity (<10 nm). Figure 4.1 shows the working principle of the FRET technique. Jensen et al. (2015) used the FRET technique to study the function of the milk-clotting enzyme chymosin from bovine and camel sources. In the current study, caseins were labeled with a donor dye and whey proteins were labeled with an acceptor dye to determine the casein– whey protein interactions in MPC. As shown in Figure 4.1, no energy transfer occurs between the donor and acceptor when the labeled casein and whey proteins are not interacting or are separated by a distance greater than the Förster radius. However, radiation-free energy transfer between the donor and acceptor dyes occurs when the

labeled proteins are within the Förster radius (<10 nm). The Förster radius is defined as the distance at which 50% of the excited donors transfer energy to acceptors. As the labeled proteins come close during interaction, the acceptor and donor dyes are within their Förster radius, leading to the accepter dye emitting the accepter wavelength (560 nm) as shown in Figure 4.1.

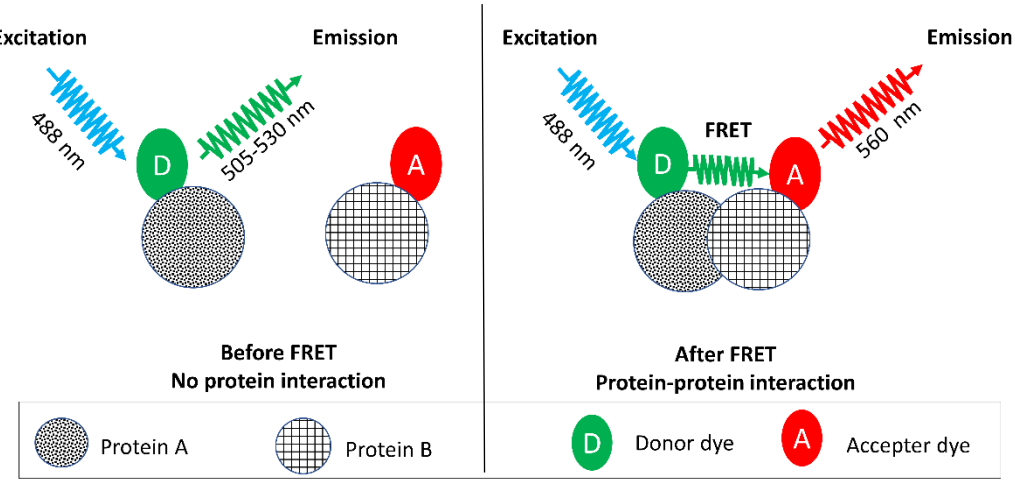

Figure 4.1 Schematic diagram describing Förster resonance energy transfer (FRET) effect.

Fluorescent dye labeling and sample preparation for FRET analysis.

The FRET analysis was carried out using the fluorescent dyes ATTO 488 NHS ester and ATTO 532 NHS ester (ATTO-TEC GmbH) as donor and acceptor dyes, respectively (Glover et al., 2020). For labeling of the proteins in the MCC, the pH of the MCC dispersion (8% protein) was increased to 8.3 using 1 M sodium bicarbonate and subsequently divided into 2 equal parts. ATTO 488 NHS ester (1 mg) was dissolved in dimethyl sulfoxide (20 µL) and added to the first part of MCC dispersion (1.2 mL) in Eppendorf tubes, as suggested by Glover et al. (2020), and then mixed thoroughly. Further, the mixture was intermittently vortexed every 15 min for up to 1

h. Fluorescent dye was not added to the second part of the MCC, which was considered unlabeled. Subsequently, the pH of both labeled and unlabeled MCC solutions was adjusted to pH 7 using 1 N hydrochloric acid. Similarly, the mWPI solution (2% protein) was divided into 2 equal parts. The first part (0.7 mL) was labeled with 0.15 mg ATTO 532 NHS ester dissolved in dimethyl sulfoxide (3 μL) and was termed as labeled. The second part did not receive a fluorescent dye and was termed as unlabeled.

For FRET analysis, the donor-only sample was prepared by mixing 1 part of ATTO 488 MCC solution (250 μL) with 1 part of unlabeled mWPI solution (250 μL); this sample was termed as the donor-only control model MPC. An accepter-only sample was prepared by mixing 1 part of unlabeled MCC solution with 1 part of ATTO 532 mWPI, and it was termed as the accepter-only control model MPC. The FRET sample was prepared by mixing 1 part of ATTO 488 MCC with 1 part of ATTO 532 mWPI solution, and it was termed as the FRET control model MPC. Similarly, donor only fibrillated model MPC, accepter-only fibrillated model MPC, and FRET fibrillated model MPC were prepared by using fibrillated mWPI solution in place of the mWPI solution. Acid gels of all control and fibrillated model MPC were prepared by heating labeled and unlabeled model MPC dispersions to 90°C for 10 min, followed by cooling to 30°C. Then, a precalculated amount of glucono-δ-lactone was added and mixed for 1 min, followed by incubation at 30°C for 4 h. The acid gels were used to acquire confocal laser scanning microscopic images for FRET analysis.

Imaging of acid gel samples for FRET analysis.

All acid gels prepared from control and fibrillated model MPC samples were carefully mounted on glass slides, avoiding gel disruption, and viewed on an Axioplan 2 microscope

equipped with confocal laser scanning LSM 5 Pascal (Carl Zeiss) version 3.2 SP2. A Plan-Apochromat ×100/1.4 oil objective was used for image acquisition. The donor-only acid gels were excited with 488 nm argon laser line with primary dichroic-HFT 488/543/633 to excite ATTO 488 NHS ester, while secondary dichroic NFT 545 was used to separate emission from the fluorescent dye. The emission signal was collected using a 505- to 530-nm band pass filter with the image collected by channel 2 [photomultiplier tube for detecting ATTO 488 NHS ester (green)]. The acceptor-only acid gel was excited with a 543-nm helium-neon laser line with primary dichroic HFT 488/543/633 to excite ATTO 532 NHS ester, while secondary dichroic NFT 545 was used to separate emission from the fluorescent dye. The emission signal was collected using a 560-nm long-pass filter with image collected by channel 1 [for detecting ATTO 532 NHS ester (red)]. The FRET acid gels were excited with a 488-nm argon laser line with primary dichroic- HFT 488/543/633 to excite the fluorescent dye, while secondary dichroic NFT 545 was used to separate emission from the fluorescent stain. The emission signal was collected using a 560-nm long-pass filter with images collected by channel 1 [for detecting FRET (blue)]. The captured 8-bit images were maximized using a dynamic range indicator associated with the acquisition software (Hochreiter et al., 2019).

Analysis of FRET index.

Donor-only, accepter-only, and FRET images were analyzed to derive the FRET index, using a FRET Analyzer plugin of ImageJ software (version 1.53f; ImageJ, National Institutes of Health). Donor and accepter images were analyzed for bleed-through analysis and checked for standard error and Pearson r value. The FRET images were analyzed for the FRET index, which was further analyzed using the color counter plugin of ImageJ software to get the hexacolor code with a pixel number to quantify the concentration of each color in the FRET index images to

quantify the FRET index for both control and fibrillated model MPC. Hexacolor codes were converted to RGB (red, green, blue) combination and further clustered into black, blue, red, yellow, and white depending upon the dominance of the R, G, or B value in the RGB combination and their respective broad color classification.

Preparation of acid gels from control and fibrillated model MPCs

Both control and fibrillated model MPC dispersions were heated to 90°C for 10 min, immediately cooled to 4°C, and kept at refrigerated temperature overnight for further analysis. The following day, model MPC dispersions were tempered to 30°C, 2 g of glucono-δ-lactone (Fisher Scientific) was added per 100 mL, and the solutions were mixed using a magnetic stirrer for 1 min. Immediately afterward, part of the model MPC mixed with glucono-δ-lactone was transferred to a temperature- controlled water bath (Cole Parmer) maintained at 30°C for continuous pH measurement using the portable pH meter. Simultaneously, the remaining model MPC was used to monitor rheological characteristics during acid gelation.

Small amplitude oscillation.

Acid gel formation was monitored using a stressstrain- controlled rheometer (MCR-92 Anton Paar) with a cup-and-bob geometry consisting of a coaxial cylinder (bob length, 60 mm; bob diameter, 38.7 mm, and cup diameter, 42 mm). The cup-and-bob geometry was preheated to 30°C. Vegetable oil was added to the model MPC surface to avoid evaporation during measurement. During acid gelation, the sample oscillated at a constant frequency of 1 Hz with an applied strain of 0.5%, which caused minimal disruption during the development of the gel network (Peng et al., 2009). Measurements were taken every 5 min until the pH reached 4.6. The derived parameters included storage modulus (G′) and loss tangent (LT). Gelation was arbitrarily

defined as the moment when the G′ of gels was greater than 1 Pa (Peng et al., 2009). Samples were analyzed in duplicate using 2 independent lots, and results were averaged.

Statistical Analysis.

Statistical analysis was performed using Excel (Microsoft Corp., Redmond, WA). One-way ANOVA and Tukey's multiple range test were done using SAS Version 9.4 (SAS Institute Inc.).

Results and Discussion

Characteristics of control and fibrillated model MPCs

Thioflavin T values for control and fibrillated model MPC were 247.1 ± 11 AU and 367.7 ± 33.2 AU, respectively, and found to be significantly ($P < 0.05$) different. A higher thioflavin T value for the fibrillated model MPC indicated the presence of whey protein fibrils. In addition to a higher thioflavin T value, the presence of fibrils in the fibrillated model MPC was also confirmed using TEM (images not shown) and found to be similar to a previous study (Rathod and Amamcharla, 2021). Importantly, the commercial mWPI used in this study for fibrillation contained casein in addition to whey proteins. Coppola et al. (2014) and Carter et al. (2021) reported the possibility of a fraction of caseins (up to 1–20%) leaking through the microfiltration membrane along with whey proteins depending on the processing conditions, such as filtration temperature. However, concentrations of casein in WPI derived from cheese whey are low and are attributed to the higher selectivity of rennet enzyme compared with microfiltration membranes (Carter et al., 2021). Casein fractions such as αS1-CN, αS2-CN, β-CN, and κ-CN in mWPI intended for fibrillation of whey proteins can have a chaperone effect and can inhibit the whey protein fibrillation (Bhattacharyya and Das, 1999; Morgan et al., 2005; Treweek et al., 2011). However, previous studies were carried out under nearly neutral pH

conditions. In addition, β-CN also acts as a molecular chaperone at high temperatures (>75°C) and neutral pH (O'Kennedy and Mounsey, 2006; Kehoe and Foegeding, 2011; Yong and Foegeding, 2008), but it is unclear whether the chaperone-like function persists during heating under acidic pH conditions. Recently, Dave et al. (2016) studied the chaperone-like effect of β-CN in the context of β-LG fibrillation at pH 2 and 80°C. The authors reported that the fibril formation was somewhat retarded at lower β-CN concentrations. However, at higher concentrations of β-CN, whey protein fibrillation was not further inhibited by the presence of β-CN and was attributed to the diversion of β-CN monomers, peptides, or both into self-assembled micelles. Reducing sodium dodecyl sulfate-polyacrylamide gel electrophoresis images from a previous study (Rathod and Amamcharla, 2021) showed a clear band for β-CN in nonfibrillated mWPI. However, the β-CN band was absent in fibrillated mWPI at pH 2 as well as at pH 6.7. In addition, TEM images from a previous work by Rathod and Amamcharla (2021) showed the presence of visible fibrils in fibrillated mWPI as well as in fibrillated model MPC. Similarly, TEM imaging of whey protein fibrils (Figure 4.2) from the current work confirms the presence of fibrils in fibrillated model MPC. Further, control and fibrillated model MPC were further evaluated in terms of apparent viscosity (at 100 S−1) and found to be 12.69 ± 0.87 and 17.3 ± 2.54 mPaS, respectively; these values were also significantly ($P < 0.05$) different from each other. These results showed that the presence of fibrils increased the viscosity of the MPC dispersions. Similar findings were reported by Rathod and Amamcharla (2021) and other studies on whey protein fibrils (Loveday et al., 2012; Dave et al., 2013; Farrokhi et al., 2019).

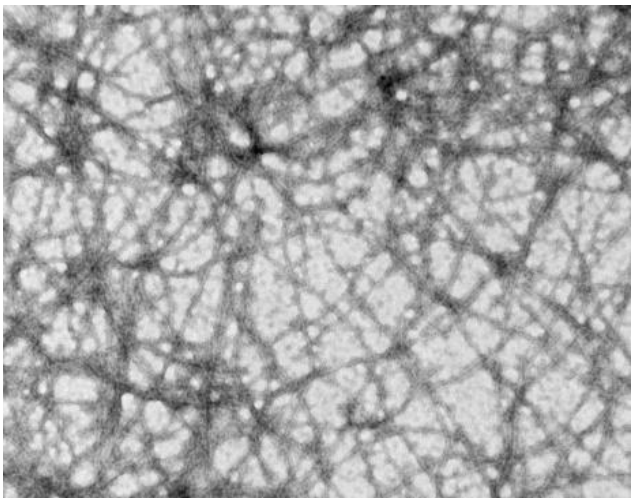

Figure 4.2 A typical transmission electron microscopic image of fibrillated milk whey protein isolate (mWPI) (Scale-200 nm, Magnification-34000x).

Acid-Base titration curve.

The acid-base titration curves of control and fibrillated model MPC are shown in Figure 4.3. Figure 4.3A shows the change in pH with respect to the addition of 0.5 N HCl. The control and fibrillated model MPC required the same amount of acid (2 mL) to reach pH 5.1 and thereby exhibited a similar buffering capacity. Both model MPC contained the same concentration of caseins, as they were prepared by mixing the same amount of MCC; therefore, both MPC contained the same colloidal calcium phosphate (CCP), which was in equilibrium with calcium and phosphate of the serum phase (Eshpari et al., 2016). Acidification of the model MPC dispersions to pH ~5.0 led to a complete solubilization of CCP (Corredig et al., 2019). However, below pH 5.0, the buffering capacity was mostly contributed by the caseins and their side groups as most of the CCP were already dissolved from casein micelles (Lucey et al., 1996).

The control model MPC required 4 mL of acid to reduce the pH from 5.1 to 3.0. Whey proteins in the control model MPC contributed to buffering capacity between pH 4.0 and 3.0,

which was attributed to the presence of acidic amino acids (Salaün et al., 2005). However, the fibrillated model MPC needed 4.6 mL of acid to attain a similar drop in pH. During acidification between pH 5.1 and 3.0, the fibrillated model MPC required a higher amount of acid than the control model MPC to lower the pH, possibly due to the presence of fibrillated whey proteins in the fibrillated model MPC. To further understand the differences in buffering capacity between native whey proteins and whey protein fibrils, nonfibrillated mWPI solution (2% wt/wt) and fibrillated mWPI solution (2% wt/wt) were analyzed in terms of their acid–base titration curves, similar to model MPC. Figure 4.3B shows that the fibrillated mWPI required a higher amount of acid to change the pH from 6.7 to 3 than nonfibrillated mWPI.

During back-titration from pH 3.0 to 7.0 (Figure 4.3C), the fibrillated model MPC needed more alkali (7.2 mL) to reach pH 7.0 from pH 3.0 than the control model MPC (6.2 mL). A higher alkali requirement for the fibrillated model MPC could be attributed to the presence of whey proteins such as fibrils in this MPC. During the fibrillation process, native globular whey proteins are hydrolyzed and rearranged into multistranded twisted structures that are rich in β-sheets perpendicular to the fibril axis (Akkermans et al., 2008; Kroes-Nijboer et al., 2012; Loveday et al., 2017). The structural rearrangement changes the position and interactions of charged groups, possibly due to the higher buffering capacity of the fibrillated model MPC compared with the control model MPC. To confirm the role of whey protein fibrils in acid-base buffering curves, nonfibrillated mWPI and fibrillated mWPI solutions that were previously acidified to pH 3.0 during acid titration were back-titrated to pH 7.0 with incremental amounts of 0.5 N NaOH. Fibrillated mWPI needed a higher amount of alkali to reach pH 7.0 than nonfibrillated mWPI (Figure 4.3D). This observation proves that fibrillated mWPI is the reason for the higher buffering capacity of fibrillated model MPC. Figure 4.3C showed that no change

occurred in the alkali addition rate during neutralization in the pH range of 5.1 to 7.0. During the acidification process, CCP continued to solubilize from the casein to the serum phase. When the same solution with destabilized CCP structure was neutralized during back-titration with alkali, the CCP structure was not fully recovered (Ezeh and Lewis, 2011); thereby, CCP may not have provided buffering capacity at pH 5.1. The buffering capacity of proteins can mostly be attributed to ionizable amino acid side groups, carboxyl, and amine groups liberated during enzymatic hydrolysis (Luo et al., 2018). Similarly, whey proteins were hydrolyzed (Akkermans et al., 2008) during acidification and subsequently rearranged into fibrils during the fibrillation process. Therefore, the differences in buffering capacity between control and fibrillated model MPC could be due to the presence of fibrils as functional groups rearranged during the fibrillation process, resulting in different buffering capacities at a lower pH range.

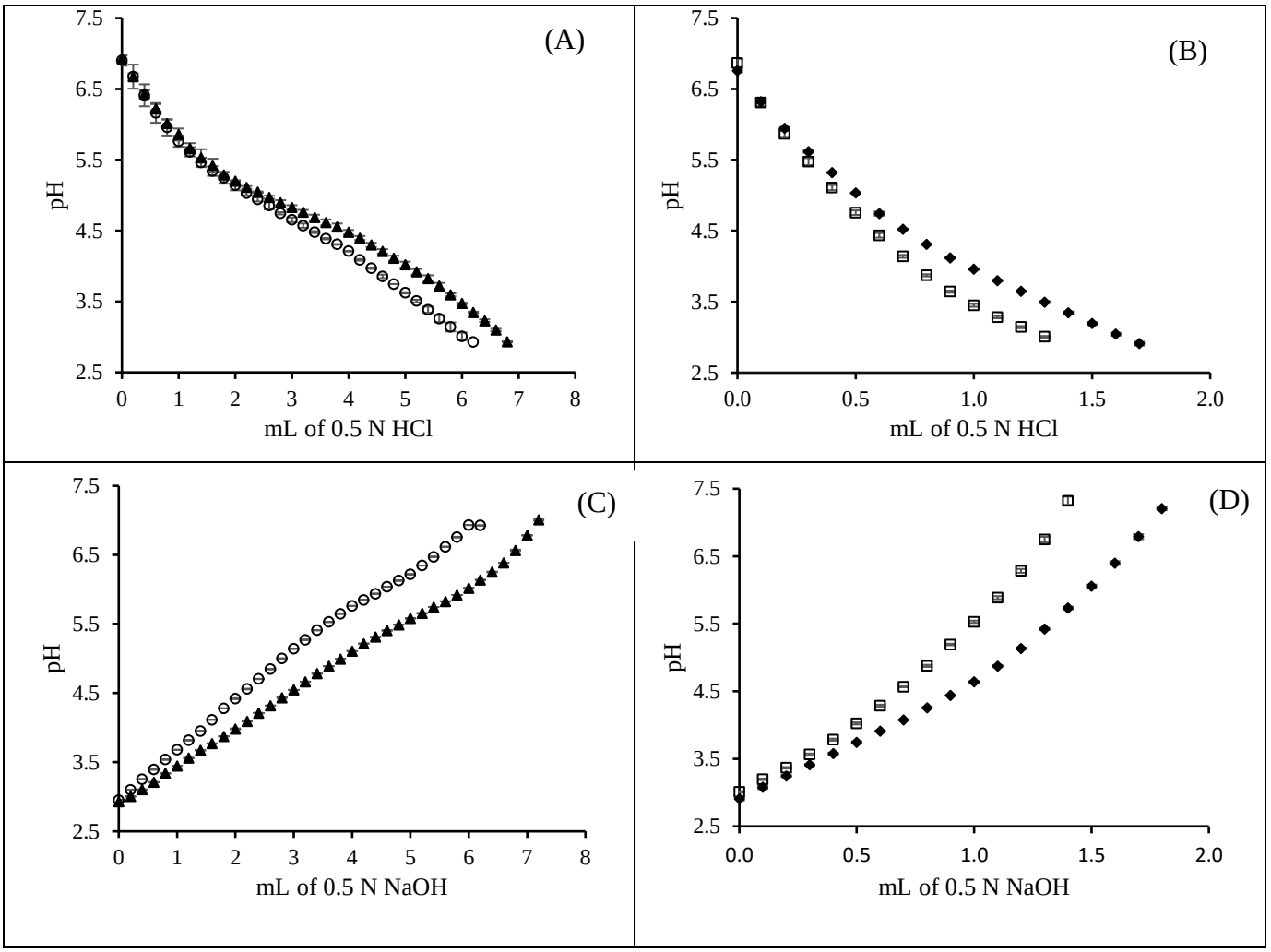

Figure 4.3 Acid-Base titration curves (A) Acidification of control and fibrillated model milk protein concentrates (MPC) from pH 6.7 to 3.0, (B) Acidification of non-fibrillated and fibrillated milk whey protein isolates (mWPI) solution from pH 6.7 to 3.0, (C) Neutralization of control and fibrillated model MPC from pH 3 to 7, (D) Neutralization of non-fibrillated and fibrillated milk mWPI solution from pH 3 to 7 (○- Control Model MPC, ▲-Fibrillated Model MPC, □-Non-fibrillated mWPI, ♦-Fibrillated mWPI). n=2.

FRET microscopy.

Figure 4.4 shows images from the FRET analysis of control and fibrillated model MPC. The donor-in-donor-only image (Figure 4.4A) shows a bright fluorescent green, which confirmed labeling of proteins in MCC and their distribution in the acid gel prepared from control model MPC. The FRET-in-donor-only image (Figure 4.4B) shows a very low fluorescence signal, indicating negligible crosstalk or bleed-through of ATTO 488 dye in the FRET signal. The accepter-in-accepter-only image (Figure 4.4C) shows a fluorescent red, which confirmed the labeling of whey proteins in mWPI in the acid gel. The color intensity of the FRET-in-accepter-only image (Figure 4.4D) is also low, indicating a minimal bleedthrough of ATTO 532 in the FRET signal. Similar to the control model MPC, images of the fibrillated model MPC (donor-in-donor only [Figure 4.4H], FRET-in-donor only [Figure 4.4I], accepter-in-accepter only [Figure 4.4J], FRET-in-accepter only [Figure 4.4K)] also indicate minimal bleed-through and crosstalk. Additionally, bleed-through analysis of donor-FRET (Figures 4.4A and 4.4B; Figures 4.4H and 4.4I) and accepter-FRET (Figures 4.4C and 4.4D; Figures 4.4J and 4.4K) images in control and fibrillated model MPC, respectively, also showed a low standard error and Pearson r value greater than 0.95 (data not shown), indicating that the FRET interactions were highly significant ($P < 0.05$) in both MPC during the gelation process. These observations support that the proteins in MCC and mWPI were interacting in the acid gels.

The FRET index image of control model MPC (Figure 4.5A) was obtained by confocal laser scanning microscopic images (Figures 4.4E, 4.4F, and 4.4G) using ImageJ software. Similarly, the FRET index image of fibrillated model MPC (Figure 4.5B) was obtained by processing confocal laser scanning microscopic images (Figures 4.4L, 4.4M, and 4.4N). In the FRET index images (Figures 4.5A and 4.5B), the black-colored area indicates no FRET

interaction between proteins in MCC suspension and mWPI solution, while the colors ranging from blue to red indicate a moderate to higher number of molecular interactions within the Förster radius for these 2 fluorochromes. However, white indicates saturation of the detector caused by an extremely high number of protein-protein interactions. Clustering of the color pixel of FRET index images showed 4.3% white, followed by 0.7% yellow, 92.9% red-orange, 1.4% blue, and 0.7% black for the control model MPC. However, the fibrillated model MPC showed 61.0% white, followed by 3.7% yellow, 28.5% red-orange, 0.1% blue, and 6.8% black. These findings suggest that the fibrillated model MPC had higher protein-protein interactions between MCC and fibrillated mWPI than the control model MPC. Fibrillated model MPC contained whey protein as fibrils with ordered β-sheets (Dave et al., 2013) and exposed disulfide bonds. Also, fibrils have a simpler secondary structure (Loveday et al., 2017) that is more open than the tertiary and quaternary structure of native proteins (Damodaran, 1997). Consequently, fibrils were more reactive and readily interacted with caseins during heating and acid gelation.

In addition, the FRET index image (Figure 4.5A) and the donor-in-donor only image (Figure 4.4A) collectively show that the acid gel of control model MPC was uniformly structured (denoted by a uniform red-orange area) with little or no porous structure (denoted by the lack of a blue-black area). However, the FRET index image (Figure 4.5B) and donor-in-donor only image (Figure 4.4H) for fibrillated model MPC show pores in the gel structure with protein-dense area. Possible reasons could be higher interactions between caseins and whey proteins and the mounting of the acid gel on glass slides.

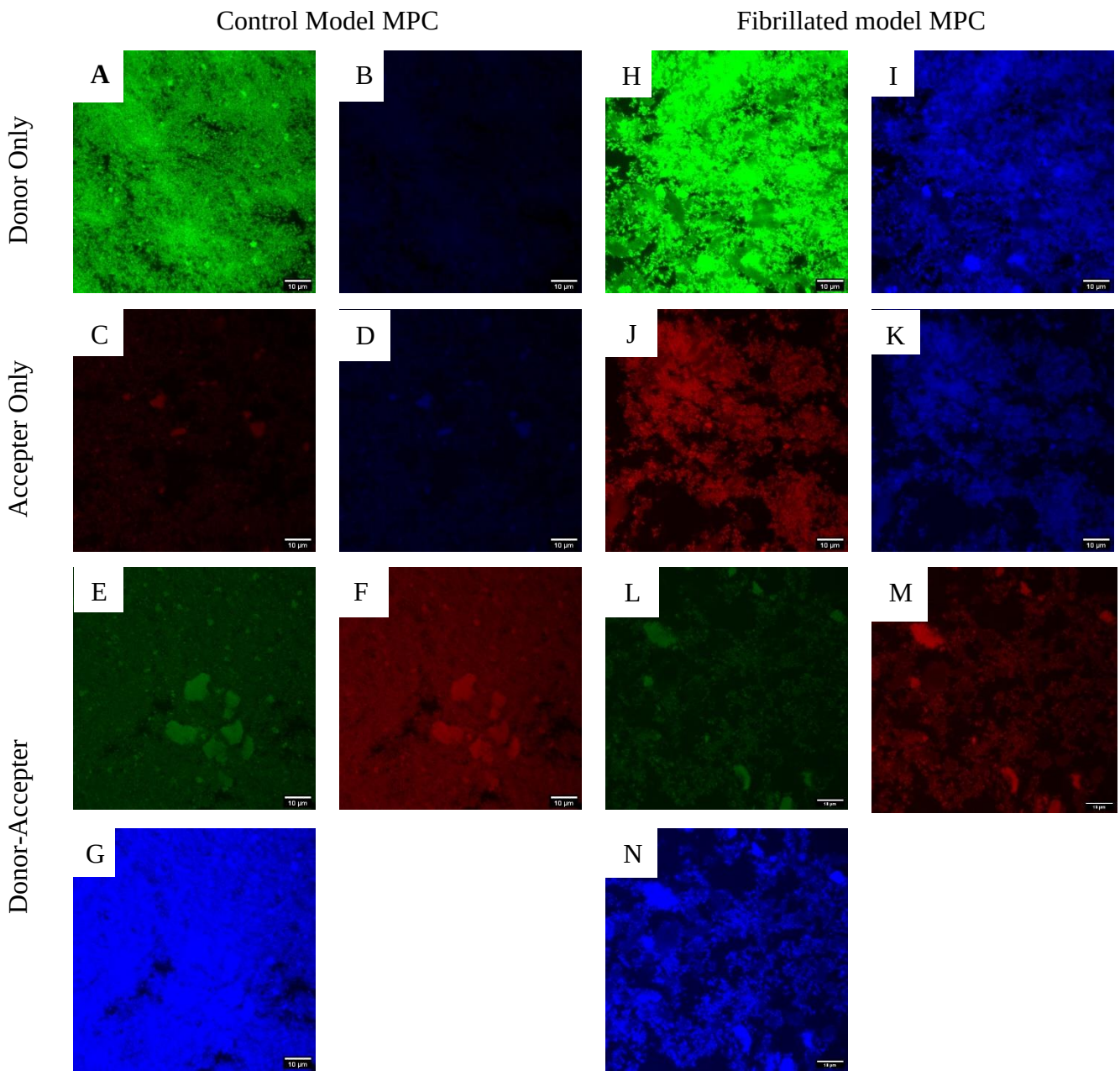

Figure 4.4 Confocal laser scanning microscopic images of control model MPC ((A) donor-in-donor only (B) FRET-in-donor only, (C) accepter-in-accepter only, (D) FRET-in-accepter only (E) donor-in-donor -accepter, (F) accepter-in-donor-accepter, (G) FRET-in-donor accepter) and fibrillated model MPC((H) donor-in-donor only, (I) FRET-in-donor only, (J) accepter-in-accepter only, (K) FRET-in-accepter only (L) donor-in-donor-accepter (M) accepter-in-donor-accepter (N) FRET-in-donor accepter).

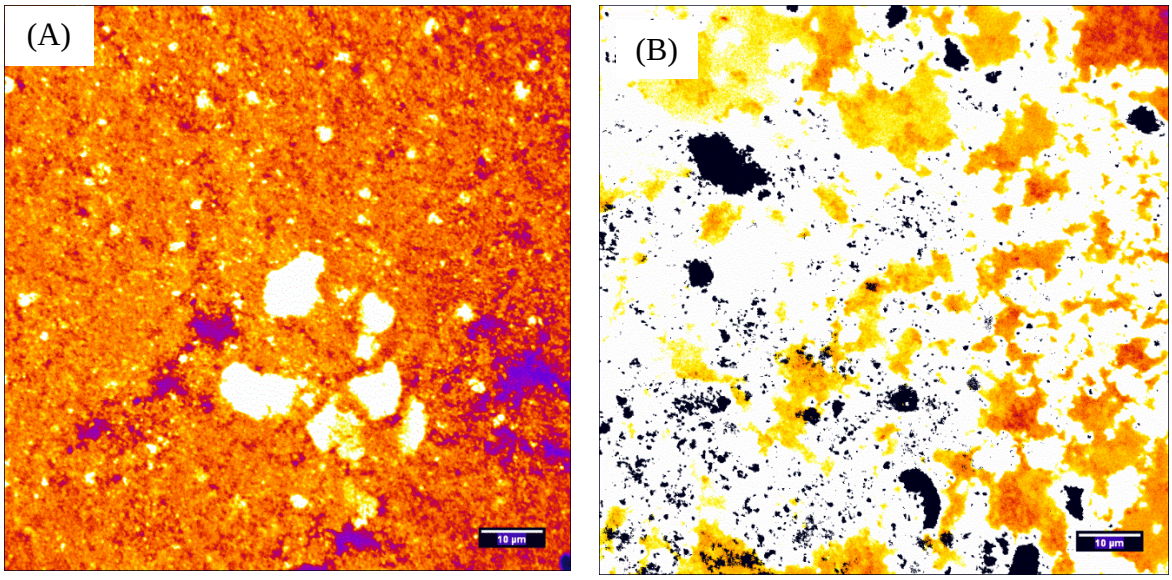

Figure 4.5 FRET (Förster resonance energy transfer) index images of acid gels prepared using control model MPC (A) and fibrillated model MPC (B).

Rheological properties of acid gel prepared from control and fibrillated model MPC

The gelation behavior of control and fibrillated model MPC is shown in Figure 4.6, and extracted gelation parameters are presented in Table 4.1. The gelation times for control model MPC and fibrillated model MPC were found to be 30.0 ± 1.3 and 28.8 ± 3.3 min, respectively, and they were not significantly different ($P < 0.05$) (Table 4.1). However, the gelation pH for the control model MPC and the fibrillated model MPC was 5.46 ± 0.03 and 5.55 ± 0.00, respectively, which were significantly different ($P < 0.05$). The possible reason for early gelation could be attributed to fibrillated whey proteins and very high casein–whey protein interactions in the fibrillated model MPC. During fibril formation, whey proteins are hydrolyzed into peptides and self-arrange to form systematic β-sheet fibrils (Dave et al., 2013; Loveday et al.,2017) with disulfide bonds between the sheets. Fibrils have an open secondary structure with more exposed

reactive groups in comparison to tertiary and quaternary structures of nonfibrillated whey proteins (Loveday et al., 2017). Higher interactions of caseins and fibrillated whey proteins were also evident from the FRET analysis.

Both control and fibrillated model MPC showed a gradual increase in storage modulus (G′) (Figure 4.6A). However, once gelation started, the increase in G′ was greater for fibrillated model MPC than for control model MPC. The possible reason for this behavior could be the presence of MCC, which was 80% of the total protein, and resistance to pH change through CCP until CCP was completely dissolved at ~pH 5.1. Gelation behavior is mainly governed by casein in MCC at a pH greater than 5.1. However, whey proteins or fibrils and their interactions with casein influence the gelation behavior at a pH below 5.1. Overall, the fibrillated model MPC showed a higher G′ over the entire gelation time until the pH reached 4.6. The G′ of the control model MPC increased to 336.9 ± 11.3 Pa (G′ max) at pH 4.79, which occurred at 158.8 ± 3.9 min; afterward, the G′ declined to 284.8 ± 10.3 Pa at pH 4.6. However, the G′ of the fibrillated model MPC increased to 546.9 ± 15.5 Pa (G′ max) at pH 4.64, which occurred at 209.3 ± 9.9 min; afterward, the G′ slightly declined to 541.8 ± 15.9 Pa at pH 4.6. The G′ of the fibrillated model MPC was significantly higher than that of the control model MPC, which indicates that the fibrils contributed to a firmer gel (Table 4.1). The G′ represents solid-like elastic behavior, hence a higher storage modulus implies higher solid-like behavior and elasticity of fibrillated model MPC (Cruz et al., 2013).

The plot between LT and pH (Figure 4.6B) shows that the control model MPC had higher LT than the fibrillated model MPC until pH 5.15, after which the fibrillated model MPC showed slightly higher LT till pH 4.8. Thereafter, the control model MPC showed an increased LT again until the final pH reached 4.6. For both MPC, the value of LT was below 1, which shows that the

elastic behavior dominated (Mariotti et al., 2009) once gelation started in both MPC until pH 4.6. Figure 4.6B also shows that LT of the fibrillated model MPC was lower than the control model MPC. This observation suggests that acid gels of the fibrillated model MPC were more elastic (solid-like) than the control model MPC after the gelation point. Further, a maximum LT was seen for both MPC near pH 5.2, which is slightly above previously reported results for stirred yogurt (pH 5.0–5.1; Lee and Lucey, 2006). The gelation behavior of the control model MPC was found to be similar to earlier reported acid gels from MPC (Meletharayil et al., 2015, 2018). However, the fibrillated model MPC formed a stronger elastic gel than the control model MPC owing to strong interaction between whey protein fibrils and casein, which can be seen in the FRET index image (Figure 4.5B).

Table 4.1 Rheological parameters obtained during gelation of acid gels of control and fibrillated model MPC (From the plot of storage modulus (G′) v/s pH).

Sample		Control model MPC	Fibrillated model MPC
Gelation point	Time (min)	30.0±1.3[a]	28.6±3.3[a]
	pH	5.46±0.03[b]	5.55±0.02[a]
At Max. Storage Modulus	G′ (Pa)	336.9±11.3[b]	546.9±15.5[a]
	pH	4.79±0.01[a]	4.64±0.01[b]
	Time (min)	158.8±3.9[b]	209.3±9.9[a]
Storage Modulus at pH 4.6 (Pa)		284.8±10.3[b]	541.8±15.9[a]

[a-b] Mean within a row with different superscripts differ ($P<0.05$); n=2

[1]From the plot of storage modulus (G′) versus pH (Figure 4.6).

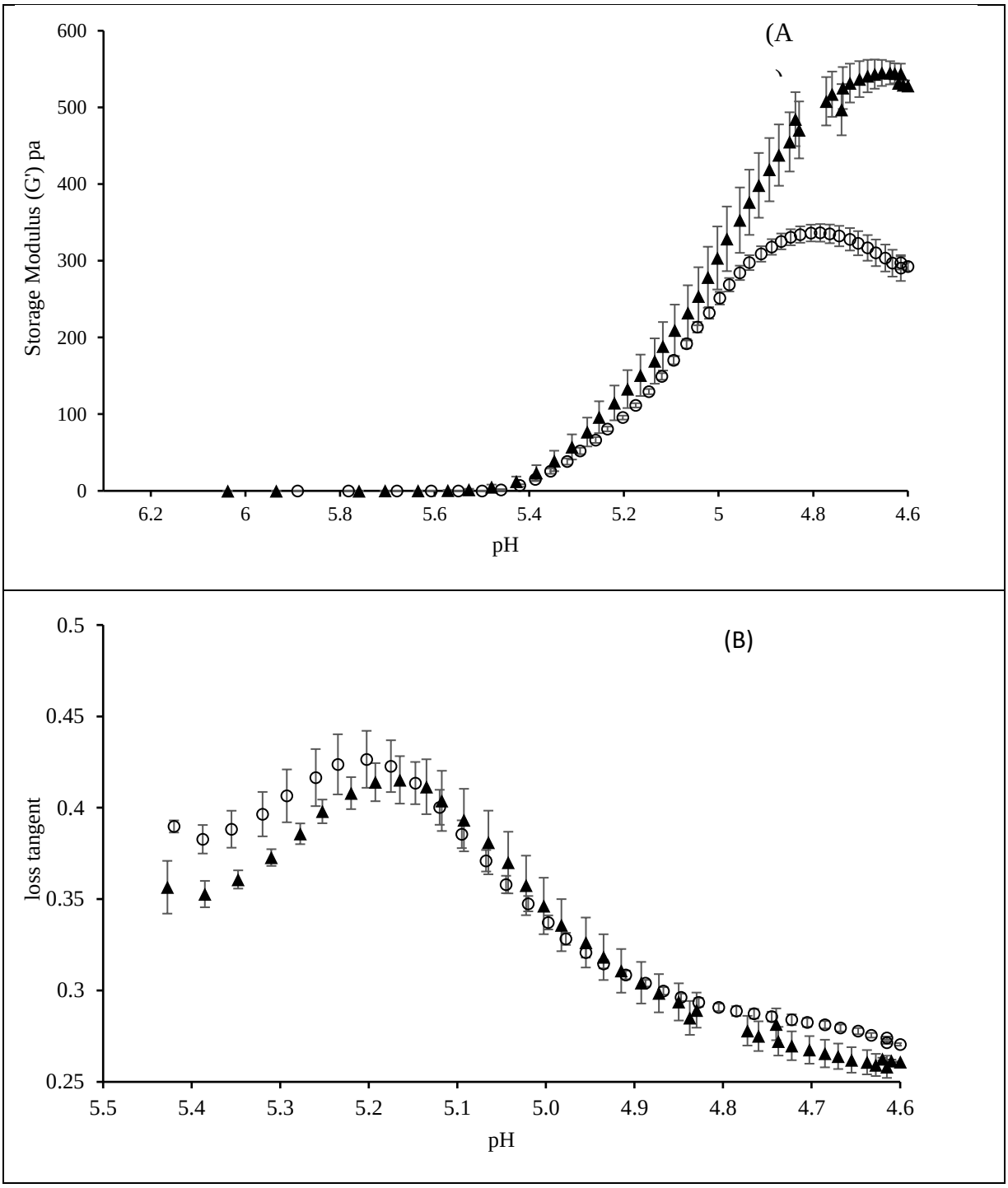

Figure 4.6 Changes in rheological behavior during gelation of control and fibrillated model milk protein concentrates (MPC) (A) storage modulus (G¢) v/s pH during gelation, (B) Loss tangent v/s pH during gelation (○- Control Model MPC, ▲-Fibrillated Model MPC). n=2.

Conclusion

The acid gelation properties of a control model MPC and a newly developed fibrillated model MPC were studied. The molecular interactions between casein and whey proteins were observed to be higher in the fibrillated model MPC compared with the control model MPC, and they consequently produced a firmer acid gel with improved microstructure. The fibrillated model MPC produced a more elastic and solid-like gel compared with the control model MPC. Further, acid gels of the fibrillated model MPC showed a higher gel strength than the control model MPC. It can be concluded that selective fibrillation of whey proteins in fibrillated model MPC can be used to improve acid gelation properties.

Acknowledgements

We are highly thankful to the National Dairy Council and Midwest Dairy Foods Research Center (St. Paul, MN) for their financial support. This project was conducted under Kansas State Research and Extension contribution number 21-157-J. This work was partially supported by the USDA National Institute of Food and Agriculture (Washington, DC) Hatch project 1014344.

References

Akkermans, C., P. Venema, A. J. van der Goot, H. Gruppen, E. J. Bakx, R. M. Boom, and E. van der Linden. 2008. Peptides are building blocks of heat-induced fibrillar protein aggregates of β-lactoglobulin formed at pH 2. Biomacromolecules 9:1474–1479. https://doi.org/10.1021/bm7014224.

Anema, S. G., S. K. Lee, E. K. Lowe, and H. Klostermeyer. 2004. Rheological properties of acid gels prepared from heated pH-adjusted skim milk. J. Agric. Food Chem. 52:337–343. https://doi.org/10.1021/jf034972c.

Baba, W. N., K. Jan, H. A. Punoo, T. A. Wani, M. M. Dar, and F. A. Masoodi. 2018. Techno-functional properties of yoghurts fortified with walnut and flaxseed oil emulsions in guar gum. Lebensm. Wiss. Technol. 92:242–249. https://doi.org/10.1016/j.lwt.2018.02.007.

Bhattacharyya, J., and K. P. Das. 1999. Molecular chaperonelike properties of an unfolded protein, αs-casein. J. Biol. Chem. 274:15505–15509. https://doi.org/10.1074/jbc.274.22.15505.

Carter, B. G., N. Cheng, R. Kapoor, G. H. Meletharayil, and M. A. Drake. 2021. Invited review: Microfiltration-derived casein and whey proteins from milk. J. Dairy Sci. 104:2465–2479. https://doi.org/10.3168/jds.2020-18811.

Coppola, L. E., M. S. Molitor, S. A. Rankin, and J. A. Lucey. 2014. Comparison of milk-derived whey protein concentrates containing various levels of casein. Int. J. Dairy Technol. 67:467–473. https://doi.org/10.1111/1471-0307.12157.

Corredig, M., P. K. Nair, Y. Li, H. Eshpari, and Z. Zhao. 2019. Invited review: Understanding the behavior of caseins in milk concentrates. J. Dairy Sci. 102:4772–4782. https://doi.org/10.3168/jds.2018-15943.

Cruz, A. G., R. N. Cavalcanti, L. M. R. Guerreiro, A. S. Sant'Ana, L. C. Nogueira, C. A. F. Oliveira, R. Deliza, R. L. Cunha, J. A. F. Faria, and H. M. A. Bolini. 2013. Developing a prebiotic yogurt: Rheological, physico-chemical and microbiological aspects and adequacy of survival analysis methodology. J. Food Eng. 114:323– 330. https://doi.org/10.1016/j.jfoodeng.2012.08.018.

Damodaran, S. 1997. Food proteins: An overview. Pages 1–24 in Food Proteins and Their Applications. 1st ed. S. Damodaran and A. Paraf, ed. Marcel Dekker.

Dave, A. C., S. M. Loveday, S. G. Anema, T. S. Loo, G. E. Norris, G. B. Jameson, and H. Singh. 2013. β-Lactoglobulin self-assembly: Structural changes in early stages and disulfide bonding in fibrils. J. Agric. Food Chem. 61:7817–7828. https://doi.org/10.1021/jf401084f.

Dave, A. C., S. M. Loveday, S. G. Anema, and H. Singh. 2016. β-casein will chaperone β-lactoglobulin during nanofibril assembly, but prefers familiar company at high concentrations. Int. Dairy J. 57:39– 43. https://doi.org/10.1016/j.idairyj.2016.02.035.

Donato, L., M. Alexander, and D. G. Dalgleish. 2007. Acid gelation in heated and unheated milks: Interactions between serum protein complexes and the surfaces of casein micelles. J. Agric. Food Chem. 55:4160–4168. https://doi.org/10.1021/jf063242c.

Eshpari, H., P. S. Tong, and M. Corredig. 2016. Changes in particle size, calcium and phosphate solubilization, and microstructure of rehydrated milk protein concentrates, prepared from partially acidified milk. Dairy Sci. Technol. 96:329–343. https://doi.org/10.1007/s13594-015-0270-1.

Ezeh, V. N., and M. J. Lewis. 2011. Milk reversibility following reduction and restoration of pH. Int. J. Dairy Technol. 64:179–187. https://doi.org/10.1111/j.1471-0307.2010.00649.x.

Farrokhi, F., F. Badii, M. R. Ehsani, and M. Hashemi. 2019. Functional and thermal properties of nanofibrillated whey protein isolate as functions of denaturation temperature and solution pH. Colloids Surf. A Physicochem. Eng. Asp. 583:124002. https://doi.org/10.1016/j.colsurfa.2019.124002.

Fox, P. F., T. Uniacke-Lowe, P. L. H. McSweeney, and J. A. O'Mahony. 2015. Milk proteins. Pages 145–239 in Dairy Chemistry and Biochemistry. Springer.

Glover, Z. J., M. J. Francis, A. H. Bisgaard, U. Andersen, L. B. Johansen, M. J. Povey, M. J. Holmes, J. R. Brewer, and A. C. Simonsen. 2020. Dynamic moisture loss explored through quantitative superresolution microscopy, spatial micro-viscosity, and macroscopic analyses in acid milk gels. Food Hydrocoll. 101:105501. https://doi.org/10.1016/j.foodhyd.2019.105501.

Gunasekaran, S., and O. Solar. 2012. Heat-induced casein-whey protein interactions. Pages 199–228 in Food Proteins and Peptides. Chemistry, Functionality, Interactions, and Commercialization. N. S. Hettiarachchy, ed. CRC Press.

Hochreiter, B., M. Kunze, B. Moser, and J. A. Schmid. 2019. Advanced FRET normalization allows quantitative analysis of protein interactions including stoichiometries and relative affinities in living cells. Sci. Rep. 9:8233. https://doi.org/10.1038/s41598-019-44650-0.

Jensen, J. L., J. Jacobsen, M. L. Moss, F. Rasmussen, K. B. Qvist, S. Larsen, and J. M. van den Brink. 2015. The function of the milkclotting enzymes bovine and camel chymosin studied by a fluorescence resonance energy transfer assay. J. Dairy Sci. 98:2853–2860. https://doi.org/10.3168/jds.2014-8672.

Karam, M. C., C. Gaiani, C. Hosri, J. Burgain, and J. Scher. 2013. Effect of dairy powders fortification on yogurt textural and sensorial properties: A review. J. Dairy Res. 80:400–409. https://doi.org/10.1017/S0022029913000514.

Kehoe, J. J., and E. A. Foegeding. 2011. Interaction between β-casein and whey proteins as a function of pH and salt concentration. J. Agric. Food Chem. 59:349–355. https://doi.org/10.1021/jf103371g.

Khubber, S., K. Chaturvedi, N. Thakur, N. Sharma, and S. K. Yadav. 2021. Low-methoxyl pectin stabilizes low-fat set yoghurt and improves their physicochemical properties,

rheology, microstructure and sensory liking. Food Hydrocoll. 111:106240. https://doi.org/10.1016/j.foodhyd.2020.106240.

Kroes-Nijboer, A., P. Venema, and E. van der Linden. 2012. Fibrillar structures in food. Food Funct. 3:221–227.

Lee, W. J., and J. A. Lucey. 2004. Structure and physical properties of yogurt gels: Effect of inoculation rate and incubation temperature. J. Dairy Sci. 87:3153–3164. https://doi.org/10.3168/jds.S0022-0302(04)73450-5.

Lee, W. J., and J. A. Lucey. 2006. Impact of gelation conditions and structural breakdown on the physical and sensory properties of stirred yogurts. J. Dairy Sci. 89:2374–2385. https://doi.org/10.3168/jds.S0022-0302(06)72310-4.

Loveday, S. M., S. G. Anema, and H. Singh. 2017. β-Lactoglobulin nanofibrils: The long and the short of it. Int. Dairy J. 67:35–45. https://doi.org/10.1016/j.idairyj.2016.09.011.

Loveday, S. M., J. Su, M. A. Rao, S. G. Anema, and H. Singh. 2012. Whey protein nanofibrils: The environment–morphology–functionality relationship in lyophilization, rehydration, and seeding. J. Agric. Food Chem. 60:5229–5236. https://doi.org/10.1021/jf300367k.

Lucey, J. A., C. Gorry, B. O'Kennedy, M. Kalab, R. Tan-Kinita, and P. F. Fox. 1996. Effect of acidification and neutralization of milk on some physico-chemical properties of casein micelles. Int. Dairy J. 6:257–272. https://doi.org/10.1016/0958-6946(95)00014-3.

Lucey, J. A., C. T. Teo, P. A. Munro, and H. Singh. 1997. Rheological properties at small (dynamic) and large (yield) deformations of acid gels made from heated milk. J. Dairy Res. 64:591–600. https://doi.org/10.1017/S0022029997002380.

Luo, Q., W. Zhan, R. M. Boom, and A. E. Janssen. 2018. Interactions between acid and proteins under in vitro gastric condition—a theoretical and experimental quantification. Food Funct. 9:5283– 5289. https://doi.org/10.1039/C8FO01033A.

Marafon, A. P., A. Sumi, D. Granato, M. R. Alcântara, A. Y. Tamime, and M. Nogueira de Oliveira. 2011. Effects of partially replacing skimmed milk powder with dairy ingredients on rheology, sensory profiling, and microstructure of probiotic stirred-type yogurt during cold storage. J. Dairy Sci. 94:5330–5340. https://doi.org/10.3168/jds.2011-4366.

Mariotti, M., M. Lucisano, M. A. Pagani, and P. K. Ng. 2009. The role of corn starch, amaranth flour, pea isolate, and Psyllium flour on the rheological properties and the ultrastructure of glutenfree doughs. Food Res. Int. 42:963–975. https://doi.org/10.1016/j.foodres.2009.04.017.

Meletharayil, G. H., H. A. Patel, and T. Huppertz. 2015. Rheological properties and microstructure of high protein acid gels prepared from reconstituted milk protein concentrate powders of different protein contents. Int. Dairy J. 47:64–71. https://doi.org/10.1016/j.idairyj.2015.02.005.

Meletharayil, G. H., H. A. Patel, L. E. Metzger, C. Marella, and T. Huppertz. 2018. Influence of partially demineralized milk proteins on rheological properties and microstructure of acid gels. J. Dairy Sci. 101:1864–1871. https://doi.org/10.3168/jds.2017-13670.

Modler, H. W., M. E. Larmond, C. S. Lin, D. Froehlich, and D. B. Emmons. 1983. Physical and sensory properties of yogurt stabilized with milk proteins. J. Dairy Sci. 66:422–429. https://doi.org/10.3168/jds.S0022-0302(83)81809-8.

Mohammadian, M., and A. Madadlou. 2016. Cold-set hydrogels made of whey protein nanofibrils with different divalent cations. Int. J. Biol. Macromol. 89:499–506. https://doi.org/10.1016/j.ijbiomac.2016.05.009.

Morgan, P. E., T. M. Treweek, R. A. Lindner, W. E. Price, and J. A. Carver. 2005. Casein proteins as molecular chaperones. J. Agric. Food Chem. 53:2670–2683. https://doi.org/10.1021/jf048329h.

Munialo, C. D., A. H. Martin, E. Van Der Linden, and H. H. De Jongh. 2014. Fibril formation from pea protein and subsequent gel formation. J. Agric. Food Chem. 62:2418–2427. https://doi.org/10.1021/jf4055215.

O'Kennedy, B. T., and J. S. Mounsey. 2006. Control of heat-induced aggregation of whey proteins using casein. J. Agric. Food Chem. 54:5637–5642. https://doi.org/10.1021/jf0607866.

Okamoto, K., and Y. Sako. 2017. Recent advances in FRET for the study of protein interactions and dynamics. Curr. Opin. Struct. Biol. 46:16–23. https://doi.org/10.1016/j.sbi.2017.03.010.

Peng, Y., M. Serra, D. S. Horne, and J. A. Lucey. 2009. Effect of fortification with various types of milk proteins on the rheological properties and permeability of nonfat set yogurt. J. Food Sci. 74:C666–C673. https://doi.org/10.1111/j.1750-3841.2009.01350.x.

Rathod, G., and J. K. Amamcharla. 2021. Process development for a novel milk protein concentrate with whey proteins as fibrils. J. Dairy Sci. 104:4094–4107. https://doi.org/10.3168/jds.2020-19409.

Sahoo, H. 2011. Förster resonance energy transfer—A spectroscopic nanoruler: Principle and applications. J. Photochem. Photobiol. C 12:20–30. https://doi.org/10.1016/j.jphotochemrev.2011.05.001.

Salaün, F., B. Mietton, and F. Gaucheron. 2005. Buffering capacity of dairy products. Int. Dairy J. 15:95–109. https://doi.org/10.1016/j.idairyj.2004.06.007.

Treweek, T. M., D. C. Thorn, W. E. Price, and J. A. Carver. 2011. The chaperone action of bovine milk αS1- and αS2-caseins and their associated form αS-casein. Arch. Biochem. Biophys. 510:42–52. https://doi.org/10.1016/j.abb.2011.03.012.

Yong, Y. H., and E. A. Foegeding. 2008. Effects of caseins on thermal stability of bovine β-lactoglobulin. J. Agric. Food Chem. 56:10352– 10358. https://doi.org/10.1021/jf801658u.

Chapter 5 - Development of spray dried functional milk protein concentrate containing whey proteins as fibrils

Abstract

Globular proteins such as whey proteins can be converted into fibrillated whey proteins by prolong heating to a temperature above 80°C at low pH. Fibrillation of whey protein results in new functionalities and could potentially open doors to applications in other untapped food product categories. Therefore, fibrillated milk protein concentrate (MPC) was produced by selective fibrillation of whey proteins in our previous study, which showed higher viscosity and gelation characteristics. Considering its potential as a functional ingredient, fibrillated MPC was spray dried to extend shelf-life. The developed fibrillated MPC powder was characterized in terms of survival of whey protein fibrils and retention of functionality. Observations from Thioflavin T fluorescence value, transmission electron microscopy, gel electrophoresis, rheology, and turbidity confirmed the presence of fibrils in reconstituted fibrillated MPC. However, fibrils in reconstituted fibrillated MPC were thin compared to the fibrils observed before spray drying, and aggregation of fibrils was seen in reconstituted fibrillated MPC. Further, rheological analysis of reconstituted fibrillated MPC at different total solids showed that reconstituted fibrillated MPC has significantly ($P<0.05$) high viscosity, consistency, and shear thinning behavior. Consequently, reconstituted fibrillated MPC also showed significantly ($P<0.05$) lower surface tension and interfacial tension and significantly ($P<0.05$) higher emulsification capacity, foaming capacity, and foam stability. Also, the functionality of fibrillated MPC was retained after spray drying and subsequent reconstitution. Fibrillated MPC powder can be used as a functional ingredient in dairy and food formulations. Fibrillated MPC in

powder form can potentially reduce the need for non-dairy additives and serve as a clean-label ingredient.

Keywords: Fibrillated MPC, viscosity, emulsification capacity, foaming capacity

Introduction

Proteins are polypeptide chains arranged in a simpler primary structure to a complex quaternary structure depending upon their amino acid makeup, the position of amino acids on the peptide chain, and interaction within amino acid side chains (Damodaran, 2017). Despite having a stable protein structure, globular proteins can self-assemble into protein fibrils through hydrophobic interactions, hydrogen bonds, electrostatic, and van der Waals forces (Meng et al., 2022). The fibrillation process is influenced by intrinsic factors including amino acid composition, hydrophobicity, and confirmational rearrangement, and extrinsic factors including temperature, time, ionic strength, pH, and shear (Lambrecht et al., 2019). Fibrils are made up of a cross-β structure, where the β-sheets are organized parallel to the fibril axis and β-strands are organized perpendicular to this axis (Farrokhi et al., 2018). The protein fibrils are highly ordered and unbranched structures with a diameter of a few nanometers and a length of a few micrometers (Wang et al., 2020). Food protein fibrils are formed in controlled environmental conditions (at low pH, ionic strength, high temperature, and longer heating) and they are non-toxic and digestible (Mohammadian and Madadlou, 2018). Compared to natural food proteins, fibrillated food proteins showed improved functionality such as thickening, gelling, emulsifying, foaming, antioxidant, and antimicrobial activities (Mohammadian and Madadlou, 2016; Loveday et al., 2017; Meng et al., 2022). Most food proteins such as whey proteins have a globular structure, with a complex tertiary and quaternary structure. Globular food proteins can be converted into fibrillar form through the fibrillation process which involves heating of protein solution at low pH and low ionic strength. After the fibrillation of whey proteins, fibrillated whey proteins showed higher viscosity, gelling, emulsification, and foaming capacity (Oboroceanu et al., 2014; Peng et al., 2016; Loveday et al., 2017; Mohammadian and Madadlou,

2018). These fibrillated proteins have stable structure; however, they are affected by environmental conditions such as pH, salt, and moisture (Mantovani et al., 2016: Loveday et al., 2017). Whey protein fibrils are generally formed at pH ~2 (Cao and Mezzenga, 2019), which showed aggregation at their isoelectric pH and entanglement upon pH adjustment to pH 7 (Farrokhi et al., 2020). Therefore, pH alteration toward neutral pH alters from thin fibrils to thick, entangled, and rope-like fibrils. However, the use of surfactants such as lecithin improved the pH stability of fibrils during the pH change to neutral pH (Mantovani et al., 2016). The addition of divalent salts such as calcium showed the formation of highly flexible fibrils with increased viscosity when calcium was added before fibril formation (Loveday et al., 2011). However, the addition of calcium after fibrils formation, resulted in cold set gels due to crosslinked fibrils (Bolder et al., 2006). In other reported literature, fibrils were dehydrated using freeze drying, where they observed breakage of fibril structure and reduction in viscosity and solubility upon rehydration of the fibrils (Maurstad et al., 2009; Loveday et al., 2012; Farrokhi et al., 2018). The reason could be ice crystal formation and structural shrinkage during freeze drying. During freeze drying of cell culture, cryoprotectants such as maltodextrin were used which act as cushioning to cells, protect the cells from ice crystals, and act as filter material (Reddy et al., 2009). Considering milk protein composition in milk, where whey proteins and casein are in a 20:80 ratio, micellar casein can potentially act as a filler material to protect fibrils during spray drying. Combining whey protein fibrils with micellar casein yields milk protein concentrate, which showed enhanced functionality such as viscosity and gelation (Rathod and Amamcharla, 2021; Rathod et al., 2022), showing no inhibiting effect of casein on the functionality of pre-formed whey protein fibrils. Therefore, the presence of micellar casein in whey proteins fibril containing milk protein concentrate can act as filler and reduce structural

damage to whey protein fibrils during spray drying and help in retaining the functionality of whey protein fibrils. Therefore, the current study was planned to study survival of whey protein fibrils and retention of functionality of fibrillated MPC after spray drying.

Materials and methods

Experimental Approach

Casein-rich micellar casein concentrate (MCC) dispersion was mixed with fibrillated milk whey proteins isolate (mWPI) solution at neutral pH, keeping casein to whey protein ratio similar to milk, to manufacture fibrillated MPC. Similarly, control MPC was prepared by mixing MCC dispersion with mWPI solution without any treatment. Both MPCs were spray dried and checked for the survival of fibrils and functional properties after reconstitution. The whole study was replicated using two independent lots of mWPI.

Preparation of control and fibrillated MPC

Fibrillated MPC was prepared as per the protocol described by Rathod & Amamcharla, (2021) and the whole manufacturing process is shown in Figure 5.1. Briefly, MCC was reconstituted to 14% total solids using reverse osmosis filtered water maintained at 45-50°C with continuous stirring for 45 minutes using an overhead stirrer (at 500 rpm) and kept overnight in refrigerated storage (4°C) to ensure complete rehydration of MCC. Similarly, mWPI was reconstituted to 2% (Wt/Wt) protein and kept overnight in refrigerated storage to ensure complete rehydration. The following day, the mWPI solution was adjusted to pH 2 using 6 N Hydrochloric acid and kept for an hour to stabilize pH. The pH of the mWPI solution was readjusted to pH 2, if needed. Subsequently, mWPI solution at pH 2 was heated to 80°C for 14 h for the fibrillation of whey proteins, followed by rapid cooling in an ice bath and refrigerated storage (4°C). The cooled mWPI fibril solution at pH 2 was adjusted to pH 6.7 using 3 N NaOH.

The 2% mWPI fibrils solution at pH 6.7 was mixed with 14% MCC solution to make fibrillated MPC keeping casein to whey protein ratio 80:20. Similar to fibrillated MPC, control MPC was manufactured by mixing 14% MCC solution and 2% (Wt/Wt) protein mWPI solution without any further treatment (Process shown in gray color boxes in Figure 5.1 were omitted for the manufacture of control MPC). After mixing, the total protein content of both mixtures was ~7%. Both fibrillated and control MPCs were adjusted to pH 6.7 before they were subjected to spray drying. Both MPCs were preheated to 55°C and then spray dried at 180°C inlet temperature and 90-95 °C outlet temperature using a single-stage spray dryer (Niro atomizer, Copenhagen, Denmark). Fibrillated MPC powders were checked for the survival of fibrils and functional properties after reconstitution.

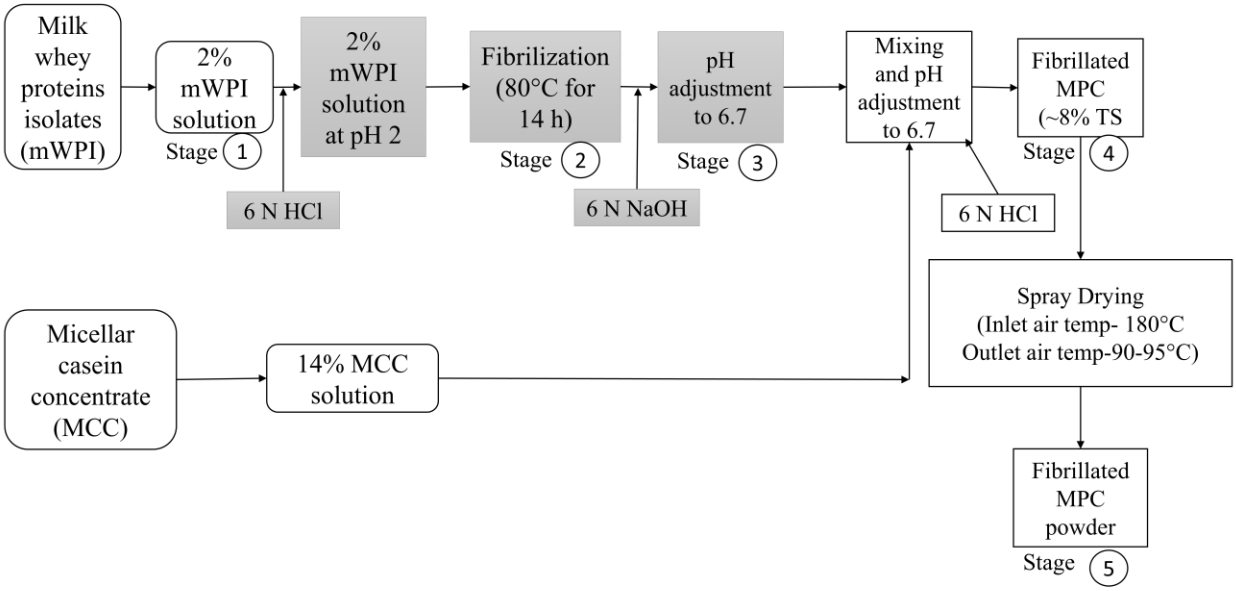

Figure 5.1 Process flow diagram for the manufacture of fibrillated milk protein concentrate powder (Representative sample was taken in different stages: Stage-1. 2% mWPI solution

Stage-2. Fibrillated mWPI at pH 2 Stage-3. Fibrillated mWPI at pH 6.7 Stage-4. Fibrillated MPC, Stage-5. Fibrillated MPC powder)

Confirmation of fibril formation at different stages of production of control and fibrillated MPC

Both control and fibrillated samples analyzed for fibril formation where control samples were not expected to have fibrils as they did not treated with fibrillation process. However, they were tested to see the difference between control and fibrillated sample. Representative samples were taken at different stages of fibrillated MPC manufacturing (Stage-1: 2% mWPI solution; Stage-2: Fibrillated mWPI at pH 2; Stage-3: Fibrillated mWPI at pH 6.7; Stage-4: Fibrillated MPC, Stage 5. Fibrillated MPC powder) to confirm fibrillation during the process. In addition, MPC powders (Stage 5) were reconstituted (5% Wt/Wt protein) in distilled water (45°C) with continuous stirring at 500 rpm using a magnetic stirrer for 45 minutes and kept overnight in the refrigerator for complete rehydration. Samples collected at Stage-4 and reconstituted MPC (Stage-5) samples were subjected to ultracentrifugation (100,000×g) to remove casein (as a pallet) and the supernatant was used for confirmation of the presence of fibril. Fibril formation was confirmed using different techniques such as Thioflavin T fluorescence value (an indirect indicator of fibrillation), transmission electron microscopy, sodium dodecyl sulfate-polyacrylamide gel electrophoresis (SDS-PAGE), and rheology using the methods described by Rathod and Amamcharla, (2021). Tricine-SDS-PAGE was also used to observe the conversion of whey protein into protein hydrolysate which are building blocks of fibrils.

Tricine SDS-PAGE

The liquid samples of both MPCs before spray drying (Stage-4 sample) and reconstituted samples (Stage-5) of both MPCs powders were diluted to 0.5% protein content using distilled water. Samples were diluted with Tris-Tricine sample buffer in a 1:2 ratio, mixed thoroughly, and incubated at 37°C for 15 minutes in a water bath. A 15 µL sample was loaded in the 16.5% precast Tris-Tricine gel (Bio-Rad Laboratories, Hercules, CA) fitted into an electrophoresis assembly (Bio-Rad Mini Gel system, Bio-Rad Laboratories, Hercules, CA) filled with 1X Tris-Tricine sample buffer (Bio-Rad Laboratories, Hercules, CA) prepared from 10X Tris-Tricine buffer by mixing sample buffer, and distilled water in 1:9 ratio. The gel electrophoresis was started with a constant current of 20 mA for 15 minutes for stacking and increased to 25 mA until the dye reached the bottom (Schägger, 2006). The gel was fixed using 10% Trichloroacetic acid solution for one hour and subsequently in staining solution (Coomassie brilliant blue R-250, Bio-Rad Laboratories, Hercules, CA) with continuous shaking for 24 hours. Destaining was carried out in a solution containing 10% methanol, 10% acetic acid, and 80% double distilled water for 24 hours with continuous shaking. The gel images were scanned using Invitrogen iBright 1500 imager (Invitrogen, Carlsbad, CA).

Color

The color analysis of both MPC before spray drying (Stage-4; Figure 5.1) and after spray drying (reconstituted MPC; Stage-5) was performed by following the method described by Rathod and Kairam, (2018) at the same protein content. Approximately 6-8 mL of liquid samples were poured on the plastic Petri dish and placed on the white platform. Then, the samples were scanned using Mini Scan™ XE plus (Hunter Color Lab, Reston, VA) for L*, a*, and b* values. The total color was determined using the following equation.

$$\text{Total color} = \sqrt{(L^*)^2 + (a^*)^2 + (b^*)^2}$$

Turbidity

Turbidity of control and fibrillated MPC was carried out as per the method suggested by Jiang et al., (2022). Briefly, 5% (Wt/Wt) reconstituted MPC solution was further diluted to 0.1 (Wt/Wt) protein solution using distilled water. The diluted sample was analyzed for %Transmission at 600 nm using UV-5200 UV/VIS Spectrophotometer (Metash Shanghai, China). Turbidity was calculated by subtracting the %Transmission value from 100.

Functional Properties of control and fibrillated MPC

Rheology

Control and fibrillated MPC samples were reconstituted at 5%, 10%, and 20% total solids in distilled water (45°C) with continuous stirring at 500 rpm using a magnetic stirrer for 45 minutes and kept overnight in the refrigerator for complete rehydration. The next day, reconstituted MPC samples were tempered to 20°C and continuous rotational flow data were collected at 20°C using a stress-strain-controlled rheometer (MCR-92 Anton Paar, Vernon Hills, IL) fitted with a 50-mm diameter stainless steel cone with 1° angle and 101-μm gap. A shear ramp was used, and the shear rate varied from 0.01 s^{-1} to 200 s^{-1} at 20°C. Along with viscosity, the consistency coefficient and flow behavior index were calculated using the power-law model (Rathod and Amamcharla, 2021).

Surface tension and interfacial tension

The surface tension and interfacial tension of reconstituted control and fibrillated MPC (5% Wt/Wt protein) were measured using an automatic surface tensiometer (Model BZY102, Anhui, China) as per the manufacturer's protocol (Yusoff et al., 2021). Vegetable oil (Great Value,

Walmart, Bentonville, AR) was gently added on top of the sample as oil phase to create oil-water interface for measuring interfacial tension.

Emulsification capacity

Emulsification capacity was measured as suggested by Zaitoun et al., (2022). Reconstituted control and fibrillated MPC (5% Wt/Wt protein) samples were diluted to 0.05% protein using distilled water, and 120 mL of diluted sample was taken in a 600 mL beaker at room temperature. The handheld homogenizer (CAT Scientific X120 Poly-Science, Niles, IL, USA) and conductivity meter electrode (Accumet™ AP75; Fisher Scientific, PA) was placed in the beaker containing the diluted sample. Vegetable oil (Great Value, Walmart, Bentonville, AR) was filled in a 125 mL separatory funnel and placed just above the beaker. Subsequently, vegetable oil addition was started by opening the 125 mL separatory funnel valve all the way up with continuous blending. Initially, blending was done at a slow rate (speed 1), then blending speed was increased to speed 3. Oil addition was stopped when the emulsion breakpoint was detected, which was marked when conductivity becomes zero due to an increase in electric resistance upon emulsion collapse. Emulsification capacity was expressed as the total g of oil emulsified per mg of soluble protein (Acton and Saffle, 1972).

Foaming capacity and foam stability

Foam capacity and foam stability of control and fibrillated MPC were measured according to the method described by Sinha et al. (2007). Reconstituted MPC (5% Wt/Wt protein) samples were diluted to 3% protein with distilled water, and 100 mL of diluted sample was taken into a 400 mL beaker. The diluted sample was whipped for 3 min at high speed using a handheld homogenizer (CAT Scientific X120 Poly-Science, Niles, IL, USA). The foam was poured immediately into a 500 ml measuring cylinder and the total volume of the liquid was

measured immediately after 30 s. The difference in the volume was expressed as the volume of the foam. The foam stability was determined by measuring the fall in the volume of the foam after 30 min. All the experiments were performed in triplicate and the results are the average of three values.

Heat Coagulation Time

Heat coagulation time was performed by the method suggested by Rathod and Amamcharla, (2021). Briefly, reconstituted MPC samples (5% Wt/Wt proteins) were adjusted to pH 6.7 and kept overnight in the refrigerator. pH was readjusted to 6.7 if needed. After that, 2.5 mL of the sample was filled in heat-resistant screw cap test tubes (8 mL, 17 mm dia. x 63 mm height) (DWK Life Science, Millville, NJ). The test tubes were inserted into the stainless-steel rack. The rack along with tubes was immersed in an oil bath (Narang Scientific Works Pvt. Ltd, New Delhi, India) maintained at 140°C and placed on the rocker. Heat coagulation time was noted as the time in seconds elapsed between immersing the sample vials in the hot oil bath and the onset of visible clots/flakes.

Protein oxidation

Protein oxidation was studied according to the method given by (Scheidegger et al., 2010; Keppler et al., 2019). Briefly, reconstituted control and fibrillated MPC (5% Wt/Wt protein) dispersion was further diluted to 0.1 % protein content using distilled water followed by vortex mixing. Protein oxidation was measured in terms of decay in two amino acids *viz.*, Tryptophan and tyrosine, and their respective oxidation products that are N-formyl kynurenine and Di-tyrosine. Diluted protein solutions were analyzed in quartz cuvette using a spectrofluorometer (LS-55; Perkin Elmer, Waltham, MA) using right angle assembly for tryptophan (excitation and emission wavelength- 294 nm and 340 nm, respectively) and L-tyrosine (excitation and emission

wavelength- 274 nm and 310 nm, respectively) using 1% attenuation filter with 10 nm excitation slit width and 20 nm emission slit width. Similarly, oxidation products N-formyl kynurenine (excitation and emission wavelength- 325nm and 435 nm, respectively) and Di-tyrosine (excitation and emission wavelength-284 nm and 415 nm, respectively) were also measured. The fluorescence intensity was recorded to compare the concentration of a specific component in control and fibrillated MPC.

Statistical Analysis

Statistical analysis was performed using Excel (Microsoft Corp., Redmond, WA). One-way ANOVA and Tukey's multiple range test were done using SAS Version 9.4 (SAS Institute Inc.).

Results and discussion

Confirmation of fibril formation and viability during the manufacture of fibrillated MPC and comparison with control MPC

Thioflavin T fluorescence (Th T) value

The results of the Th T value were shown in Table 5.1. The Th T value was measured for the liquid MPC sample before spray drying (Stage-4) and reconstituted MPC samples after spray drying (Stage-5) keeping the same total protein. In both samples (liquid before spray drying and reconstituted after spray drying), fibrillated MPC showed a significantly *($P<0.05$*) higher Th T value than the control MPC, which indicates the presence of whey protein fibrils in liquid fibrillated MPC before spray drying as well as reconstituted fibrillated MPC after spray drying. Since these Th T values were taken in MPC where micellar casein is also present, for further confirmation, MPC was subjected to ultracentrifugation to remove micellar casein, and the

remaining supernatant was analyzed for Th T value. The supernatant of fibrillated MPC showed a higher Th T value than control MPC for both liquid fibrillated MPC before spray drying as well as reconstituted fibrillated MPC after spray drying. The above results suggest that fibrils present in the fibrillated MPC survived the spray drying process. Similarly, an increase in the Th T value for fibrillated MPC and fibrillated mWPI was reported in the earlier study (Rathod and Amamcharla, 2021).

Table 5.1 Chemical and physical properties of control and fibrillated MPC before spray drying and after spray drying (Reconstituted).

Parameters	Before Spray Drying (5% Wt/Wt solution)(Stage-4)		After Spray Drying (5% Wt/Wt solution) (Stage-5)	
	Control MPC	Fibrillated MPC	Control MPC	Fibrillated MPC
Thioflavin T Fluorescence (Th T) value	226.5±5.4[a]	305.0±6.5[b]	248.4±3.0[a]	361.9±16.0[b]
Th T value of Supernatant of ultracentrifugation	14.8±0.9[a]	26.0±3.0[b]	13.2±1.4[a]	26.1±4.1[b]
Viscosity (mPa.s @ $100s^{-1}$	3.28±0.29[a]	7.10±0.85[b]	2.26±0.10[a]	2.60±0.31[b]
Consistency Coefficient (mPa.s)	17.71±8.78[a]	52.67±38.18[a]	3.55±0.85[a]	7.51±4.41[a]
Flow Behavior Index	0.662±0.112[a]	0.634±0.162[a]	0.908±0.053[a]	0.809±0.114[a]
L* value	89.52±0.25[b]	89.01±0.70[a]	90.75±0.42[b]	89.31±0.71[a]
a* value	-2.05±0.02[a]	-1.58±0.12[b]	-1.89±0.01[a]	-1.52±0.07[b]
b* value	2.63±0.04[a]	3.60±0.27[b]	3.26±0.02[a]	4.01±0.20[b]
Total Color	89.58±0.24[b]	89.10±0.70[a]	90.83±0.42[b]	89.41±0.70[a]
Turbidity	51.9±6.2[a]	69.8±2.6[b]	52.3±1.5[a]	81.5±0.3[b]

[a-b] Mean within a row with different superscripts differ for the stage-4 and stage-5 seperately ($P<0.05$); n=2

Transmission electron microscopy (TEM)

TEM images of control and fibrillated MPC were shown in Figure 5.2. TEM images of fibrillated MPC before spray drying (Stage-4; Figure 5.2A) showed the presence of whey protein fibrils also after spray drying (Stage-5), reconstituted fibrillated MPC has also shown the presence of fibrils (Figure 5.2 B). For further confirmation, both MPC was ultracentrifuged to remove caseins and the supernatant was analyzed, where TEM images showed the presence of fibrils in the supernatant of fibrillated MPCs (Figures 5.2 C&D). TEM images shown here were similar to those reported in the earlier study on liquid fibrillated model MPC(Rathod and Amamcharla, 2021). However, for spray-dried fibrillated MPC after reconstitution, the fibrils were thin, shorter, and more aggregated compared to the liquid fibrillated MPC. The possible reason could be shear-induced damage to fibrils owing to pumping and atomization during spray drying of liquid MPC as well as due to continuous stirring during reconstitution of fibrillated MPC. Loveday et al., (2012) reported that whey protein fibrils with a semi-flexible straight structure are broken into short rods due to freezing drying. Farrokhi et al. (2018) reported that lower solubility for fibrillated whey proteins than the native whey proteins because amyloid-like fibrils having a dominant β-sheet structure are less soluble compared to the native protein, which is due to increase in surface hydrophobicity due to exposure of hydrophobic groups. Mohammadian and Madadlou (2016) also reported a decrease in solubility of whey proteins upon fibrillation due to the formation of stranded nanofibrils and an increase in protein surface hydrophobicity. So, due to the dominant β-sheet structure, higher surface hydrophobicity, and lower solubility, these fibrils might keep themselves in aggregated form. Despite the loss of fibrils after spray drying, there are still visible fibrils seen in the reconstituted powder showing the survival of fibrils after spray drying.

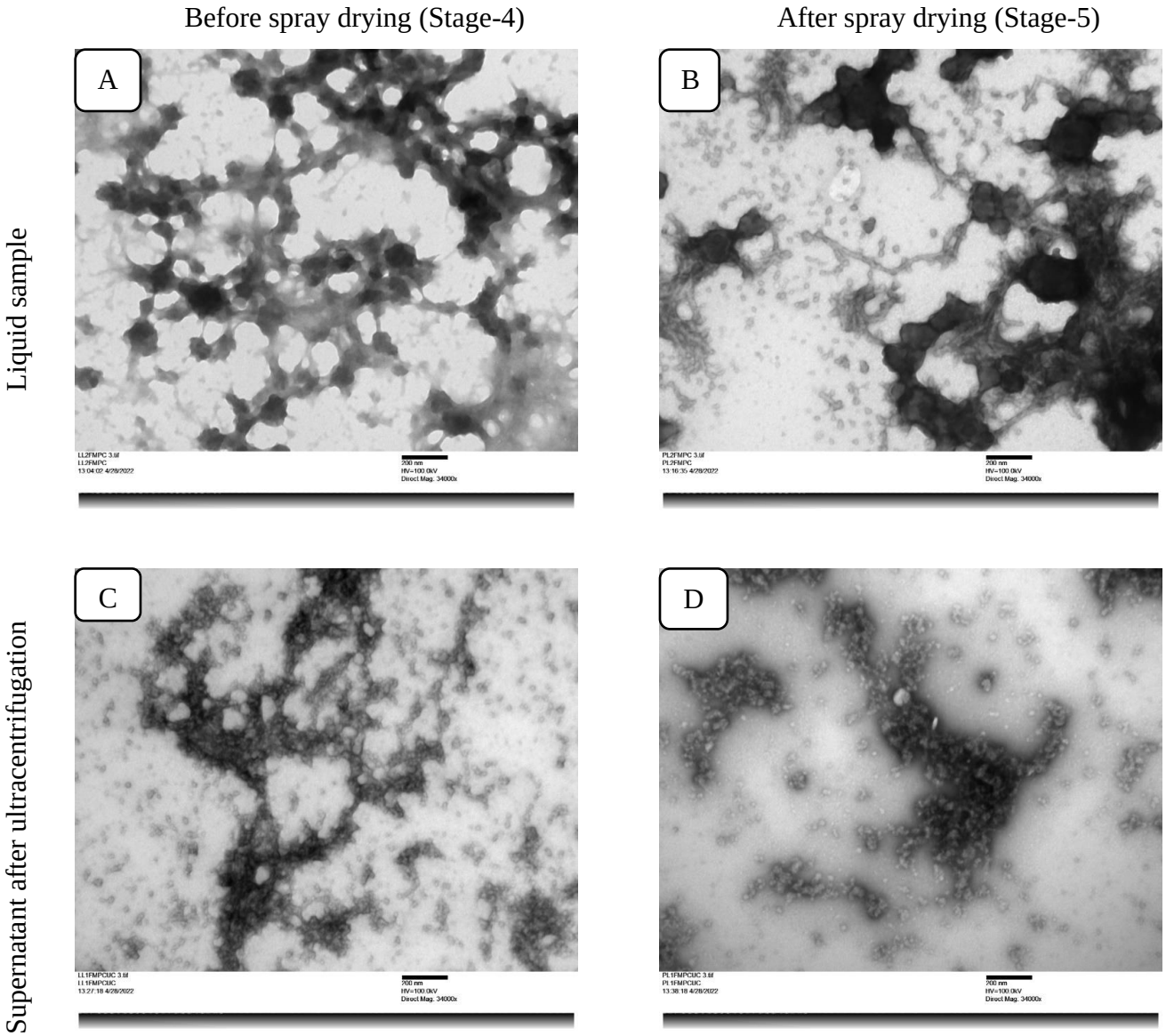

Figure 5.2. Transmission electron microscopic images of fibrillated MPC liquid (Stage-4) before spray drying (A), reconstituted fibrillated MPC powder (Stage-5) (B) supernatant of fibrillated MPC liquid before spray drying (C), and supernatant of reconstituted fibrillated MPC powder (D) (Magnification: 34000x, Scale 200 nm).

Gel electrophoresis

SDS-PAGE gel image was shown in Figure 5.3A and Tricine SDS-PAGE gel image was shown in Figure 5.3B. There is a clear band of α-lactalbumin (14.4 kDa) and β-lactoglobulin (18.2 kDa), that can be seen in all the MPCs. For the liquid MPC sample before spray drying (Stage-4), control MPC showed a thick and clear band of α-lactalbumin and β-lactoglobulin and no presence of any smaller peptide bands. While for the fibrillated MPC samples, bands of α-lactalbumin and β-lactoglobulin were thinner than control MPC showing conversion of whey protein into whey protein fibrils, however, bands of caseins were almost similar. Further, both fibrillated MPC samples (liquid before spray drying (Stage-4) and reconstituted samples after spray drying (Stage-5)) showed peptides in the range of 2-8 kDa (Figure 5.3 B). Peptides in the 2-8 kDa range are building blocks for the fibrils (Akkermans et al., 2008a). Therefore, the presence of peptides in the range of 2-8 kDa and reduction of band intensity of α-lactalbumin and β-lactoglobulin, confirm fibril formation from whey proteins. A similar kind of protein bands in SDS-PAGE gel was seen by Rathod and Amamcharla, (2021) for liquid fibrillated MPC. After spray drying, gel bands for control and fibrillated MPC were almost similar, therefore it could be said that fibrils were present in fibrillated MPC even after drying.

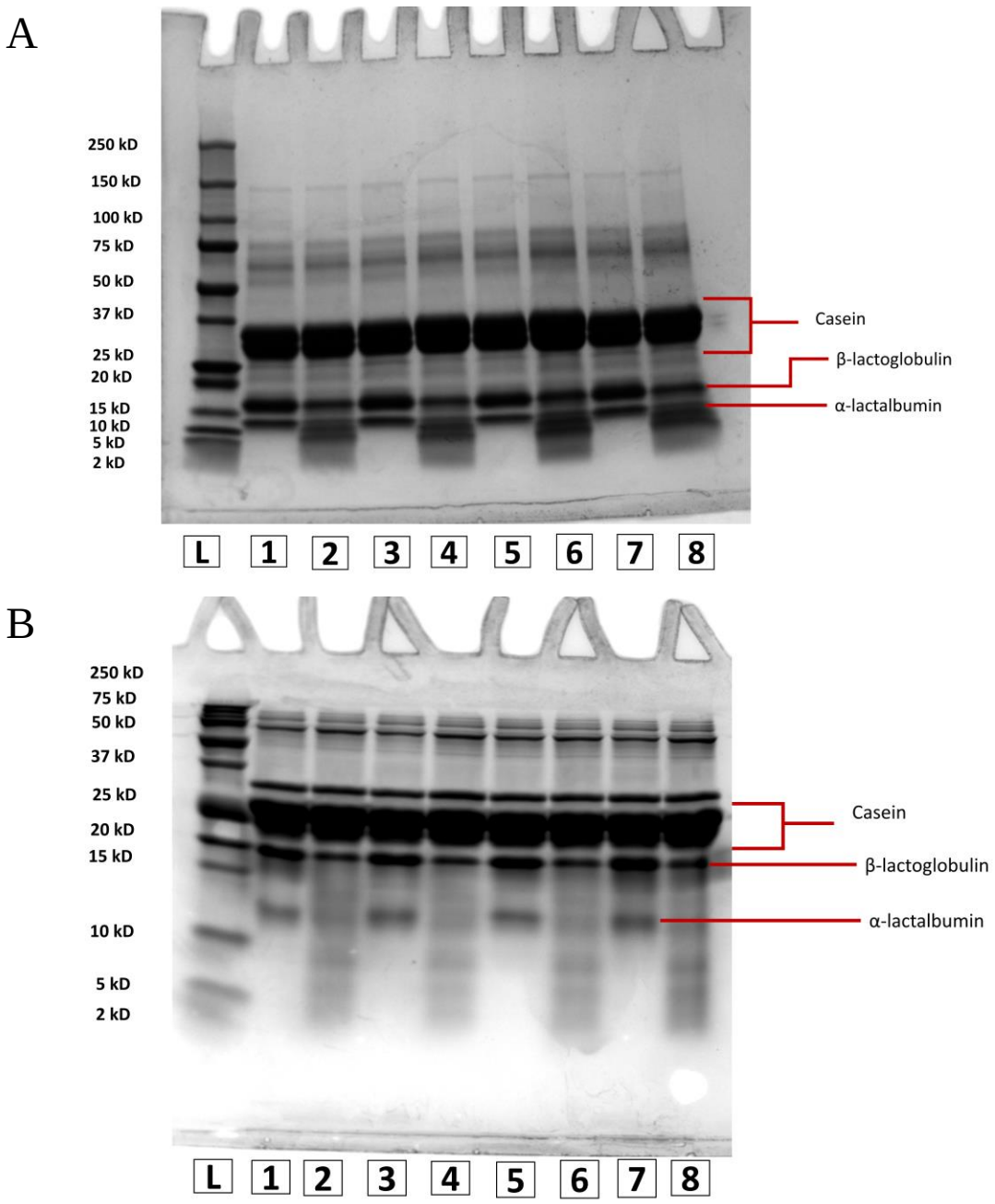

Figure 5.3 Gel electrophoresis of control MPC (C-MPC) and fibrillated MPC (F-MPC) A) SDS-PAGE B) Tricine-SDS-PAGE (Lanes- L-Ladder, before spray drying (1-Lot 1 C-MPC, 2-Lot 1 F-MPC, 3-Lot 2 C-MPC, 4-Lot 2 F-MPC) After spray drying (5-Lot 1 C-MPC, 6-Lot 1 F-MPC, 7-Lot- 2 C-MPC, 8-Lot-2 F-MPC))

Rheology

The result of the rheology of control and fibrillated MPCs was shown in Table 5.1. For before spray drying sample (Stage-4), fibrillated MPC showed significantly ($P<0.05$) higher viscosity and consistency coefficient than control MPC, and a lower flow behavior index showing that fibrillated MPC is more shear thinning than control MPC. The results of rheology were similar to that were reported earlier by Rathod and Amamcharla, (2021). However, reconstituted MPC samples after spray drying (Stage-5) showed lower viscosity and consistency coefficient than the liquid MPC before spray drying. In an earlier study, whey protein fibrils were freeze-dried and upon reconstitution, the viscosity of reconstituted whey protein fibrils was lower than the original whey protein fibrils. The original whey protein fibrils were straight compared to curly fibrils of reconstituted whey protein fibrils. Freeze dying of fibrils might have fractured the straight whey protein fibrils (Loveday et al., 2012). Breakage of fibrils into shorter fibrils and subsequent aggregation of fibrils can be seen in the TEM images (Figure 5.2). Another probable reason could be the shear thinning behavior of both samples. For proper reconstitution, MPC was stirred at 500 rpm for 45 minutes at 45-50°C which might affect their rheological properties. Despite of reduction in viscosity and consistency coefficient, reconstituted fibrillated MPC showed significantly ($P<0.05$) higher viscosity, consistency coefficient, and lower flow rate index than the reconstituted Control MPC.

Color

The result of the instrumental color of control and fibrillated MPC was shown in Table 5.1. Results for the MPC before drying (Stage-4) showed that fibrillated MPC has significantly ($P<0.05$) less L* value and total color value and higher a* and b* value, however, the difference was smaller. During fibrillation, the whey protein solution was heated at 80°C for 14 h, which

resulted in darkening the color of fibrillated whey protein solution, which was subsequently mixed with micellar casein concentrated solution to make fibrillated MPC. Therefore, the resultant fibrillated MPC was slightly darker giving a lesser L* value, however visible color difference is negligible. Compared to an earlier study on fibrillated MPC (Rathod and Amamcharla, 2021), L* and Total color values were higher for the MPC produced in the current study, which may be due to the compositional difference in the raw material used and lower heating time for fibrillation (14h) in the current study compared to 20 h in the previous study. After spray drying (Stage-5), both MPC showed a positive shift in all the color parameters for reconstituted MPCs than liquid MPC, however, the results were similar to that of liquid MPC. Reconstituted fibrillated MPC showed significantly ($P<0.05$) lower L* and Total color values and higher a* and b* values.

Turbidity

The result of turbidity of control and fibrillated MPC was shown in Table 5.1. For liquid MPC samples (before spray drying; Stage-4), turbidity was significantly ($P<0.05$) higher for fibrillated MPC than the control MPC, which may be due to the presence of whey proteins fibrils, as the presence of fibrils makes the solution turbid than the non-fibrillated ones (Akkermans et al., 2008b; Jiang et al., 2022). Further, whey protein fibrils were formed at pH 2 which was subsequently raised to pH 7. This transition goes through the isoelectric point of whey proteins. Therefore, after pH adjustment to pH 7, aggregation in whey protein fibrils was seen, leading to an increase in turbidity (Mantovani et al., 2018). The aggregation of fibrils can be seen in the TEM images (Figure 5.2). So, fibrillated MPC showed higher turbidity than the control MPC. After spray drying turbidity of both the MPCs was increased, however, fibrillated MPC after reconstitution (Stage-5) showed higher turbidity than the control MPC. As seen in the TEM

images, reconstituted fibrillated MPC showed higher aggregation which could be the potent reason for the higher turbidity of reconstituted fibrillated MPC (Figure 5.2). Martin et al. (2007) also reported higher turbidity for the reconstituted skim milk powders than the fresh skim milk, which could be due to alteration in casein micelles surface due to spray drying. The alteration results in an increase in particle size due to casein-whey protein interaction on the micellar surface (at pH 6.7), and association of casein and whey protein during water removal from droplet during drying, and migration of calcium from serum to micelle (Vasbinder and De Kruif, 2003; Martin et al., 2007). In the current study, the particle size of fibrillated MPC after reconstitution was higher than the control MPC as well as fibrillated MPC before spray drying (data not shown). Unlike the skim milk study, MPCs were not heated in the current study however, spray drying-induced changes will occur. Further, unlike whey proteins, whey protein fibrils have higher surface hydrophobicity (Mohammadian and Madadlou, 2016), therefore whey protein fibrils have a higher probability of interacting with micellar casein after mixing during pre-heating and subsequent spray drying. Further, aggregates of fibrils will also contribute to an overall particle size of the fibrillated MPC and thereby its turbidity.

Comparison of functional properties of control and fibrillated MPC

Rheology

The rheology of reconstitute control and fibrillated MPC at different total solids was shown in Table 5.2. Results showed that the viscosity of reconstituted fibrillated MPC at all the total solids was significantly ($P<0.05$) higher than the reconstituted control MPC and there was an increase in viscosity with an increase in total solids of both reconstituted MPCs. Except for 5% total solids, the viscosity of reconstituted fibrillated MPC was almost double that of the reconstituted Control MPC. A similar trend was seen for the consistency coefficient, where

reconstituted fibrillated MPC showed a significantly (*P<0.05*) higher consistency coefficient than reconstituted control MPC, and the increased consistency coefficient was positively correlated with an increase in total solids. Further, reconstituted fibrillated MPC showed shear thinning behavior at all the total solids levels. The possible reason for the higher viscosity and consistency is the presence of fibrillated whey proteins as they bind to more water and form a network that thickens the solution and increases the viscosity (Rathod and Amamcharla, 2021). With an increase in total solids, the total amount of solids and fibrils was increased which led to an increase in viscosity at an elevated total solids level.

Table 5.2 Comparison of the rheology of control and fibrillated MPC at different total solids

Total Solids % (wt/wt)	Viscosity (mPa.s) @100s-1		Consistency Coefficient (mPa.s^n)		Flow Behavior Index	
	Control MPC	Fibrillated MPC	Control MPC	Fibrillated MPC	Control MPC	Fibrillated MPC
5%	2.26± 0.10^a	2.60± 0.31^b	3.55± 0.85^a	7.51± 4.41^a	0.908± 0.053^a	0.809± 0.114^a
10%	4.23± 0.54^a	9.7± 0.34^b	5.60± 1.11^a	15.999± 4.02^b	0.942± 0.019^a	0.896± 0.049^a
20%	667.4± 19.7^a	1228.7± 77.7^b	18718± 8855^a	24839± 11684^a	0.308± 0.101^a	0.375± 0.095^a

$^{a-b}$ Mean within a row with different superscripts differ (*P*<0.05); n=2

Surface tension and interfacial tension

The result of surface tension and interfacial tension of reconstituted control and fibrillated MPC was given in Table 5.3. The surface tension and interfacial tension of reconstituted fibrillated MPC were significantly (*P<0.05*) lower than control MPC. Both the interfacial properties are important as surface tension and interfacial tension are especially important

parameters to study foaming and emulsification properties, respectively. Faster adsorption at the air-water or oil-water interface reduces the interfacial tension between two immiscible phases. Compared to native protein, fibrillation of protein showed a reduction in surface tension by faster mass transfer on the air-water interface as the fibrillated system has small peptides in form of free peptides and peptide aggregates (Wan et al., 2016). Interfacial tension was a helpful parameter to analyze the adsorption of protein molecules on the oil-water interface and thereby emulsification property (Fan et al., 2021). The adsorption of food proteins occurs in three main steps. First, protein adsorption at the interface by a rapid decrease in interfacial tension, secondly, protein unfolding, and third, a slow rearrangement of protein (Beverung et al., 1999). Unlike native whey proteins, fibrillated whey proteins are already unfolded proteins due to high heat treatment during the fibrillation process (Mantovani et al., 2018). Also, compared to native whey proteins fibrillated whey proteins have a high aspect ratio and surface hydrophobicity that facilitates adsorption on the oil-water interface leading to a reduction in interfacial tension compared to native proteins (Fan et al., 2021). Therefore, the reduction in surface tension and interfacial tension of reconstituted fibrillated MPC was due to the presence of whey protein fibrils. The reduction in tension at the interface might positively help to improve functionality such as emulsification and foaming.

Table 5.3 Comparision of functional properties of control and fibrillated MPC

Functional Property	Control MPC	Fibrillated MPC
Surface Tension (mN/m)	45.9±0.1[b]	42.9±0.5[a]
Interfacial Tension(mN/m)	13.4±0.5[a]	13.1±0.3[a]
Emulsification Capacity (g of oil per mg of protein)	2.13±0.07[a]	2.45±0.06[b]
Foaming Capacity (mL/g)	36.7±4.7[a]	52.2±6.3[b]
Foam Stability (mL/g)	14.2±2.0[a]	20.8±2.0[b]
Heat Coagulation Time (s)	61.3±6.1[b]	37.8±0.7[a]

[a-b] Mean within a row with different superscripts differ ($P<0.05$); n=2

Emulsification capacity

Results of the emulsification capacity of reconstituted control and fibrillated MPC was shown in Table 5.3. The emulsification capacity of fibrillated MPC was significantly (*P<0.05*) higher than control MPC. Emulsification capacity is one of the important functional properties of food products (Fan et al., 2021). This property is mainly related to the ability to unfold and adsorb on the oil-water interface owing to the amphiphilicity, and ability to bind with fat and water (Lam and Nickerson, 2015). As protein is made up of both hydrophilic and lipophilic groups, it possesses amphiphilicity and the ability to get adsorbed at oil-water interphase (Gao et al., 2017). Therefore, proteins can form a viscoelastic interfacial film for oil droplet stabilization through intermolecular interactions including hydrophobic interaction, electrostatic interaction, and hydrogen bonding (Lam and Nickerson, 2015). Studies suggest that compared to native β-lactoglobulin (major whey proteins), fibrillated β-Lactoglobulin can effectively adsorb onto the Oil-water interface with higher viscoelasticity of the interfacial layer (Hu et al., 2019). Similarly, compared to native whey proteins, whey protein fibrils showed higher emulsification capacity and emulsion stabilization (Peng et al., 2016). Further, Mantovani et al., (2018) found that fibril-

stabilized emulsions at pH 7 were more stable due to higher viscosity and faster migration of fibrils to interface compared to fibrils at lower pH. In the current study, whey protein fibrils were at pH 6.7 in fibrillated MPC, which might enhance the emulsification capacity. Therefore, the presence of whey protein fibrils in reconstituted fibrillated MPC increases the emulsification capacity compared to reconstituted control MPC.

Foaming capacity and foam stability

Results of Foaming capacity and foam stability of reconstituted control and fibrillated MPC were shown in Table 5.3. The foaming capacity and foam stability of reconstituted fibrillated MPC were significantly ($P<0.05$) higher than reconstituted Control MPC. Foaming capacity and stability are extremely important functionality in aerated products such as ice cream (Ho et al., 2020). As discussed earlier, compared to untreated whey proteins, whey protein fibrils have lower surface tension and interfacial tension, due to their ability to get adsorbed at the air-water interface, and thereby they can provide higher foaming capacity and foam stability. Oboroceanu et al. (2014) found that foam produced by whey protein fibrils has improved foam capacity and foam stability compared to non-fibrillar whey proteins. Similarly, higher foamability and foam stability for β-lactoglobulin fibrils at pH 7 were also reported (Peng, Yang, Li, Tang, & Li, 2017). Therefore, due to the presence of fibrillated whey proteins in fibrillated MPC, fibrillated MPC showed higher foaming capacity and foaming stability. Other than, the interfacial properties of whey protein fibrils, viscosity enhancement provided by whey protein fibrils can also restrict air cell movement and thereby coalescence of air cells and drainage of liquid, leading to higher foam stability (Oboroceanu et al., 2014).

Heat coagulation time

The result of heat coagulation time of reconstituted control and fibrillated MPC was shown in Table 5.3. Heat coagulation time of fibrillated MPC was significantly ($P<0.05$) lower than the control MPC which is similar to the results reported by Rathod and Amamcharla, (2021) for fibrillated MPC. Heat coagulation time denotes the heat stability of milk protein dispersions and heat stability is required because dairy products are subjected to thermal pasteurization or sterilization for microbiological safety and quality (Liu and Zhong, 2013). In the heat coagulation test, heat-induced coagulation of milk proteins concentrates solution is the result of aggregation of the milk proteins. Due to heat, κ- casein dissociates from micelles, and due to heat-induced acidification κ-casein brush on the micelle surface collapse, leading to destabilization of the micelles, followed by aggregation of milk proteins (Huppertz, 2016). Heat-induced coagulation of casein is also affected by denatured whey proteins and their interaction with casein, as whey proteins attached to casein protrude from the casein micelles and contribute to more rapid coagulations and gelation, mostly pH 6.7 and below as κ-casein and whey protein complex will be on micelle surface (Vasbinder and De Kruif, 2003; Huppertz, 2016). In an earlier study, whey protein fibrils showed higher interaction with micellar casein compared to whey proteins when they were heated (90°C for 10 minutes) and gelled subsequently. Liu and Zhong, (2013) also reported that nanofibrils of whey protein are known to form a gel upon heating. Therefore, in the current study, due to higher interaction between whey protein fibrils and casein at pH 6.7, higher viscosity of the fibrillated solution and reactivity due to open fibrillar structure, fibrillated MPC might have shown early gelation and aggregation upon heating 140°C, leading to lower heat stability than control MPC. Liu and Zhong, (2013) reported that the heat stability of whey protein fibrils can be further improved by glycation, which can be

used as possible means to improve heat stability, but their overall effect on the functionality of resultant fibrillated MPC needs another detailed study.

Protein oxidation

Results of the protein oxidation study of reconstituted control and fibrillated MPC were shown in Table 5.4. Here, to see the loss of essential amino acid, Tryptophan and L-tyrosine were chosen whereas, Di-tyrosine and N-formyl kynurenine was chosen as oxidation marker(Keppler et al., 2019). Results showed that the corresponding fluorescence intensity of reconstituted fibrillated MPC for Tryptophan as well as L-tyrosine was lower than the reconstituted control MPC, where the difference was significant ($P<0.05$) for L-tyrosine while non-significant for Tryptophan. The reduction in fluorescence intensity of Tryptophan and tyrosine for fibrillated MPC showed that fibrillation treatment reduces the number of essential amino acids. Further, the corresponding fluorescence intensity of reconstituted fibrillated MPC for Di-tyrosine and N-formyl kynurenine was significantly ($P<0.05$) higher than reconstituted control MPC, which indicates that heating for longer periods during fibrillation leads to an increase in the formation of oxidation products. However, the amount of oxidation products not high compared to reconstituted control MPC. The presence of oxidation products even in reconstituted control MPC shows that these oxidation products also generated during the processing of milk proteins.

Table 5.4 Comparison of protein oxidation in control and fibrillated MPC

Sample	Control MPC	Fibrillated MPC
Tryptophan (AU)	277.7±15.3[a]	271.6±7.0[a]
Tyrosine (AU)	643.4±47.7[b]	588.8±10.1[a]
Di-tyrosine (AU)	112.8±4.8[a]	126.6±3.5[b]
N-formyl kynurenine (AU)	16.0±1.4[b]	12.7±1.1[a]

[a-b] Mean within a row with different superscripts differ ($P<0.05$); n=2

Conclusion

Fibrillation enhances the functional properties of whey proteins, which was coined by making fibrillated MPC with higher functionalities such as thickening and gelling. Fibrillated MPC was spray dried and compared with control MPC, where fibrillated MPC showed survival of fibrils after spray drying. Also, reconstituted fibrillated MPC showed higher viscosity, emulsification capacity, foaming capacity, foam stability, and lower surface tension interfacial tension after reconstitution. Therefore, considering the functional properties of reconstituted fibrillated MPC, fibrillated MPC powder can be used as a functional ingredient to improve the functionality of dairy and food products. Fibrillated MPC powder can reduce the need for non-dairy additives and can be marketed as clean-label ingredients.

Acknowledgments

We thank Dairy Management Inc. andMidwest Dairy Foods Research Center (St. Paul, MN) for their partial financial support. We acknowledge Dr. Daniel Boyle, Director KSU microscopy facility for his help in performing TEM analysis.

References

Acton, J.C., and R.L. Saffle. 1972. Emulsifying capacity of muscle protein: phase volumes at emulsion collapse. J. Food Sci. 37:904–906. doi:10.1111/J.1365-2621.1972.TB03699.X.

Akkermans, C., A.J. Van der Goot, P. Venema, E. Van der Linden, and R.M. Boom. 2008a. Properties of protein fibrils in whey protein isolate solutions: Microstructure, flow behaviour and gelation. Int. Dairy J. 18:1034–1042. doi:10.1016/J.IDAIRYJ.2008.05.006.

Akkermans, C., P. Venema, A.J. van der Goot, H. Gruppen, E.J. Bakx, R.M. Boom, and E. van der Linden. 2008b. Peptides are building blocks of heat-induced fibrillar protein aggregates of β-lactoglobulin formed at pH 2. Biomacromolecules 9:1474–1479. doi:10.1021/BM7014224/SUPPL_FILE/BM7014224-FILE002.PDF.

Beverung, C.J., C.J. Radke, and H.W. Blanch. 1999. Protein adsorption at the oil/water interface: characterization of adsorption kinetics by dynamic interfacial tension measurements. Biophys. Chem. 81:59–80. doi:10.1016/S0301-4622(99)00082-4.

Bolder, S.G., H. Hendrickx, L.M.C. Sagis, and E. van der Linden. 2006. Ca2+-induced cold-set gelation of whey protein isolate fibrils. Appl. Rheol. 16:258–264. doi:10.1515/ARH-2006-0018/MACHINEREADABLECITATION/RIS.

Cao, Y., and R. Mezzenga. 2019. Food protein amyloid fibrils: Origin, structure, formation, characterization, applications and health implications. Adv. Colloid Interface Sci. 269:334–356. doi:10.1016/J.CIS.2019.05.002.

Damodaran, S. 2017. Food Proteins: An Overview. Food Proteins their Appl. 1–24. doi:10.1201/9780203755617-1.

Fan, Y., G. Peng, X. Pang, Z. Wen, and J. Yi. 2021. Physicochemical, emulsifying, and interfacial properties of different whey protein aggregates obtained by thermal treatment.

LWT 149:111904. doi:10.1016/J.LWT.2021.111904.

FAOSTAT. 2022. FAOSTAT. Accessed September 6, 2022. https://www.fao.org/faostat/en/#data/QCL/visualize.

Farrokhi, F., F. Badii, M.R. Ehsani, and M. Hashemi. 2020. Effect of pH-dependent fibrillar structure on enzymatic hydrolysis and bioactivity of nanofibrillated whey protein. LWT 131:109709. doi:10.1016/J.LWT.2020.109709.

Farrokhi, F., M.R. Ehsani, F. Badii, and M. Hashemi. 2018. Structural and thermal properties of nanofibrillated whey protein isolate in the glassy state. LWT 95:274–281. doi:10.1016/J.LWT.2018.05.001.

Gao, Z., J. Zhao, Y. Huang, X. Yao, K. Zhang, Y. Fang, K. Nishinari, G.O. Phillips, F. Jiang, and H. Yang. 2017. Edible Pickering emulsion stabilized by protein fibrils. Part 1: Effects of pH and fibrils concentration. LWT - Food Sci. Technol. 76:1–8. doi:10.1016/J.LWT.2016.10.038.

Ho, T.M., B. Bhandari, and N. Bansal. 2020. Influence of Milk Fat on Foam Formation, Foam Stability and Functionality of Aerated Dairy Products. Dairy Fat Prod. Funct. 583–606. doi:10.1007/978-3-030-41661-4_24.

Hu, J., J. Yang, Y. Xu, K. Zhang, K. Nishinari, G.O. Phillips, and Y. Fang. 2019. Comparative study on foaming and emulsifying properties of different beta-lactoglobulin aggregates. Food Funct. 10:5922–5930. doi:10.1039/C9FO00940J.

Huppertz, T. 2016. Heat stability of milk. Adv. Dairy Chem. Vol. 1B Proteins Appl. Asp. Fourth Ed. 179–196. doi:10.1007/978-1-4939-2800-2_7/COVER.

IDFA. 2021. U.S. Dairy Industry’s Economic Impact Totals $753 Billion - IDFA. Accessed September 6, 2022. https://www.idfa.org/news/u-s-dairy-industrys-economic-impact-totals-

753-billion.

Insight, C.M. 2020. Micellar Casein Market Size, Trends And Forecast To 2027. Accessed September 6, 2022. https://www.coherentmarketinsights.com/market-insight/micellar-casein-market-3717.

Insight, F. business. 2022. Whey Protein Market Size, Share & Growth Report [2022-2029]. Accessed September 6, 2022. https://www.fortunebusinessinsights.com/whey-protein-market-106555.

Jiang, F., Y. Pan, D. Peng, W. Huang, W. Shen, W. Jin, and Q. Huang. 2022. Tunable self-assemblies of whey protein isolate fibrils for pickering emulsions structure regulation. Food Hydrocoll. 124:107264. doi:10.1016/J.FOODHYD.2021.107264.

Keppler, J.K., T.R. Heyn, P.M. Meissner, K. Schrader, and K. Schwarz. 2019. Protein oxidation during temperature-induced amyloid aggregation of beta-lactoglobulin. Food Chem. 289:223–231. doi:10.1016/j.foodchem.2019.02.114.

Khalesi, M., and R.J. FitzGerald. 2021. Insolubility in milk protein concentrates: potential causes and strategies to minimize its occurrence. https://doi.org/10.1080/10408398.2021.1908955. doi:10.1080/10408398.2021.1908955.

Khubber, S., K. Chaturvedi, N. Thakur, N. Sharma, and S.K. Yadav. 2021. Low-methoxyl pectin stabilizes low-fat set yoghurt and improves their physicochemical properties, rheology, microstructure and sensory liking. Food Hydrocoll. 111:106240. doi:10.1016/J.FOODHYD.2020.106240.

Lam, R.S.H., and M.T. Nickerson. 2015. The effect of pH and temperature pre-treatments on the physicochemical and emulsifying properties of whey protein isolate. LWT - Food Sci. Technol. 60:427–434. doi:10.1016/J.LWT.2014.07.031.

Lambrecht, M.A., K.J.A. Jansens, I. Rombouts, K. Brijs, F. Rousseau, J. Schymkowitz, and J.A. Delcour. 2019. Conditions Governing Food Protein Amyloid Fibril Formation. Part II: Milk and Legume Proteins. Compr. Rev. Food Sci. Food Saf. 18:1277–1291. doi:10.1111/1541-4337.12465.

Liu, G., and Q. Zhong. 2013. Dispersible and thermal stable nanofibrils derived from glycated whey protein. Biomacromolecules 14:2146–2153. doi:10.1021/BM400521B/ASSET/IMAGES/LARGE/BM-2013-00521B_0010.JPEG.

Loveday, S.M., S.G. Anema, and H. Singh. 2017. β-Lactoglobulin nanofibrils: The long and the short of it. Int. Dairy J. 67:35–45. doi:10.1016/J.IDAIRYJ.2016.09.011.

Loveday, S.M., J. Su, M.A. Rao, S.G. Anema, and H. Singh. 2011. Effect of calcium on the morphology and functionality of whey protein nanofibrils. Biomacromolecules 12:3780–3788. doi:10.1021/BM201013B/SUPPL_FILE/BM201013B_SI_001.PDF.

Loveday, S.M., J. Su, M.A. Rao, S.G. Anema, and H. Singh. 2012. Whey protein nanofibrils: The environment-morphology-functionality relationship in lyophilization, rehydration, and seeding. J. Agric. Food Chem. 60:5229–5236. doi:10.1021/JF300367K/ASSET/IMAGES/LARGE/JF-2012-00367K_0008.JPEG.

Makin, O.S., and L.C. Serpell. 2005. Structures for amyloid fibrils. FEBS J. 272:5950–5961. doi:10.1111/J.1742-4658.2005.05025.X.

Mantovani, R.A., J. Fattori, M. Michelon, and R.L. Cunha. 2016. Formation and pH-stability of whey protein fibrils in the presence of lecithin. Food Hydrocoll. 60:288–298. doi:10.1016/J.FOODHYD.2016.03.039.

Mantovani, R.A., G. de Figueiredo Furtado, F.M. Netto, and R.L. Cunha. 2018. Assessing the potential of whey protein fibril as emulsifier. J. Food Eng. 223:99–108.

doi:10.1016/J.JFOODENG.2017.12.006.

Martin, G.J.O., R.P.W. Williams, and D.E. Dunstan. 2007. Comparison of Casein Micelles in Raw and Reconstituted Skim Milk. J. Dairy Sci. 90:4543–4551. doi:10.3168/JDS.2007-0166.

Maruyama, S., N.A. Streletskaya, and J. Lim. 2021. Clean label: Why this ingredient but not that one?. Food Qual. Prefer. 87:104062. doi:10.1016/J.FOODQUAL.2020.104062.

Maurstad, G., M. Prass, L.C. Serpell, and P. Sikorski. 2009. Dehydration stability of amyloid fibrils studied by AFM. Eur. Biophys. J. 38:1135–1140. doi:10.1007/S00249-009-0526-X/FIGURES/4.

Meena, G.S., A.K. Singh, N.R. Panjagari, and S. Arora. 2017. Milk protein concentrates: opportunities and challenges. J. Food Sci. Technol. 54:3010–3024. doi:10.1007/S13197-017-2796-0/FIGURES/2.

Meng, Y., Z. Wei, and C. Xue. 2022. Protein fibrils from different food sources: A review of fibrillation conditions, properties, applications and research trends. Trends Food Sci. Technol. 121:59–75. doi:10.1016/J.TIFS.2022.01.031.

Mohammadian, M., and A. Madadlou. 2016. Characterization of fibrillated antioxidant whey protein hydrolysate and comparison with fibrillated protein solution. Food Hydrocoll. 52:221–230. doi:10.1016/J.FOODHYD.2015.06.022.

Mohammadian, M., and A. Madadlou. 2018. Technological functionality and biological properties of food protein nanofibrils formed by heating at acidic condition. Trends Food Sci. Technol. 75:115–128. doi:10.1016/J.TIFS.2018.03.013.

Oboroceanu, D., L. Wang, E. Magner, and M.A.E. Auty. 2014. Fibrillization of whey proteins improves foaming capacity and foam stability at low protein concentrations. J. Food Eng.

121:102–111. doi:10.1016/J.JFOODENG.2013.08.023.

Peng, D., J. Yang, J. Li, C. Tang, and B. Li. 2017. Foams Stabilized by β-Lactoglobulin Amyloid Fibrils: Effect of pH. J. Agric. Food Chem. 65:10658–10665. doi:10.1021/ACS.JAFC.7B03669/ASSET/IMAGES/LARGE/JF-2017-036699_0006.JPEG.

Peng, J., J.R. Simon, P. Venema, and E. Van Der Linden. 2016. Protein Fibrils Induce Emulsion Stabilization. Langmuir 32:2164–2174. doi:10.1021/ACS.LANGMUIR.5B04341/ASSET/IMAGES/LARGE/LA-2015-04341B_0010.JPEG.

Rathod, G., and J.K. Amamcharla. 2021. Process development for a novel milk protein concentrate with whey proteins as fibrils. J. Dairy Sci. 104:4094–4107. doi:10.3168/JDS.2020-19409.

Rathod, G., D.L. Boyle, and J.K. Amamcharla. 2022. Acid gelation properties of fibrillated model milk protein concentrate dispersions. J. Dairy Sci. 105:4925–4937. doi:10.3168/jds.2021-20695.

Rathod, G., and N. Kairam. 2018. Preparation of omega 3 rich oral supplement using dairy and non-dairy based ingredients. J. Food Sci. Technol. 55:760–766. doi:10.1007/S13197-017-2988-7/TABLES/3.

Reddy, K.B.P.K., S.P. Awasthi, A.N. Madhu, and S.G. Prapulla. 2009. Role of Cryoprotectants on the Viability and Functional Properties of Probiotic Lactic Acid Bacteria during Freeze Drying. http://dx.doi.org/10.1080/08905430903106811 23:243–265. doi:10.1080/08905430903106811.

Research, A.M. 2021. Milk Protein Concentrate Market Size, Share, Trends & Forecast, 2027. Accessed September 6, 2022. https://www.alliedmarketresearch.com/milk-protein-

concentrate-market-A10558.

Schägger, H. 2006. Tricine–SDS-PAGE. Nat. Protoc. 2006 11 1:16–22. doi:10.1038/nprot.2006.4.

Scheidegger, D., R.P. Pecora, P.M. Radici, and S.C. Kivatinitz. 2010. Protein oxidative changes in whole and skim milk after ultraviolet or fluorescent light exposure. J. Dairy Sci. 93:5101–5109. doi:10.3168/JDS.2010-3513.

Sinha, R., C. Radha, J. Prakash, and P. Kaul. 2007. Whey protein hydrolysate: Functional properties, nutritional quality and utilization in beverage formulation. Food Chem. 101:1484–1491. doi:10.1016/J.FOODCHEM.2006.04.021.

USDA. 2022. United States Department of Agriculture Foreign Agricultural Service Dairy Production and Trade Developments.

Vasbinder, A.J., and C.G. De Kruif. 2003. Casein–whey protein interactions in heated milk: the influence of pH. Int. Dairy J. 13:669–677. doi:10.1016/S0958-6946(03)00120-1.

Wan, Z., X. Yang, and L.M.C. Sagis. 2016. Contribution of Long Fibrils and Peptides to Surface and Foaming Behavior of Soy Protein Fibril System. Langmuir 32:8092–8101. doi:10.1021/ACS.LANGMUIR.6B01511/ASSET/IMAGES/LARGE/LA-2016-01511J_0007.JPEG.

Wang, Y., Y. Shen, G. Qi, Y. Li, X.S. Sun, D. Qiu, and Y. Li. 2020. Formation and physicochemical properties of amyloid fibrils from soy protein. Int. J. Biol. Macromol. 149:609–616. doi:10.1016/J.IJBIOMAC.2020.01.258.

Wong, D.W.S., W.M. Camirand, A.E. Pavlath, D.N. Parris, and D.M. Friedman. 2009. Structures and functionalities of milk proteins∗. https://doi.org/10.1080/10408399609527751 36:807–844. doi:10.1080/10408399609527751.

Yusoff, S.F., F.F. Haron, N. Asib, M.T.M. Mohamed, and S.I. Ismail. 2021. Development of Vernonia amygdalina Leaf Extract Emulsion Formulations in Controlling Gray Mold Disease on Tomato (Lycopersicon esculentum Mill.). Agron. 2021, Vol. 11, Page 373 11:373. doi:10.3390/AGRONOMY11020373.

Zaitoun, B.J., N. Palmer, and J.K. Amamcharla. 2022. Characterization of a Commercial Whey Protein Hydrolysate and Its Use as a Binding Agent in the Whey Protein Isolate Agglomeration Process. Foods 2022, Vol. 11, Page 1797 11:1797. doi:10.3390/FOODS11121797.

Chapter 6 - Production of fibrillated non-fat dried milk and studying its functional properties

Abstract

Milk and milk products are widely consumed due to their nutritional benefits. Unlike household cooking, several additives such as gums, stabilizers, emulsifiers, and texture modifiers are used in commercial manufacturing to get the best product appearance and maintain the product quality. These additives are non-dairy based. However, consumers want products without these non-dairy additives. Recently, fibrillation emerged as a new technique to convert globular proteins such as whey proteins into fibrils which give enhanced viscosity, foaming, and emulsification capacity. Therefore, skim milk was subjected to microfiltration and ultrafiltration to separate whey proteins. Then, whey proteins were selectively fibrillated and mixed back with other constituents of skim milk to get fibrillated skim milk. Fibrillated skim milk was spray-dried to get fibrillated non-fat dried milk (NDM). Visible whey protein fibrils were observed in reconstituted fibrillated NDM which showed survival of fibrils in fibrillated NDM. Fibrillated NDM showed significantly ($P<0.05$) higher viscosity than control NDM. Fibrillated NDM also showed higher emulsification capacity, foaming capacity, and stability than the control NDM but lower gel strength. Considering the improved functionality of fibrillated NDM, they can be used in product formulations such as ice cream mix where the thickening of a solution, good emulsification, and foaming properties are required.

Keywords: Fibrillated NDM, viscosity, emulsification capacity, foaming capacity

Introduction

Milk is an important source of nutrition and source of essential amino acids, fatty acids, and minerals. Milk is converted to a variety of products such as yogurt, ice-cream, and cheese which increase milk consumption and omit the limitation of lower shelf life of milk. However, these products must have desirable product properties for customer acceptance such as yogurt with a thick gel and no syneresis (Peng et al., 2009), drier ice cream with optimum meltdown; cheese and cheese spread without excessive oiling off. Therefore, different additives such as texture modifiers, emulsifiers, stabilizers, and gelling agents are added to the product formulation to meet customer acceptance and retain product quality (Baba et al., 2018; Khubber et al., 2021). However, consumers want products free of non-dairy ingredients or added with clean label ingredients without impacting the product quality. These desirable product qualities can be incorporated by enhancing the functionality of milk protein ingredients such as milk proteins.

Among milk constituents, milk protein can provide better gelation by forming a three-dimensional network (Donato et al., 2007), and interfacial properties such as emulsification and foaming properties by adsorbing at the oil-water and air-water interface, respectively. Therefore, manufacturers are adding additional protein to the formulation using protein-rich ingredients such as milk protein concentrate, nonfat dried milk, and micellar casein concentrate. However, milk proteins are costly ingredients in milk product formulation, therefore the addition of milk protein ingredients will increase the overall cost of manufacturing. Further, the additional total solids from proteins will also change the physical properties of the product (such as viscosity) which might create difficulties in processing the product. Therefore, processing interventions are needed to enhance functionality with similar protein content. Recently, fibrillation emerged as a

new technique to modify globular proteins such as whey proteins into fibrils. The fibrillar structure of a protein is known to provide enhanced functional properties such as gelling, foaming (Oboroceanu et al., 2014), emulsification (Mantovani et al., 2018), viscosity (Loveday et al., 2012) than native globular proteins (Loveday et al., 2017).

Recently, Rathod and Amamcharla (2021) reported a process to manufacture the fibrillated milk protein concentrate (MPC) by selective conversion of globular whey proteins into fibrils, which showed improved functional properties than the control MPC. Non-fat dried milk is a widely used ingredient in milk product formulation and improving functionality can help to reduce the use of non-dairy ingredients. Therefore, the current study was focused on improving the functionality of non-fat dried milk using selective fibrillation of whey proteins. Hence, skim milk was subjected to microfiltration and ultrafiltration to separate whey proteins. Separated whey proteins were subjected to fibrillation followed by mixing back with other membrane-separated constituents to get fibrillated skim milk. This fibrillated skim milk was spray-dried to get fibrillated non-fat dried milk (NDM). Then, the fibrillated NDM was checked for the survival of fibrils and other functional properties after reconstitution.

Materials and methods

Experimental Approach

Pasteurized skim milk was subjected to microfiltration (MF) to separate casein in MF retentate and whey proteins in MF permeate. MF permeate was subjected to ultrafiltration (UF) to further increase the whey protein concentration in UF retentate. Then, UF retentate was standardized for 2% protein and divided into two equal parts. One part was stored in a cold store without any treatment and termed as control UF retentate.

The second portion was subjected to fibrillation process to convert whey proteins into fibrils (Figure 6.1) and termed a fibrillated UF retentate. Control UF retentate was mixed with casein-rich MF retentate and UF permeate keeping the ratio of all the constituents similar to skim milk and termed a control skim milk. Similar to control UF retentate, fibrillated UF retentate was also mixed with MF retentate and UF permeates and termed fibrillated skim milk. Both control and fibrillated skim milk were spray dried and termed as control non-fat dried milk (NDM) and fibrillated NDM, respectively. Both NDMs were characterized for their functional properties. The whole experiment was replicated with three independent lots of skim milk.

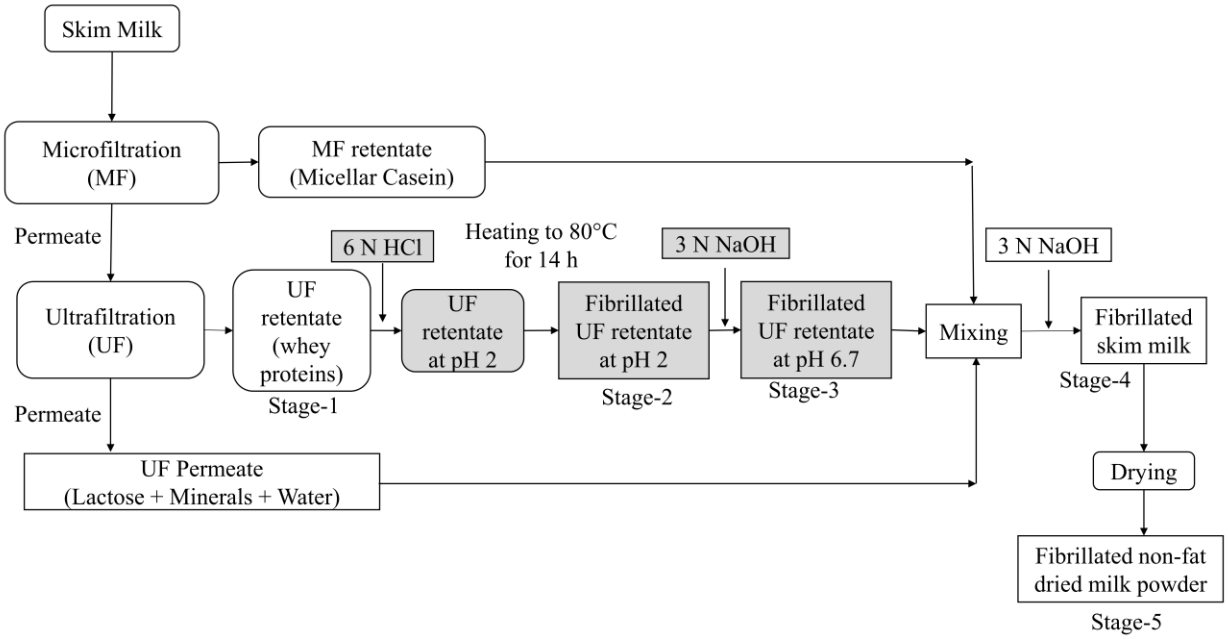

Figure 6.1 Process flow diagram for manufacturing control and fibrillated non-fat dried milk (Representative sample was taken in different stages: Stage-1. UF retentate at pH 2, Stage-2. Fibrillated UF retentate at pH 2, Stage-3. Fibrillated UF retentate at pH 6.7, Stage-4. Fibrillated skim milk, Stage-5. Fibrillated non-fat dried milk powder) (Shaded portion was omitted for control NDM)

Preparation of control and fibrillated NDM.

Control and fibrillated NDM were prepared as shown in Figure 6.1. Briefly, pasteurized skim milk was collected from the Davis dairy plant, South Dakota State University, SD. Pasteurized skim milk was warmed to 23.3 °C and subjected to MF to get casein-rich MF retentate and whey proteins in MF permeate. MF was performed using two 0.1 µm ceramic microfiltration membrane. Microfiltration was performed at 23.3 °C using a transmembrane pressure of 86.2 kPa (34.5 kPa inlet and 103.4 kPa differential). MF retentate was cooled, divided into two parts, and kept in cold storage(4°C). MF permeate was ultrafiltered using an ultrafiltration (UF) membrane to fractionate and concentrate whey proteins in UF retentate and non-protein parts in UF permeate. UF was performed using two 10 kDa polyether sulfone spiral wound membranes (3838 element format, Dominick Hunter Filtration Division-N. A, Parker Hannifin Corporation, Oxnard, CA, USA) arranged in parallel. Each membrane element was 97 mm in diameter and 965 mm in length with a 1.1 mm feed spacer and a total surface area of 5.7 m2. Ultrafiltration was performed at 23.3 °C using a 276 kPa transmembrane pressure (207 kPa inlet and 138 kPa differential). UF retentate was diluted to 2% protein using UF permeate and divided into two halves. The first half was used as a control and stored in cold storage (4°C) without giving any further treatment and termed as control UF retentate. Another half was acidified to pH 2 using 6 N HCl and heated to 80°C for 14 hours under constant stirring, followed by immediate cooling to 4°C using an ice bath to get fibrillated UF retentate. Fibrillated UF retentate was further neutralized to pH 6.7 using 3 N NaOH and stored in cold storage. MF retentate, control UF retentate, and UF permeate were mixed keeping the mixture composition similar to skim milk and termed control skim milk. Similar to control skim milk, MF retentate, fibrillated UF retentate and UF permeate were mixed and termed fibrillated skim milk. Control and fibrillated skim milk

were dried using a two-stage spray drier with an external vibrating fluidized bed and termed Control NDM and Fibrillated NDM, respectively. The whole study was conducted using three independent lots of skim milk.

Confirmation of fibril formation at different stages of production of control and fibrillated NDM

Representative samples were taken at each manufacturing stage (Stage-1. UF retentate at pH 2, Stage-2. Fibrillated UF retentate at pH 2, Stage-3. Fibrillated UF retentate at pH 6.7, Stage-4. Fibrillated skim milk, Stage-5. Fibrillated non-fat dried milk powder) as shown in Figure 6.1 to confirm fibril formation and survival. Fibrillated NDM sample was reconstituted to 10% (Wt/Wt) total solids in distilled water (45°C) with constant stirring for 30 minutes using an overhead stirrer (Caframo^{TM} Ontario, Canada) at 500 rpm), followed by overnight storage in the refrigerator (4°C) to ensure complete rehydration. A reconstituted fibrillated NDM sample was ultracentrifuged (90000×g) for 1 hour and the supernatant was collected. The presence of fibrils was confirmed by Thioflavin T fluorescence value and transmission electron microscopy as suggested by Rathod and Amamcharla (2021). Tricine-sodium dodecyl sulfate-polyacrylamide gel electrophoresis (SDS-PAGE) was used to determine the conversion of whey proteins into fibrils.

Tricine SDS-PAGE

Samples collected at differnet stages (Figure 6.1) were diluted to 0.5% protein content using distilled water and vortexed. Diluted samples were mixed with tris-tricine sample buffer in a 1:2 ratio and vortexed. The mixture was incubated at 37°C for 15 minutes. Then, a 15 µl mixture was loaded in the 16.5% precast Tris-Tricine gel (Bio-Rad Laboratories, Hercules, CA)

fitted into an electrophoresis assembly (BioRad Mini Gel system, Bio-Rad Laboratories, Hercules, CA) filled with 1X Tris-Tricine sample buffer (Bio-Rad Laboratories, Hercules, CA) prepared from 10X Tris-Tricine buffer by mixing sample buffer, and double distilled water in 1:9 ratio. The gel was run at 20 mA for 15 minutes for stacking. Then, adjusted to 25 mA for 90 minutes (Schägger, 2006). The gels were removed when the dye reached the bottom line. The gel was fixed in 10% Trichloroacetic acid solution for one hour. The gel was removed and dipped into a tray filled with staining solution (Coomassie brilliant blue R-250, Bio-Rad Laboratories, Hercules, CA) with continuous shaking for 24 hours. Then, the staining solution was replaced with a destaining solution (10% methanol, 10% acetic acid, 80% double distilled water) and kept for 24 hours with continuous shaking. The gel was placed on a transparency slide and scanned using a scanner to get an image of the gel.

Functional Properties of control and fibrillated NDM

Rheology

Both NDM samples were reconstituted in distilled water (at 45°C) at 10%, 15%, and 20% total solids with constant stirring for 30 minutes using an overhead stirrer (Caframo^{TM} Ontario, Canada) at 500 rpm), followed by overnight storage in the refrigerator (4°C) to ensure complete rehydration. The next day, skim milk and reconstituted samples were tempered to 20°C using temperature controlled water bath, and continuous rotational flow data were collected at 20°C using a stress-strain-controlled rheometer (MCR-92 Anton Paar, Vernon Hills, IL) fitted with a cup and bob geometry (Bob Length-60 mm, Bob diameter-38.7 mm, and Cup diameter- 42 mm) at a varied shear rate from 0.01 s^{-1} to 200 s^{-1} at 20°C. Along with viscosity, the consistency coefficient and flow behavior index were also calculated using the power-law model (Rathod and Amamcharla, 2021).

Acid-base titration curve

Acid-base titration profiles of reconstituted control and fibrillated NDM (10% Wt/Wt total solids) were carried out by using the method described by Rathod et al., 2022. Briefly, both control and fibrillated NDM were reconstituted in distilled water (45°C) to 10% (Wt/Wt total solids) with continuous stirring using an overhead stirrer (Caframo^{TM} Ontario, Canada) at 500 rpm, followed by overnight refrigerated storage to ensure complete hydration. The following day, samples were tempered to 30°C using a temperature-controlled water bath and used for analysis. Samples were titrated from their initial pH of 6.7 to pH 3.0 by adding 0.2 mL of 0.5 N HCl in increments under constant stirring and constant temperature of 30°C using a temperature-controlled water bath (Cole Parmer, Vernon Hills, IL) attached with a magnetic stirrer. The pH was recorded using Accumet™ AP110 Portable pH Meter (Fisher Scientific, Waltham, MA) after every 0.2 mL incremental addition of hydrochloric acid. Once the pH reached 3.0, the same sample was back titrated to pH 7.0 by 0.2 mL incremental addition of 0.5 N sodium hydroxide under constant stirring. The pH was also recorded after every addition of 0.2 mL sodium hydroxide.

Acid gelation

Both reconstituted NDM dispersions (10% Wt/Wt total solids) were heated to 90°C for 10 min, immediately cooled to 4°C, and kept at refrigerated temperature (4°C) overnight before further analysis.

Acid gel rheology. The reconstituted NDM dispersions were tempered to 30°C (using a temperature-controlled water bath). Then, a calculated quantity of glucono-δ-lactone (GDL; Fisher Scientific, Waltham, MA) was added to reconstituted NDM (@ 2 g of per 100 mL) and mixed using a magnetic stirrer for 2 min. Immediately, a part of the GDL mixed reconstituted

NDM was transferred to a temperature-controlled water bath (Cole Parmer, Vernon Hills, IL) maintained at 30°C for continuous pH measurement using Accumet™ AP110 Portable pH Meter (Fisher Scientific, Waltham, MA). Simultaneously, the remaining reconstituted NDM was used to monitor rheological characteristics during acid gelation using a stress-strain-controlled rheometer (MCR-92 Anton Paar, Vernon Hills, IL) with a cup and bob geometry consisting of a coaxial cylinder (Bob Length-60 mm, Bob diameter-38.7 mm, and Cup diameter- 42 mm). Cup and bob geometry was preheated to 30°C. During acid gelation, the sample oscillated at a constant frequency of 1 Hz with an applied strain of 0.5%, which caused minimal disruption of acid gels during the development of the gel network (Peng et al., 2009). Measurements were taken every 5 minutes until the pH reached 4.6.

Acid gel microstructure. Reconstituted NDM (30 mL) was transferred to a beaker and tempered to 30°C. Then, the pre-estimated quantity of GDL was added to reconstituted NDM to reach the final acid gel pH of 4.6. The mixture was stirred using a magnetic stirrer for 3 minutes to ensure complete mixing of GDL. Then, 45 μL of the sample-GDL mixture was transferred on the glass slide having silicon spacer (0.5 mm height and 9 mm diameter) and covered with a coverslip. Then, the glass slide with the sample-GDL mixture and left-over sample with GDL in the beaker was incubated at 30°C for 4 h, then kept in the refrigerator overnight. The next day, the pH of the acid gel formed in the beaker was measured for confirmation of a pH drop to 4.6. The coverslip on the glass slide was gently removed, and the acid gel on the slide was stained with 10 μL of fast green FCF (5 mg dye in 5 mL water) for 5–10 min in dark and covered again with the coverslip. The stained gels were viewed under a confocal laser scanning microscope (LSM 5 Pascal: Zeiss, Thornwood, NY) version 3.2 SP2. A Plan-Neofluar 10x/0.3 and Plan-Neofluar 40x/1.3 Oil DIC objective were used for image acquisition. A 543 nm Helium-Neon

laser line and a primary dichroic HFT 543 to excite Fast green FCF. The emission signal was collected with Channel 2 using a secondary dichroic NFT 635 and an LP 650 nm filter to detect Fast Green (green) (Gandhi et al., 2017). Images were analyzed with ImageJ software (ImageJ, National Institutes of Health, Bethesda, MD) with a color pixel counter plugin to measure the green color area.

Emulsification capacity

Emulsification capacity was measured as suggested by Baheeja et al. (2022) method. Reconstituted NDM samples were diluted to 0.05% protein and 120 mL of diluted sample was taken in a 600 mL beaker at room temperature. The handheld homogenizer (CAT Scientific X120 PolyScience, Niles, IL, USA) and conductivity meter electrode (Accumet™ AP75; Fisher Scientific, PA) were placed in the beaker containing the diluted sample. Vegetable oil (locally purchased) was filled in a 125 mL separatory funnel and placed just above the beaker. Then, vegetable oil addition was started by opening the 125 mL separatory funnel valve all the way up with continuous blending. Initially, the blending of oil and the diluted sample was done at a slow rate (speed 1), then the speed was increased to speed 3. Oil addition was stopped when the emulsion breakpoint was detected. Emulsion breakpoint was marked when conductivity become zero due to an increase in electric resistance upon emulsion collapse. Emulsification capacity was expressed as the total g of oil emulsified per mg of soluble protein Acton and Saffle (1972).

Foaming capacity and foam stability

Foam capacity and foam stability were measured according to the method described by Sinha et al. (2007). Briefly, reconstitute NDM samples were diluted to 3% (Wt/Wt) protein with distilled water. 100 mL of diluted sample was taken into a 400 mL beaker. The diluted sample was whipped for 3 min at high speed using a handheld homogenizer (CAT Scientific X120

PolyScience, Niles, IL, USA). The foam was poured immediately into a 250 ml measuring cylinder and the total volume of the foam was measured immediately after 30 s. The foam stability was determined by measuring the fall in the volume of the foam after 30 min. All the experiments were performed in triplicate and the results are the average of three values.

Heat Coagulation Time

Heat coagulation time was performed by the method suggested by Rathod and Amamcharla, (2021). Briefly, reconstituted NDM samples (10% total solids) were adjusted to pH 6.9 and kept overnight in the refrigerator. Then, 2 mL of the sample was filled in heat-resistant screw cap test tubes (8 mL, 17 mm dia. x 63 mm height) (DWK Life Science, Millville, NJ). The test tubes were inserted into the stainless-steel rack. The rack along with tubes was immersed in an oil bath (Narang Scientific Works Pvt. Ltd, New Delhi, India) maintained at 140°C and placed on the rocker. Heat coagulation time was noted as the time in seconds elapsed between dipping the samples in the hot oil bath and the onset of visible clots/flakes.

Protein oxidation

Protein oxidation was studied according to the method given by Scheidegger et al. (2010) and Keppler et al. (2019). Briefly, reconstituted NDM was diluted to 0.1 % protein content using deionized water followed by vortex mixing. Protein oxidation was measured in terms of decay in two amino acids *viz.*, Tryptophan and tyrosine, and their respective oxidation products that are N-formyl kynurenine and Di-tyrosine. Diluted protein solutions were analyzed in quartz cuvette using a spectrofluorometer (LS-55; Perkin Elmer, Waltham, MA) using right angle assembly for tryptophan (excitation and emission wavelength- 294 nm and 340 nm, respectively) and L-tyrosine (excitation and emission wavelength- 274 nm and 310 nm, respectively) using 1% attenuation filter

with 10 nm excitation slit width and 20 nm emission slit width. Similarly, oxidation products N-formyl kynurenine (excitation and emission wavelength- 325nm and 435 nm, respectively) and Di-tyrosine (excitation and emission wavelength-284 nm and 415 nm, respectively) were also measured. The fluorescence intensity was recorded to compare the concentration of a specific component in control and fibrillated NDM.

Statistical Analysis

Statistical analysis was performed using Excel (Microsoft Corp., Redmond, WA). One-way ANOVA and Tukey's multiple range test were done using SAS Version 9.4 (SAS Institute Inc.).

Results and discussion

Confirmation of fibril formation and viability during the manufacture of fibrillated NDM and comparison with control NDM

Fibrillated NDM was produced as per the process as shown in Figure 6.1 and fibril formation was confirmed at every stage (Stage-1. UF retentate at pH 2, Stage-2. Fibrillated UF retentate at pH 2, Stage-3. Fibrillated UF retentate at pH 6.7, Stage-4. Fibrillated skim milk, Stage-5. Fibrillated non-fat dried milk powder) during the process using thioflavin T fluorescence (Th T) value, transmission electron microscopy and Tricine-SDS-PAGE and compared with control NDM. Table 6.1 showed that thioflavin T values of fibrillated UF retentate (both at pH 2 and 6.7) were higher than the control UF retentate. Similarly, fibrillated skim milk showed a higher Th T value than control skim milk. When both NDM was reconstituted, fibrillated NDM also showed a higher Th T value than control NDM (Table 1). Th T value is an indirect indicator of fibril formation (Pan and Zhong, 2015), therefore higher Th T

value indicate the presence of fibrils in fibrillate UF retentate, fibrillated skim milk, and fibrillated NDM. Several studies reported an increase in the Th T values after the conversion of proteins into fibrillar protein (Koudelka et al., 2012; Mantovani et al., 2016). For further confirmation of the presence of fibrils, samples were analyzed using TEM, and the result were shown in Figure 6.2. Visible fibrils were observed in TEM images of fibrillated UF retentate at pH 2 and pH 6.7. Similar TEM images of milk whey protein isolate fibrils were seen by Rathod and Amamcharla (2021) and other researchers for whey proteins fibrils (Loveday et al., 2012) and β-lactoglobulin fibrils (Dave et al., 2013). Fibrillated skim milk and Fibrillated NDM did not show visible fibrils similar to fibrillated UF retentate which could be due to the small proportion of fibrillated whey proteins (~0.8%) in fibrillated skim milk and fibrillated NDM. The higher proportion of casein might overshade whey protein fibrils. Therefore, reconstituted fibrillated NDM was ultracentrifuged (90000×g) to remove casein from the solution in form of a pallet, and the supernatant was analyzed for TEM. Visible fibrils were seen in the TEM images of the supernatant of fibrillated NDM which confirm the presence and survival of whey protein fibrils after spray drying. Tricine SDS-PAGE was used as another method for confirmation of fibrillation and images gels were shown in Figure 6.3. Here, all the fibrillated samples showed the presence of small molecular weight (2-8 kDa) peptides, which is also an indicator of fibril formation (Akkermans et al., 2008a; Rathod and Amamcharla, 2021). During fibril formation, protein is hydrolyzed due to heat and low pH and rearranges itself into an ordered fibrillar form. Due to SDS, a dissociating agent, whey protein fibrils were dissociated into hydrolysates with different molecular weights (2-8 kDa) which can be seen in the gel image (Figure 6.3). Further, Fibrillated skim milk showed higher viscosity compared to control skim milk (Table 1), and reconstituted fibrillated NDM also showed higher viscosity compared to reconstituted control

NDM. A similar increase in viscosity due to fibril formation was reported by Rathod and Amamcharla (2021) for fibrillated model milk protein concentrate. These results suggest that fibrillated samples have a presence of whey protein fibrils and whey protein fibrils survived the spray drying condition as the presence of whey protein fibrils was confirmed in reconstituted fibrillated NDM.

Table 6.1 Thioflavin T fluorescence value of control UF retentate, fibrillated UF retentate (at pH 2 and pH 6.7), control and fibrillated skim milk and NDM; and rheology of control and fibrillated skim milk and NDM.

Sample	Control UF retentate	Fibrillated UF retentate at pH 2	Fibrillated UF retentate at pH 6.7	Control skim milk	Fibrillated skim milk	Control NDM	Fibrillated NDM
Thioflavin T fluorescence value (AU)	12±1	519±55	140±91	169±16	206±29	175±9	229±14
Viscosity at 100 S^{-1} (mPa.S)				2.14±0.17	2.26±0.07	2.28±0.13^{b}	2.58±0.09^{a}

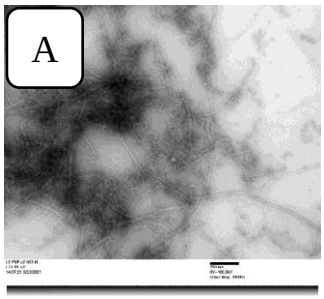

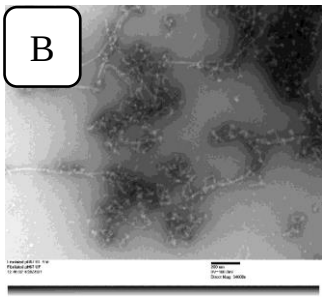

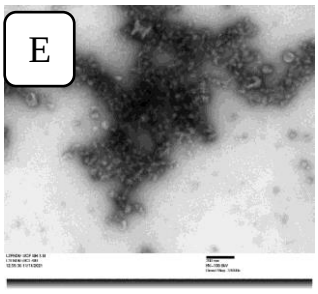

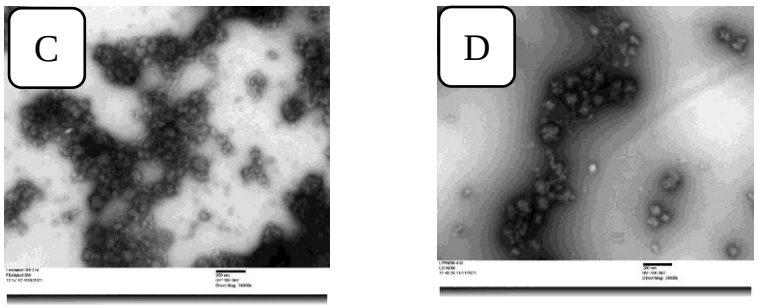

Figure 6.2 TEM images of Fibrillated UF at pH 2 (A), Fibrillated UF at 6.7 (B), Fibrillated skim milk (C), Reconstituted Fibrillated NDM (D), and Supernatant of reconstituted Fibrillated NDM (E). (Scale-200 nm)

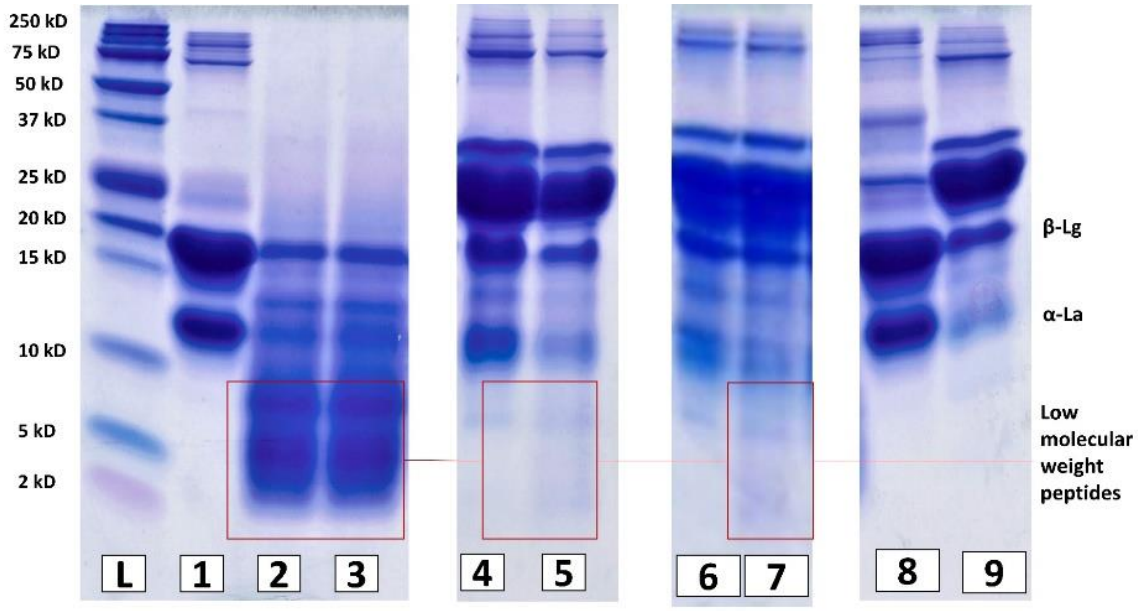

Figure 6.3 Tricine-Sodium Dodecyl Sulfate-Polyacrylamide gel (L-Ladder (2-250 kD), Lane-1-Control UF retentate, Lane-2-Fibrillated UF retentate at pH-2, Lane-3- Fibrillated UF retentate at pH-6.7, Lane-4-Control skim milk, Lane-5-Fibrillated skim milk, Lane-6-Reconstituted control NDM, Lane-7-Reconstituted Fibrillated NDM, Lane-8-Milk whey proteins isolate Lane-9-Micellar casein concentrate

Comparison of functional properties of control and fibrillated NDM

Rheology

Rheology of reconstitute control and fibrillated NDM is shown in Table 6.2. Both NDM were reconstituted at different total solids (10%, 15%, and 20%) and studied for rheology. Fibrillated NDM showed significantly ($P<0.05$) higher viscosity than the control NDM (Table 6.2). At l0% total solid, the difference in viscosity between reconstituted control and fibrillated NDM was smaller. The difference in viscosity was increased with an increase in total solids. Similarly, consistency co-efficient was also significantly ($P<0.05$) higher for reconstituted fibrillated NDM, and the difference in consistency co-efficient was also increased with an increase in total solids. However, the flow behavior index of reconstituted fibrillated NDM was significantly lower than reconstituted control NDM. At 10% total solids, both NDM showed shear thickening behavior however, with an increase in the total solids they turned shear thinning. Similarly, an increase in viscosity and consistency co-efficient was seen for fibrillated model milk protein concentrate (MPC) by Rathod and Amamcharla (2021). Also, they have seen the shear thinning behavior of both fibrillated and control model MPC. They reported that whey protein fibrils form a fibrillar network which increases overall viscosity and consistency co-efficient, therefore increase in viscosity and consistency co-efficient was seen in the reconstituted fibrillated NDM samples as compared to reconstituted control NDM. An increase in total solids further increases the number of whey protein fibrils and other constituents, which cumulatively resulted in viscosity and consistency coefficient. Due to applied shear, fibrillar network breaks and fibrils align to the direction of shear forces, which resulted in the shear thinning behavior of fibrillated samples (Akkermans et al., 2008b; Mantovani et al., 2018).

Therefore, it could be said that the presence of whey protein fibrils in the reconstituted fibrillated NDM is responsible for the change in the overall rheological behavior.

Table 6.2 Comparison of rheology (at 10%, 15%, and 20% Total solids) of control and fibrillated NDM.

Parameters	Total Solids	Control NDM	Fibrillated NDM	% increase to control NDM
Viscosity at 100 S^{-1} (mPa.S	10%	2.28±0.13[b]	2.58±0.09[a]	13.1
	15%	4.14±0.66[b]	7.92±1.04[a]	91.3
	20%	6.66±1.16[b]	16.93±3.51[a]	154.2
Consistency Co-efficient (K) (mPa.S^n	10%	0.99±0.14[b]	1.38±0.15[a]	
	15%	3.86±1.22[b]	11.12±2.1[a]	
	20%	8.36±3.46[b]	34.54±11.74[a]	
Flow Behavior index (n)	10%	1.22±0.02[a]	1.17±0.02[b]	
	15%	1.03±0.05[a]	0.93±0.01[b]	
	20%	0.98±0.04[a]	0.85±0.03[b]	

[a-b] Mean within a row with different superscripts differ ($P<0.05$); n=3

Acid-base titration

Both reconstitute control and fibrillated NDM (10% Wt/Wt total solids) were analyzed for acid-base titrations. Reconstituted fibrillated NDM uses slightly higher amount of acid (6.8 ml) to bring down pH to 3 than reconstituted control NDM (6.6 ml). Similarly, reconstituted fibrillated NDM used a slightly higher amout of base (7.6 ml) to neutralize to pH 7 than reconstituted control NDM (7.2 ml). This observation is similar to our earlier study on fibrillated model MPC where fibrillated milk whey proteins and fibrillated model MPC used a higher

amount of acid to bring down pH to 3 and higher alkali to neutralize pH to 7 (Rathod et al, 2022).

Acid gelation

Acid gel rheology. The acid gelation behavior of both reconstituted NDM was shown in Figure 6.4 and Table 6.3. The gelation pH of reconstituted control NDM was 5.19±0.06 which was higher than the reconstituted fibrillated NDM (5.12±0.01). Once the gelation started, reconstituted control NDM showed higher storage modulus (G′) than the reconstituted fibrillated NDM throughout the whole gelation period. Both reconstituted control and fibrillated NDM show continuous increase till gelation pH reached 4.6. G′ at pH 4.6 for reconstituted control NDM was 345±76 Pa which was higher than the reconstituted fibrillated NDM (237±8 Pa). These results are completely inverse to the results of our earlier studies on fibrillated model MPC. It needs further detailed investigation on whey protein fibrils and casein interaction during spray drying and subsequent reconstitution of fibrillated NDM.

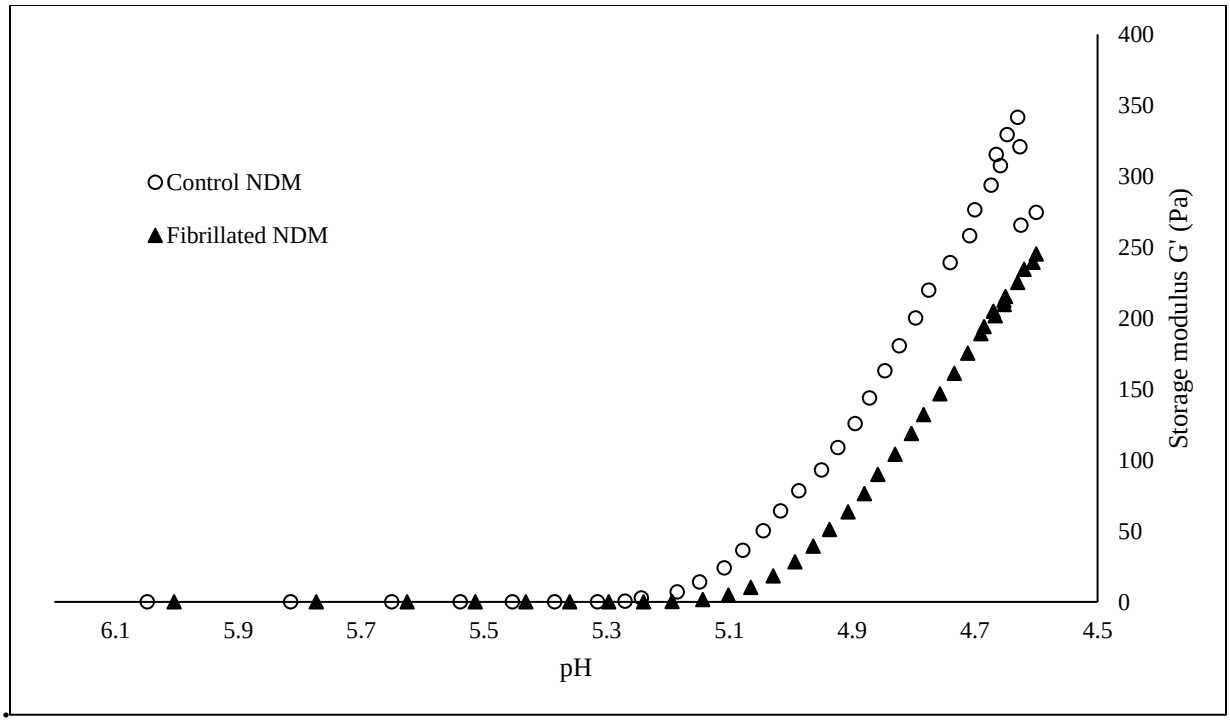

Figure 6.4 Changes in rheological behavior during gelation of control and fibrillated non-fat dried milk (NDM) storage modulus (G′) v/s pH during gelation

Table 6.3 Comparision of functional properties of control and fibrillated NDM

Functional Property	Control NDM	Fibrillated NDM
Gelation		
Gelation pH	5.19±0.06[a]	5.12±0.01[b]
Max. Storage modulus (G′)	345±76[a]	237±8[b]
Emulsification Capacity (g of oil per mg of protein)	3.12±0.13[b]	3.44±0.14[a]
Foaming Capacity (mL/g)	31.6±3.3[b]	35.3±1.9[a]
Foam Stability (mL/g)	14.3±4.6[a]	17.0±2.0[a]
Heat Coagulation Time (s)	212±37[b]	238±37[a]

[a-b] Mean within a row with different superscripts differ ($P<0.05$); n=3

Acid gel microstructure. The microstructure of the acid gel of both reconstituted NDM was shown in Figure 6.5. At 10x magnification, both the acid gels look similar with some pores. When acid gels were analyzed using the color pixel counter plugin in ImageJ software, acid gel of reconstituted control NDM showed slightly lower green pixels (99.54%) than reconstituted fibrillated NDM (99.89%) which shows that reconstituted control NDM has more empty space than reconstituted fibrillated NDM. This difference can be seen at higher magnification (40x). Reconstituted control NDM showed 76.36% and reconstituted fibrillated NDM showed 87.24% green area.

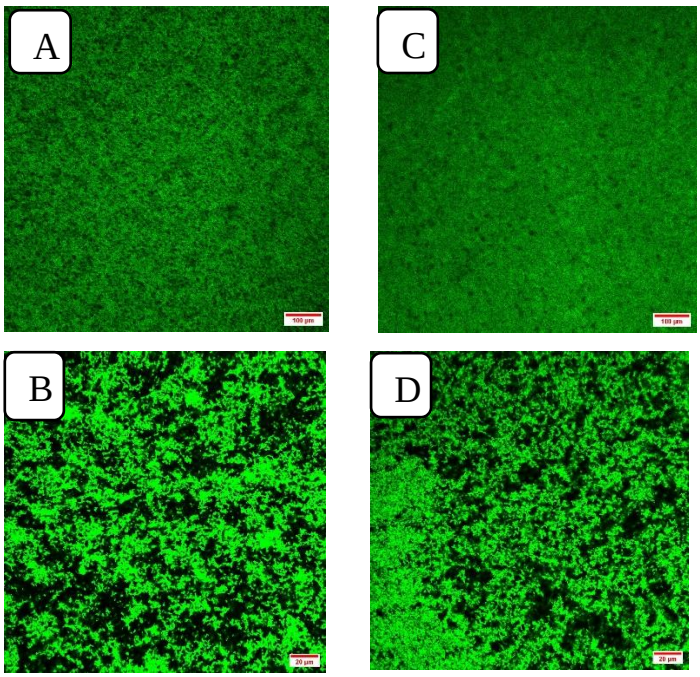

Figure 6.5 Confocal laser scanning microscopic image of acid gels of control NDM (A, B) and fibrillated NDM (C, D) at 10% (Wt/Wt) total solids.

Emulsification capacity

Results of emulsification capacity was shown in Table 6.3. The emulsification capacity (g of oil per mg of protein) of reconstituted fibrillated NDM was 3.44±0.14 which is significantly higher than the reconstituted control NDM (3.12±0.13). In reconstituted fibrillated NDM, globular whey proteins were converted to whey protein fibrils and this fibrillar structure shows a good emulsification capacity by providing higher viscosity and faster migration of whey protein fibrils to the oil-water interface (Mantovani et al., 2018; Jiang et al., 2021). The fibrillar structure is more open than the globular structure, therefore more functional groups are exposed which can interact with the aqueous phase and oil phase to form an emulsion. This could be the possible reason behind the increase in the emulsification capacity of reconstituted fibrillated NDM.

Foaming capacity and foam stability

The result of foaming capacity and foam stability was shown in Table 6.3. A sample of reconstituted fibrillated NDM (35.3±1.9) showed significantly ($P<0.05$) higher foaming capacity than the reconstituted control NDM (31.6±3.3). Similarly, reconstituted fibrillated NDM (17.0±2.0) showed higher foaming stability than the reconstituted control NDM (14.3±4.6), but the difference was statistically non-significant. When protein dispersions were whipped using a high shear mixer, the air was incorporated in the dispersion and dispersed in form of air cells. The air cells were surrounded by liquid, and an air-protein dispersion film will be formed on the air-water interface, and finally structured as an air bubble (Damodaran, 2005). This process is influenced by how protein, from the dispersion, moves over the air-water interface and is absorbed at the interface. Protein adsorption at the interface depends on the unfolding and denaturation of protein, exposure of hydrophobic residues of the protein to the air phase, and its hydrophilic segment to the aqueous phase (Oboroceanu et al., 2014). Considering the structure,

whey protein fibrils are more open structure than the native globular whey proteins. Further, whey protein fibrils at neutral pH are absorbed faster than fibrils at their formation pH (pH 2) due to the lower energy barrier to be absorbed (Wan et al., 2016). Whey protein fibrils in reconstituted fibrillated NDM were near neutral pH, therefore they could be absorbed faster at the interface which could the reason behind the higher foaming capacity of fibrillated NDM. Foam stability is mainly affected by the drainage of the liquid film and bubble coalescence. Therefore, to produce a high-volume stable protein foam, drainage of liquid from between the bubbles must be minimized (Damodaran, 2005; Oboroceanu et al., 2014). Whey protein fibrils thicken the solution by providing a 3-dimensional network, which can be seen by the higher viscosity of reconstituted fibrillated NDM. Increased solution restricts the movement of the air cell, which reduces the chance of coalescence of air cells and escape of air cells, which led to an increase in foam stability.

Heat coagulation time

Results of heat coagulation time are shown in Table 6.3. Reconstituted fibrillated NDM showed higher heat coagulation time than the reconstituted control NDM. However, lower heat stability was reported for fibrillated samples by Rathod and Amamcharla, (2021). Compared to fibrillated model milk protein concentrate, fibrillated NDM has a lower concentration of fibrils and the presence of another non-protein component. Therefore, it may show a difference in heat stability which need further investigation.

Protein oxidation

The results of the protein oxidation study are shown in Table 6.4. Both reconstituted NDMs showed a non-significant difference in Tryptophan and Tyrosine values. This indicates that there is no significant loss of essential amino acids. Oxidation products of Tryptophan and

Tyrosine were also detected, which are N-formyl kynurenine and Di-tyrosine (Feng et al., 2015). A sample of reconstituted fibrillated NDM showed significantly ($P<0.05$) higher Di tyrosine and N-formyl kynurenine value, which is an indicator of protein oxidation (Keppler et al., 2019). However, the difference between control and fibrillated NDM for Di-tyrosine value and N-formyl kynurenine was not higher. Therefore, it could be said that the fibrillation process is not severely affecting essential amino acid content.

Table 6.4 Comparison of protein oxidation in control and fibrillated NDM

Sample	Control NDM	Fibrillated NDM
Tryptophan (AU)	643 ± 2.9^{a}	640.8 ± 14.2^{a}
Tyrosine (AU)	263.6 ± 5^{a}	264.4 ± 5.9^{a}
Di-tyrosine (AU)	100 ± 2.2^{b}	104.3 ± 2.3^{a}
N-formyl kynurenine (AU)	22.49 ± 1.2^{b}	22.74 ± 1.1^{a}

[a-b] Mean within a row with different superscripts differ ($P<0.05$); n=3

Conclusion

Fibrillation of whey proteins showed improvement in functional properties such as emulsification, foaming, thickening, and gelling. Therefore, whey proteins, a globular protein in skim milk, were fractionated using the membrane process and selectively converted into the fibrillar form using the fibrillation process, and mixed back to the remaining constituents of skim milk from membrane separation. The fibril-containing fibrillated skim milk was spray dried and called fibrillated NDM. Results of Thioflavin T fluorescence value, transmission electron microscopy, and gel electrophoresis showed conversion of globular whey proteins into whey protein fibrils and survival of whey protein fibrils during further processing and spray-drying.

Further, reconstituted fibrillated NDM showed higher viscosity, emulsification capacity, foaming capacity, and foam stability. Unlike fibrillated model MPC, reconstituted fibrillated NDM showed lower storage modulus than the reconstituted control NDM during gelation. The manufactured fibrillated NDM can be checked for product applications such as ice cream to see the improvement in the functionality of the product.

Acknowledgments

We thank Dairy Management Inc. and Midwest Dairy Foods Research Center (St. Paul, MN) for their financial support. We also thank Dr. Boyle, Director of KSU Microscopy Facility for helping with TEM and Confocal Laser scanning analysis.

References

Akkermans, C., P. Venema, A.J. van der Goot, H. Gruppen, E.J. Bakx, R.M. Boom, and E. van der Linden. 2008a. Peptides are building blocks of heat-induced fibrillar protein aggregates of β-lactoglobulin formed at pH 2. Biomacromolecules 9:1474–1479. doi:10.1021/BM7014224/SUPPL_FILE/BM7014224-FILE002.PDF.

Akkermans, C., A.J. Van der Goot, P. Venema, E. Van der Linden, and R.M. Boom. 2008b. Properties of protein fibrils in whey protein isolate solutions: Microstructure, flow behaviour and gelation. Int. Dairy J. 18:1034–1042. doi:10.1016/J.IDAIRYJ.2008.05.006.

Baba, W.N., K. Jan, H.A. Punoo, T.A. Wani, M.M. Dar, and F.A. Masoodi. 2018. Techno-functional properties of yoghurts fortified with walnut and flaxseed oil emulsions in guar gum. LWT 92:242–249. doi:10.1016/J.LWT.2018.02.007.

Dave, A.C., S.M. Loveday, S.G. Anema, T.S. Loo, G.E. Norris, G.B. Jameson, and H. Singh. 2013. β-lactoglobulin self-assembly: Structural changes in early stages and disulfide

bonding in fibrils. J. Agric. Food Chem. 61:7817–7828. doi:10.1021/JF401084F/SUPPL_FILE/JF401084F_SI_001.PDF.

Donato, L., M. Alexander, and D.G. Dalgleish. 2007. Acid gelation in heated and unheated milks: Interactions between serum protein complexes and the surfaces of casein micelles. J. Agric. Food Chem. 55:4160–4168. doi:10.1021/JF063242C/ASSET/IMAGES/LARGE/JF063242CF00006.JPEG.

Feng, X., C. Li, N. Ullah, J. Cao, Y. Lan, W. Ge, R.M. Hackman, Z. Li, and L. Chen. 2015. Susceptibility of whey protein isolate to oxidation and changes in physicochemical, structural, and digestibility characteristics. J. Dairy Sci. 98:7602–7613. doi:10.3168/JDS.2015-9814.

Gandhi, G., J.K. Amamcharla, and D. Boyle. 2017. Effect of milk protein concentrate (MPC80) quality on susceptibility to fouling during thermal processing. LWT - Food Sci. Technol. 81:170–179. doi:10.1016/J.LWT.2017.03.063.

Jiang, F., Y. Pan, D. Peng, W. Huang, W. Shen, W. Jin, and Q. Huang. 2022. Tunable self-assemblies of whey protein isolate fibrils for pickering emulsions structure regulation. Food Hydrocoll. 124:107264. doi:10.1016/J.FOODHYD.2021.107264.

Keppler, J.K., T.R. Heyn, P.M. Meissner, K. Schrader, and K. Schwarz. 2019. Protein oxidation during temperature-induced amyloid aggregation of beta-lactoglobulin. Food Chem. 289:223–231. doi:10.1016/J.FOODCHEM.2019.02.114.

Khubber, S., K. Chaturvedi, N. Thakur, N. Sharma, and S.K. Yadav. 2021. Low-methoxyl pectin stabilizes low-fat set yoghurt and improves their physicochemical properties, rheology, microstructure and sensory liking. Food Hydrocoll. 111:106240. doi:10.1016/J.FOODHYD.2020.106240.

Koudelka, T., F.C. Dehle, I.F. Musgrave, P. Hoffmann, and J.A. Carver. 2012. Methionine oxidation enhances κ-casein amyloid fibril formation. J. Agric. Food Chem. 60:4144–4155. doi:10.1021/JF205168T/SUPPL_FILE/JF205168T_SI_001.PDF.

Loveday, S.M., S.G. Anema, and H. Singh. 2017. β-Lactoglobulin nanofibrils: The long and the short of it. Int. Dairy J. 67:35–45. doi:10.1016/J.IDAIRYJ.2016.09.011.

Loveday, S.M., J. Su, M.A. Rao, S.G. Anema, and H. Singh. 2012. Whey protein nanofibrils: The environment-morphology-functionality relationship in lyophilization, rehydration, and seeding. J. Agric. Food Chem. 60:5229–5236. doi:10.1021/JF300367K/ASSET/IMAGES/LARGE/JF-2012-00367K_0008.JPEG.

Mantovani, R.A., J. Fattori, M. Michelon, and R.L. Cunha. 2016. Formation and pH-stability of whey protein fibrils in the presence of lecithin. Food Hydrocoll. 60:288–298. doi:10.1016/J.FOODHYD.2016.03.039.

Mantovani, R.A., G. de Figueiredo Furtado, F.M. Netto, and R.L. Cunha. 2018. Assessing the potential of whey protein fibril as emulsifier. J. Food Eng. 223:99–108. doi:10.1016/J.JFOODENG.2017.12.006.

Oboroceanu, D., L. Wang, E. Magner, and M.A.E. Auty. 2014. Fibrillization of whey proteins improves foaming capacity and foam stability at low protein concentrations. J. Food Eng. 121:102–111. doi:10.1016/J.JFOODENG.2013.08.023.

Pan, K., and Q. Zhong. 2015. Amyloid-like fibrils formed from intrinsically disordered caseins: physicochemical and nanomechanical properties. Soft Matter 11:5898–5904. doi:10.1039/C5SM01037C.

Peng, Y., M. Serra, D.S. Horne, and J.A. Lucey. 2009. Effect of Fortification with Various Types of Milk Proteins on the Rheological Properties and Permeability of Nonfat Set Yogurt. J. Food Sci. 74:C666–C673. doi:10.1111/J.1750-3841.2009.01350.X.

Sinha, R., C. Radha, J. Prakash, and P. Kaul. 2007. Whey protein hydrolysate: Functional properties, nutritional quality and utilization in beverage formulation. Food Chem. 101:1484–1491. doi:10.1016/J.FOODCHEM.2006.04.021.

Sriniv, S.S.S.S., R. Riniv, R. Rinivasan, A. Asan Asan Asan D D D, D. Damodaran, and A. Amodaran. 2005. Protein Stabilization of Emulsions and Foams. J. Food Sci. 70:R54–R66. doi:10.1111/J.1365-2621.2005.TB07150.X.

Wan, Z., X. Yang, and L.M.C. Sagis. 2016. Contribution of Long Fibrils and Peptides to Surface and Foaming Behavior of Soy Protein Fibril System. Langmuir 32:8092–8101. doi:10.1021/ACS.LANGMUIR.6B01511/ASSET/IMAGES/LARGE/LA-2016-01511J_0007.JPEG.

Zaitoun, B.J., N. Palmer, and J.K. Amamcharla. 2022. Characterization of a Commercial Whey Protein Hydrolysate and Its Use as a Binding Agent in the Whey Protein Isolate Agglomeration Process. Foods 2022, Vol. 11, Page 1797 11:1797. doi:10.3390/FOODS11121797.

Chapter 7 - Conclusion

Milk proteins are excellent dairy ingredients that provide nutrition and functional properties such as thickening, gelling, emulsification, and foaming in dairy products. They are supplemented using protein-dense ingredients such as milk protein concentrates/isolates. However, due to the present customer and industry demand, the native protein functionality needs to be enhanced to meet the emerging demand. Among several techniques, fibrillation is a novel technique that converts globular proteins such as whey proteins into a fibrillar form and these fibrillated protein shows enhanced functionality such as thickening, gelling, emulsification, and foaming than the non-fibrillated protein. Considering the benefits of fibrillation, in the current study whey proteins were selectively fibrillated and mixed with micellar casein concentrate (keeping casein to whey proteins ratio 80:20) to get fibrillated model milk protein concentrates (F-MPC). F-MPC showed the presence of fibrils also, it showed higher viscosity and produced firmer acid gel than the control model MPC. F-MPC was spray dried which showed the presence of fibrils upon rehydration and showed higher viscosity, emulsification, and foaming properties than C-MPC. In another study, fibrillated skim milk was prepared by selective fibrillation of whey proteins (fractionated by microfiltration and ultrafiltration of skim milk) followed by spray drying to convert into fibrillated non-fat dried milk which showed higher viscosity, emulsification, and foaming properties than the control non-fat dried milk. Therefore, it could be said that selective fibrillation of whey protein can be an effective technique to increase the functionality of the existing milk protein powders. This improvement in the functionality of milk protein powder can reduce the need for non-dairy ingredients in dairy food formulations. Also, these improved milk protein powders can be considered as clean label ingredients

Appendix A - Data and SAS code for Chapter 4: Acid gelation

As a sample analysis, SAS code for one way ANOVA analysis of Thioflavin T fluorescence (ThT) value was shown below:

```
title 'AG';
data AG;
input MPC$ LOT$ ThT;
datalines;
CMPC A      252.9
CMPC A      249.44
CMPC A      242.33
CMPC A      245.44
CMPC B      234.16
CMPC B      231.31
CMPC B      260.73
CMPC B      260.72
FMPC A      401.79
FMPC A      401.76
FMPC A      397.44
FMPC A      393.35
FMPC B      342.44
FMPC B      338.74
FMPC B      333.76
FMPC B      332.55
;
proc print data=AG;
run;
proc anova data=AG;
class MPC LOT;
model ThT=MPC LOT MPC*LOT;
means MPC LOT MPC*LOT/Tukey;
random Lot;
run;
```